Draft version August 7, 2026
Typeset using LaTeX **twocolumn** style in AASTeX7.0.1

arXiv:2608.00173v2 [astro-ph.EP] 6 Aug 2026

The Dynamics of Planetary Ejection

Malena Rice,[1] William DeRocco,[2,3] and Sean N. Raymond[4]

[1] *Department of Astronomy, Yale University, 219 Prospect Street, New Haven, CT 06511, USA*
[2] *Maryland Center for Fundamental Physics, University of Maryland, College Park, 4296 Stadium Drive, College Park, MD 20742, USA*
[3] *Department of Physics & Astronomy, The Johns Hopkins University, 3400 N. Charles Street, Baltimore, MD 21218, USA*
[4] *Laboratoire d'astrophysique de Bordeaux, Univ. Bordeaux, CNRS, B18N, allée Geoffroy Saint-Hilaire, F-33615 Pessac, France*

ABSTRACT

The ubiquity of free-floating planets inferred from microlensing and direct imaging surveys suggests that planetary ejection—a process in which planets initially born encircling a stellar host become gravitationally unbound—is common. Four overarching mechanisms have been proposed to induce planetary ejection: close approaches of neighboring planets, instabilities in binary or multi-star systems, stellar and planetary flybys, and post-main-sequence stellar evolution. Here we review the mechanisms underlying planetary ejection, as well as predictions derived from each. Current and upcoming microlensing surveys offer the potential to test existing models and distinguish between potential planetary ejection mechanisms, offering further insight into the demographic-level architectures of exoplanets across stellar environments.

Keywords: Free floating planets (549) — Exoplanet dynamics (490) — Exoplanets (498) — Gravitational microlensing (672)

Contents

1. Introduction 2

2. Close approaches between neighboring planets 3
   2.1. Underlying principles 3
      2.1.1. The Safronov number 3
      2.1.2. Angular momentum deficit 6
   2.2. Evidence for scattering-induced planetary ejection in the solar system 7
   2.3. Evidence for scattering-induced planetary ejection in extrasolar systems 8
   2.4. Predictions and implications: planet-planet scattering 9
      2.4.1. The present-day population of bound planets 9
      2.4.2. The mass distribution of FFPs 10
      2.4.3. The velocity distribution of FFPs 11

3. Instabilities in systems with bound stellar companions 12
   3.1. Instabilities of circumstellar planets in binary systems 12
      3.1.1. Circumstellar planets in close stellar binaries 12
      3.1.2. Circumstellar planets in wide stellar binaries 14
   3.2. Instabilities of circumbinary planets 14
   3.3. Planetary orbital instabilities in multi-star systems 14
   3.4. Predictions and implications: instabilities in systems with bound stellar companions 15

4. Flyby-induced ejections 16
   4.1. Flyby occurrence rates 16
   4.2. Cross-sections for flyby interactions 16
   4.3. Potential outcomes from stellar flyby interactions 17
   4.4. Substellar object flybys 18
   4.5. Predictions and implications: flyby encounters 18
      4.5.1. Predictions and implications: flybys in embedded clusters 18
      4.5.2. Predictions and implications: flybys in evolved open clusters 19
      4.5.3. Predictions and implications: flybys in globular clusters 19

Corresponding author: Malena Rice
malena.rice@yale.edu

4.5.4. How often do planets remain bound to the host cluster after being liberated from their host star? 20

5. Post-main-sequence planetary ejection 21
5.1. The general variable-mass two-body problem 21
5.2. The mass-loss index Ψ 21
5.3. Direct ejection from slow mass loss 21
5.4. Direct ejection in the impulse approximation 22
5.5. Post-main-sequence planetary close encounters 22
5.6. Increased susceptibility to flyby-induced ejection 23
5.7. White dwarf kicks 23
5.8. The role of binarity in planetary ejection for evolving stellar systems 24
5.9. Predictions and implications: post-main-sequence planetary ejection 24

6. Discussion 25
6.1. Relative rates of FFP production 25
6.2. Observed properties of candidate FFPs 27
6.3. Sub-planetary-mass ejected bodies 28
6.4. Future prospects 29

7. Summary 30

1. INTRODUCTION

The signatures of multi-scale dynamic environments are imprinted on today's census of observed planetary systems. Both theoretical and observational constraints have indicated that planets' evolved configurations are often not representative of the initial outcomes of planet formation (J. C. B. Papaloizou & C. Terquem 2006; M. B. Davies et al. 2014; A. Morbidelli 2018; S. N. Raymond et al. 2020). Instead, a given main-sequence (or post-main-sequence) system reflects the integrated sculpting of millions to billions of years of processing. Orbits may evolve substantially over a system's lifetime, undergoing shifts and instabilities. In many scenarios, these orbital shifts may result in planets being ejected from their host systems.

Numerical simulations indicate that planetary ejection is a common outcome of dynamical interactions between planets and their perturbers (S. J. Weidenschilling & F. Marzari 1996; F. A. Rasio & E. B. Ford 1996; D. N. C. Lin & S. Ida 1997; S. Chatterjee et al. 2008; E. B. Ford 2014). Observational constraints, too, point toward a high rate of planetary ejection: microlensing surveys have unveiled a vast population of planets orbiting within the Milky Way, unbound from any host star (P. Mróz et al. 2017; A. Gould et al. 2022; T. Sumi et al. 2023). Correcting for survey biases, these discoveries indicate that such "free-floating planets" (FFPs)—also commonly referred to as "rogue planets"—are common, at of order ≈ 20 FFPs with masses $0.33 < M/M_{\oplus} < 6660$ per star in the Milky Way (T. Sumi et al. 2023).

While planetary ejection is a ubiquitous process, the specific outcomes of this process are elusive to directly pinpoint. Ejected planets have been removed from their host systems such that they are not, by default, illuminated by any bright source. This renders them effectively invisible to the historically lucrative transit and radial velocity methods that have been leveraged to discover and characterize most known exoplanets to date (J. L. Christiansen et al. 2025). Furthermore, some planetary ejection mechanisms suggest that FFPs may stem from birth populations that are largely distinct from the well-characterized census of bound exoplanets—a near-inevitability, for example, for many planets born into orbits that are not long-term stable.

This poses a challenge as well as an opportunity. Planetary ejection studies offer a complementary avenue toward understanding regions of parameter space in planetary systems that are only minimally accessible with most exoplanet detection and characterization methods. A bridge between the theoretical and observational constraints on planetary ejection provides a crucial piece of the puzzle when interpreting the demographic-level evolutionary cycles of planetary systems.

Depending on the birth properties and environmental factors shaping a planetary system, a range of dynamical mechanisms may induce instabilities that lead to planetary ejection. Indeed, any close encounters or instability-inducing mechanisms, such as planet-planet close approaches, dynamical perturbations from companion stars, stellar and planetary flybys, and host star evolution, have the potential to trigger the ejection of one or more initially bound planets.

We provide a schematic overview of these instability-triggering mechanisms in Figure 1 for guidance. In this manuscript, which is designed as a pedagogical overview of the dynamics of planetary ejection, we begin by discussing the underlying mechanisms that may trigger planetary ejection. We first consider interactions between neighboring planets in Section 2, then examine the influence of bound stellar companions in Section 3. We describe potential ejection from flybys of unbound objects in Section 4. Lastly, we discuss the prospects for planetary ejection from post-main-sequence stellar evolution in Section 5. We discuss the relative contributions of each planetary ejection mechanism as well as

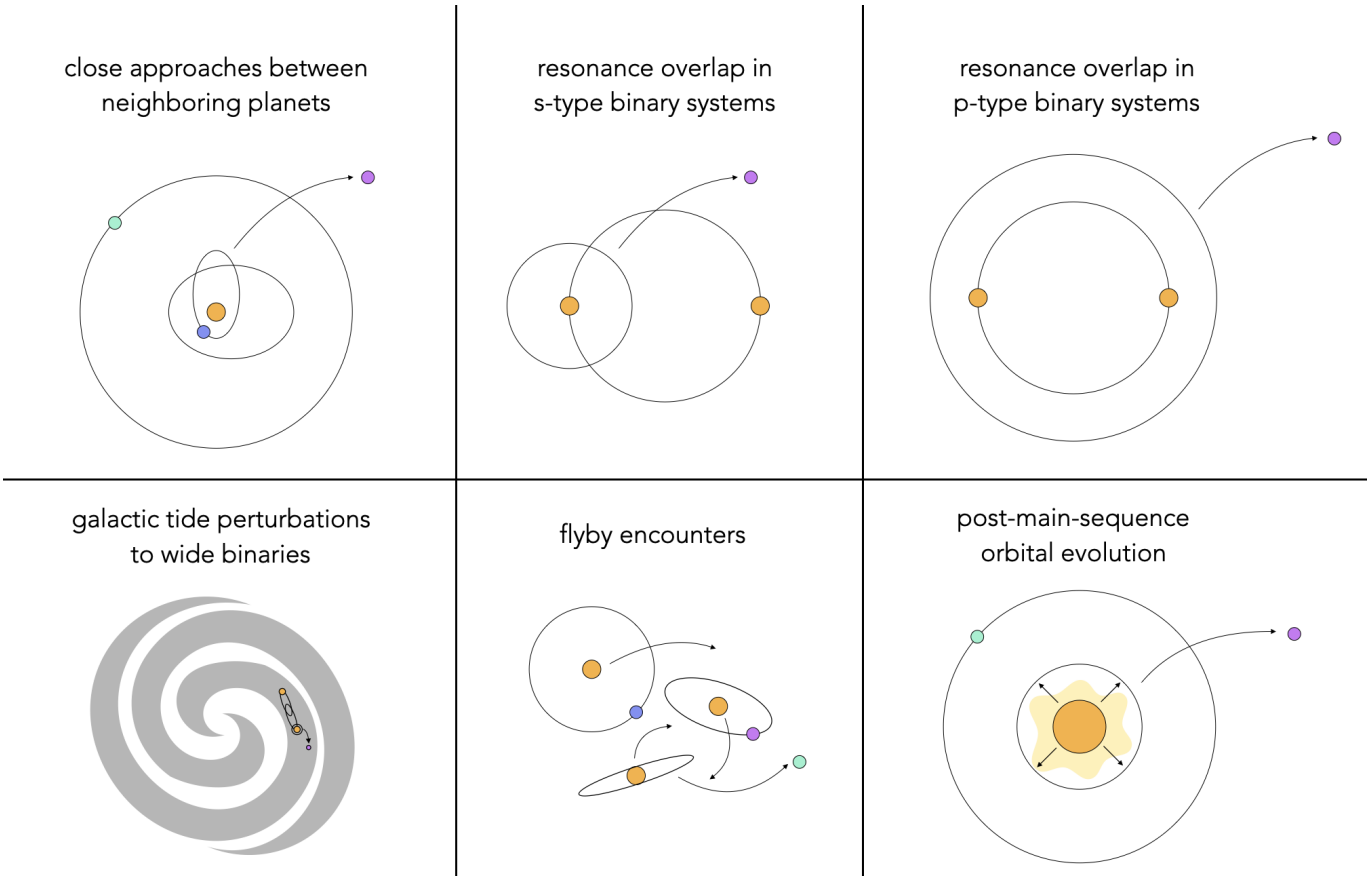

Figure 1. Schematic overview of instability-inducing mechanisms through which planets may be ejected from a system. These mechanisms, each discussed throughout this work, include close approaches between neighboring planets (top left; Section 2), binary-induced instabilities (top center and right, and bottom left; Section 3), flyby encounters (bottom center; Section 4), and post-main-sequence orbital evolution (bottom right; Section 5).

future prospects to constrain the planetary ejection rate in Section 6. We conclude with a summary of major takeaways in Section 7.

2. CLOSE APPROACHES BETWEEN NEIGHBORING PLANETS

Stellar systems that host two or more planets around a single star often undergo instabilities in which neighboring planets experience close encounters. In this process, commonly referred to as "planet-planet scattering," the close encounters may cause one or more planets to be scattered outward and unbound from the system. Conservation of the system's angular momentum implies that, in the process of planet-planet scattering, the lowest-mass planets tend to be ejected, whereas the highest-mass planets typically remain bound to the system. The remaining, bound planets are often left on dynamically excited (eccentric and/or inclined) orbits from the encounter.

In Section 2.1, we first outline some underlying principles that can be applied to describe systems' capacity for planetary ejection through planet-planet scattering. We then provide a brief overview of the evidence for planet-planet scattering in the solar system in Section 2.2 and an analogous overview for exoplanet systems in Section 2.3. We close with predictions for the free-floating planet population, drawn from single-star scattering scenarios, in Section 2.4.

2.1. *Underlying principles*

In this section we describe quantitative metrics that provide intuition for planetary systems' typical proclivity toward planetary ejection, as well as relevant timescales for instability.

2.1.1. *The Safronov number*

Depending on the physical conditions of the system, close encounters between two bodies in a planetary system may result in either a collision or an ejection. The outcome of a close encounter can be understood from first principles through examining a simple scenario in which two bodies undergo a grazing encounter.

Consider a body with mass m approaching a planet with mass M_p and radius R_p from a large distance x,

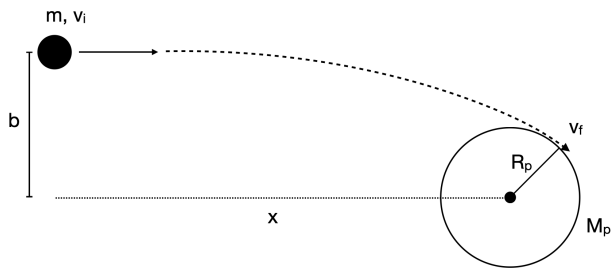

Figure 2. Schematic depiction of the grazing-encounter scenario considered in Section 2.1.1, through which the Safronov number, which is used to determine the likelihood of collisions vs. ejections as the outcome of close encounters, is derived. Here x is an initially large distance from which mass m, at initial velocity v_i, approaches a planet with mass M_p and R_p with impact parameter b. The final velocity v_f of mass m is denoted at the point of closest approach during its grazing encounter with mass M_p.

with impact parameter b and initial velocity v_i (Figure 2). Both m and M_p are in orbit around a star with mass M_*, where $M_* \gg m, M_p$.

From conservation of energy, the final velocity v_f when mass m reaches a grazing encounter with mass M_p can be obtained through the expression

$$\frac{1}{2}mv_i^2 - \frac{GM_p m}{\sqrt{x^2+b^2}} = \frac{1}{2}mv_f^2 - \frac{GM_p m}{R_p}. \tag{1}$$

For $x \to \infty$, $1/\sqrt{x^2+b^2} \approx 0$ and Equation 1 simplifies to

$$v_f^2 = v_i^2 + v_{\rm esc,p}^2, \tag{2}$$

where the escape velocity $v_{\rm esc,p}$ from planet M_p is given as

$$v_{\rm esc,p} = \sqrt{\frac{2GM_p}{R_p}}. \tag{3}$$

To examine the case of ejection, we are interested in the scenario in which mass m reaches a final velocity v_f above the escape velocity of the system $v_{\rm esc,*}$. That is, we require

$$v_f > v_{\rm esc,*} \ (\text{for ejection}), \tag{4}$$

where

$$v_{\rm esc,*} = \sqrt{\frac{2GM_*}{r}} \tag{5}$$

to escape from an orbit around the host star, for planet-star distance r at a given time.

Inspection of Equation 2 together with the condition of Equation 4 reveals that for any encounter velocity v_i, close encounters with a neighboring planet will lead to a boost above the system's escape velocity for $v_{\rm esc,p}^2/v_{\rm esc,*}^2 > 1$. Thus, the parameter Θ, defined as

$$\Theta \equiv \frac{v_{\rm esc,p}^2}{v_{\rm esc,*}^2}, \tag{6}$$

is useful in demonstrating whether encounters will typically lead to ejections—the alternative being either (1) collisions or (2) close approaches in which both bodies remain bound to the host star without merging. Θ is commonly referred to as the "Safronov number," and, in this simplified scenario, ejections occur where $\Theta > 1$. Rearranging using Equations 3 and 5, the Safronov number may also be written as

$$\Theta = \frac{M_p r}{R_p M_*}. \tag{7}$$

Equations 6 and 7 provide a generalized version of the Safronov number, which is often approximated specifically for circular orbits. For circular orbits, $a = r$ and Equation 7 may be updated accordingly. In particular, the instantaneous orbital speed at a given separation r from the star is

$$v_{\rm orb} = \sqrt{GM_*\left(\frac{2}{r} - \frac{1}{a}\right)}. \tag{8}$$

Therefore, in the limit of a circular orbit, $v_{\rm esc,*} = \sqrt{2}v_{\rm orb}$. In this case, the Safronov number may be rewritten as its commonly reported form

$$\Theta = \frac{1}{2}\frac{v_{\rm esc,p}^2}{v_{\rm orb}^2} \ \ (\text{for } e = 0). \tag{9}$$

The above approximations assume no energy transfer between the planet and the ejected body, and they do not take into consideration the encounter geometry (instead assuming a grazing geometry), which in practice influences whether m reaches the system's escape velocity (e.g. S. J. Weidenschilling 1975). Because of these limitations, the requirement for a planet to efficiently eject its neighbors may be more safely written as $\Theta \gg 1$. For planets in the regime $\Theta \ll 1$, close approaches by neighboring bodies tend to instead lead to collisions.

Equation 7 demonstrates that, in general, planets on wider orbits are more efficient at ejecting neighboring material. The majority of the currently known exoplanets were detected via the transit method, such that the census is heavily biased toward systems in which planets are difficult to eject: those in which planets are on extremely tight orbits with $\Theta \ll 1$, with a strong potential well that typically culminates in collisions, rather than ejections, from close encounters. M. C. Wyatt

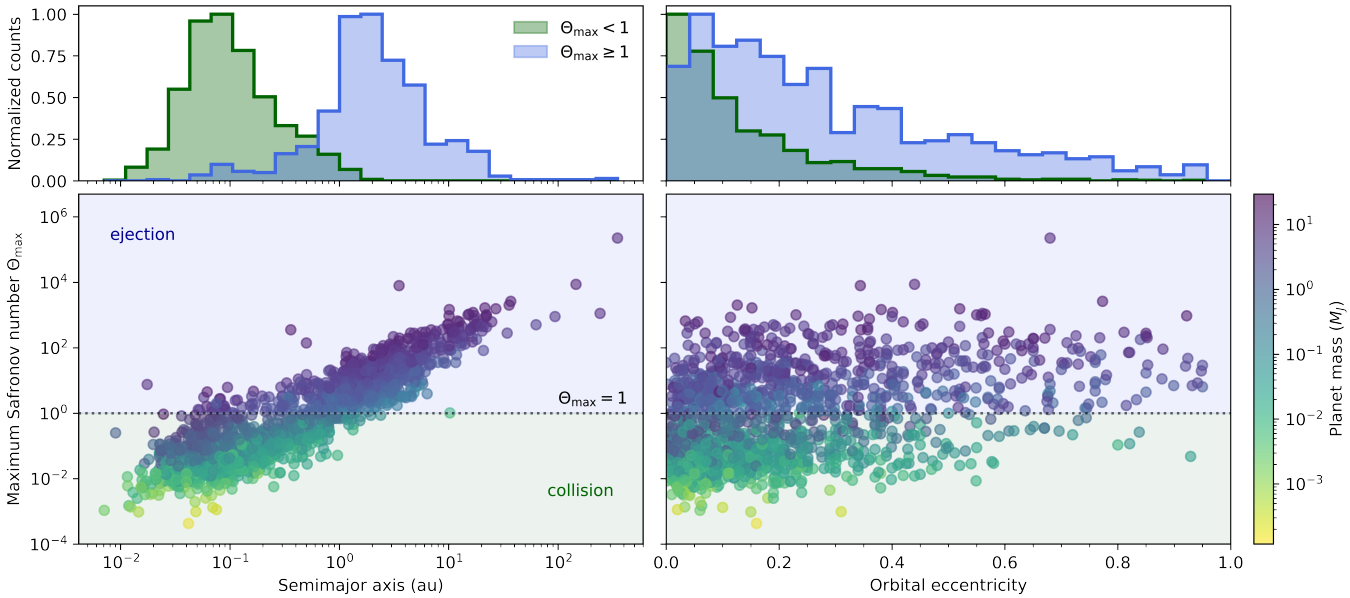

Figure 3. Maximum Safronov number of known, bound planets shown as a function of semimajor axis (left) and eccentricity (right), as a scatter plot (bottom) and histogram (top). The histograms are each normalized to peak at 1 for a clearer comparison between samples. Only planets with measured, nonzero uncertainties in orbital eccentricity are included. Though these planets remain bound to their host systems, the elevated eccentricities of planets with high Safronov numbers suggests that they may have ejected neighboring companions in their past histories. Because the Safronov number varies with location in the orbit, we take the maximum Safronov number $\Theta_{\max}$ corresponding to apoastron, where $r = a(1+e)$. The present-day maximum Safronov number calculated here is a proxy for the true value of interest, which is the pre-scattering Safronov number. This is an updated version of an earlier result first demonstrated by E. B. Ford & F. A. Rasio (2008).

et al. (2017) developed a mapping of the typical outcomes from close approaches with the known census of exoplanets—assuming circular orbits and encounters with a single planet—demonstrating this bias.

Wider-orbiting known exoplanets—largely discovered through the radial-velocity or direct-imaging methods—often have higher Safronov numbers. E. B. Ford & F. A. Rasio (2008) showed that planets with higher Safronov numbers typically have higher-eccentricity orbits than those with lower Safronov numbers, suggesting that neighboring planets may have been previously ejected from the systems. Updating this result with the current set of known planets (as of 7/1/2026) and using Equation 7 to calculate the maximum Safronov number for each orbit, we demonstrate in Figure 3 that this finding continues to hold true for the present-day census of confirmed exoplanets.

Equation 7 provides further intuition when considered in conjunction with planetary mass-radius relationships, as visualized in Figure 4. For sub-Jovian-mass planets, the scaling of R_p with M_p is sub-linear, at roughly $R_p \propto M_p^{1/3}$ for $M_p \lesssim 2M_\oplus$ and $R_p \propto M_p^{2/3}$ for $2M_\oplus \lesssim M_p \lesssim 0.4M_J$ (D. Valencia et al. 2006; J. Chen & D. Kipping 2017). In this regime, M_p grows more rapidly than R_p. For a given stellar type and assuming $e = 0$, this implies that $\Theta \propto M_p^{2/3} a$ for $M_p \lesssim 2M_\oplus$ and $\Theta \propto M_p^{1/3} a$ for $2M_\oplus \lesssim M_p \lesssim 0.4M_J$. Hence, higher-mass rocky and Neptunian planets have higher Safronov numbers, such that more massive planets are generally more efficient at ejecting material for a given orbit and host star type.

For Jovian-mass planets ($M \gtrsim 0.4M_J$), the mass-radius relationship is relatively flat at $R_p \propto M_p^0 \approx$ constant (J. Chen & D. Kipping 2017). In this regime, given a known stellar type (and thus mass M_*), the Safronov number further simplifies so that it scales only with orbital separation r—or, for circular orbits, with semimajor axis a. The Safronov number for an $e = 0$ Jovian-mass planet is then well-approximated by a linear scaling with semimajor axis, $\Theta \propto a$.

The Safronov number is not necessarily static for a given planet. A planet may migrate during or after its formation, either increasing or decreasing the Safronov number depending on the direction of migration. As giant planets cool and contract, altering their densities by a factor of a few, their Safronov numbers also accordingly shift, as explored by A. S. Bonomo et al. (2017) in the context of the CoRoT-9 b Jovian planet. This affects the branching ratios of accretion vs. ejection outcomes for close encounters.

The Safronov number also has important implications for the formation of planets. The concept of the Safronov number was originally developed in the context

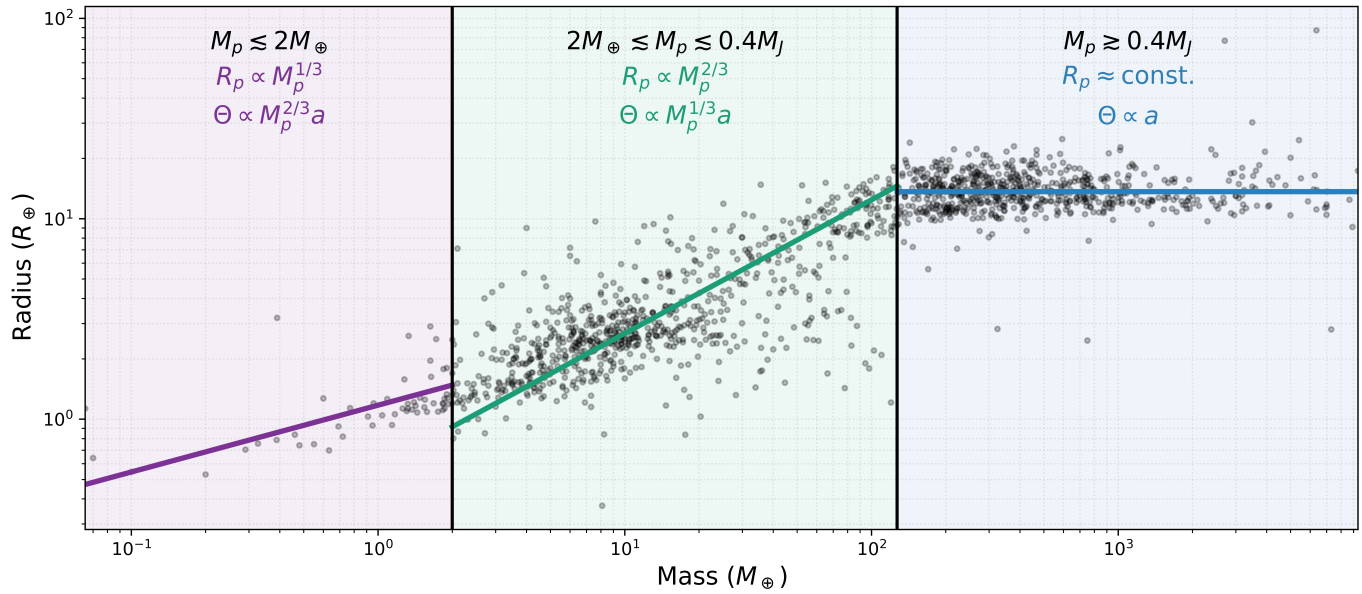

Figure 4. Theoretical, piecewise mass-radius scalings across planetary mass regimes, alongside associated scalings of the Safronov number. The census of observed exoplanets with masses and radii (including uncertainties) reported in the NASA Exoplanet Archive PSCompPars table as of 7/1/2026 is shown in gray, and the theoretical fits with fixed exponents are scaled to match this population. We note that the empirically-derived exponents fitted to each subpopulation in previous work have been observed to deviate slightly from these theoretical values, which enables improved matches at the boundaries between each subpopulation (e.g. J. Chen & D. Kipping 2017).

of gravitational focusing (see Section 4.2 for further discussion of this mechanism), as a limit for planetesimal accretion to proceed (V. S. Safronov & E. V. Zvjagina 1969). Thus, the fact that planets exist in our solar system with $\Theta > 1$ implies that they must have either migrated or formed through a separate mechanism (in the case of the solar system giant planets, primarily gas accretion). This also implies a limit for planet formation: that is, the Safronov number may be used to approximate the widest orbital separation at which a planet of a given mass and radius, around a given host star, may form through planetesimal accretion such that $\Theta < 1$ (accretion dominates over ejection). For an Earth-like planet around a solar-mass star, this limit is 14.2 AU.

2.1.2. *Angular momentum deficit*

The angular momentum deficit (AMD) is defined as the difference in angular momentum between a planetary system and the same system in which all planets are on circular, aligned orbits at the same semimajor axes. The AMD may be calculated as (P.-S. Laplace 1878; J. Laskar 1997, 2000)

$$\mathrm{AMD} = \sum_{k=1}^{N} M_{p,k}\sqrt{GM_* a_k}(1 - \sqrt{1-e_k^2}\cos i_k) \quad (10)$$

where $M_{p,k}$, a_k, e_k, and i_k are the mass, semimajor axis, eccentricity, and inclination of the kth planet, and the sum is taken over N bound planets in the system. In this expression, the inclinations are taken relative to the invariable plane of the planetary system (P.-S. Laplace 1878), which is defined as the plane perpendicular to the net angular momentum vector of the system.

For sufficiently high AMD, secular evolution can be chaotic and the planets' orbital eccentricities and inclinations may diffusively evolve toward equipartition of the secular degrees of freedom, in some cases resulting in chaotic evolution and orbit crossings (Y. Lithwick & Y. Wu 2011; Y. Wu & Y. Lithwick 2011; Y. Lithwick & Y. Wu 2014). J. Laskar & A. C. Petit (2017) presents an analytic limit for the critical AMD required for stability in compact multi-planet systems, above which the system can undergo collisions and ejections commonly driven by overlapping mean-motion resonances (B. V. Chirikov 1979; A. C. Quillen 2011; A. C. Petit et al. 2020; D. Tamayo et al. 2021). The innermost planet is typically most susceptible to significant AMD transfer (Y. Wu & Y. Lithwick 2011), which raises its eccentricity and in some cases induces instabilities that remove the inner planet from the system. In this process, the eccentricities and inclinations of the outer planets are pushed toward lower values to conserve angular momentum, such that the loss of the innermost planet culminates in a reduced system AMD.

S. Hadden & Y. Wu (2025) applied numerical simulations to demonstrate that detached planets reach

their final state when there is no longer sufficient AMD to induce orbit crossings over time. Lower-mass planets in crowded systems undergo instabilities over longer timescales than higher-mass planets (J. E. Chambers et al. 1996; F. C. Adams & G. Laughlin 2003; F. Marzari 2025). As a result, S. Hadden & Y. Wu (2025) found that while systems of scattered, detached equal-mass giant planets ($\gtrsim 10 M_{\rm Nep}$) often reach an AMD-stable configuration within 100 Myr after the first orbit-crossing, comparable systems of lower-mass Neptune analogues can take Gyr to reach this point.

2.2. *Evidence for scattering-induced planetary ejection in the solar system*

Planet-planet scattering and subsequent planetary ejection have been invoked to explain many observables in planetary systems, including the solar system. Here we briefly discuss the evidence for planetary ejection in the solar system, which serves as a relatively well-constrained case study.

Solar system models have long incorporated the influence of planetesimal-driven migration, through which planetesimals are ejected from the system as the giant planets migrate (e.g. J. A. Fernandez & W.-H. Ip 1984; R. Malhotra 1993, 1995; E. W. Thommes et al. 1999; H. F. Levison et al. 2001; R. Gomes et al. 2005; K. Tsiganis et al. 2005; A. Morbidelli et al. 2005; K. Batygin & M. E. Brown 2010; H. F. Levison et al. 2011). Over time, these models have evolved to consider possible additional planets that may have existed in the outer solar system during its past.

Several early works examined or alluded to the possibility that the solar system may have once included additional planets that no longer remain bound. For example, numerical simulations by E. W. Thommes et al. (1999, 2002), which were focused on modeling the formation of Uranus and Neptune, included scenarios in which a fifth giant planet formed and was subsequently ejected from the outer solar system. P. Goldreich et al. (2004a), too, made the claim that some planet-sized objects were likely ejected from the outer solar system at the late stages of planet formation. If the outer solar system planets formed in a packed oligarchy, then up to five Neptune-sized isolation masses could have fit between 15-25 AU at mutual separations of 5 Hill radii—a configuration that would have destabilized as the natal disk dispersed, often resulting in the ejection of one or more planets (E. B. Ford & E. I. Chiang 2007).

D. Nesvorný (2011) and K. Batygin et al. (2012) each demonstrated that numerical simulations invoking a fifth solar system giant planet—which is often ejected[5] during the solar system's instability-driven evolution—provide an excellent match to solar system observables, such as the solar system's secular modes. Follow-up work by D. Nesvorný & A. Morbidelli (2012) examined a range of possible resonant orbital configurations and showed that the inclusion of a fifth (and possibly sixth) planet in the numerical simulations enables models to much more consistently match a, e, and i of the solar system planets to present-day values.

Further numerical studies adopting this five-giant-planet+orbital instability model have demonstrated that it appropriately reproduces the capture of the Trojan asteroids (D. Nesvorný et al. 2013) and irregular satellites (D. Nesvorný et al. 2014a) in the Jupiter system; that it is possible to maintain the Galilean moon system around Jupiter despite close-approach encounters between Jupiter and the extra ice giant (R. Deienno et al. 2014; R. Cloutier et al. 2015); and that it may enable inclination excitation for Iapetus relative to Saturn's orbital plane (D. Nesvorný et al. 2014b), but that ejection of the fifth giant by Jupiter (rather than Saturn) is favored to avoid disrupting Iapetus's orbit (R. Cloutier et al. 2015). A fifth giant planet may also support the secular-resonance-driven dispersal of primordial asteroid families (P. I. O. Brasil et al. 2016), and it is consistent with the predicted orbital evolution of Neptune necessary to reproduce the observed structure of the Kuiper belt (D. Nesvorný 2015a,b; R. Deienno et al. 2017). Studies examining other aspects of the solar system's primordial configuration now often incorporate this fifth ice giant (e.g. M. S. Clement et al. 2018, 2021a,b; B. Liu et al. 2022; N. A. Kaib et al. 2024; S. N. Raymond & N. A. Kaib 2026).

Whether or not a fifth ice giant was ejected in the early solar system's history, it would be surprising if lower-mass planets were not. Collisions between planetary embryos have been modeled to build the cores of the solar system giant planets, and in this process a subset of the embryos (typically ranging from $\approx 1-6\,M_\oplus$) is commonly ejected and removed from the system (e.g. M. Jakubík et al. 2012; A. Izidoro et al. 2015). Additional planetary embryos may also be ejected at other points in the solar system's evolution—for example, in simulations presented within M. S. Clement et al. (2018), mul-

[5] In a small fraction of runs reported by K. Batygin et al. (2012), an ice giant instead merged with Saturn, similarly reproducing a configuration comparable to that of the solar system. Thus, the five-giant-planet solar system model does not require that planetary ejection is invoked to reproduce present-day outcomes.

tiple embryos from $0.25 - 2.5\,M_{\rm Mars}$ were removed from the inner solar system during the giant planet instability. If planetary embryos remained in the outer solar system at later times, after gas giant formation and disk dispersal, most would have been similarly ejected (T. Barclay et al. 2017; K. Silsbee & S. Tremaine 2018). Though the true primordial occurrence and size distribution of such lower-mass ejected planets in the solar system's early history remains relatively poorly constrained, the pervasiveness of planetary ejection in a bottom-up planet formation framework strongly suggests that it has played a role in the solar system's early evolution.

2.3. *Evidence for scattering-induced planetary ejection in extrasolar systems*

Beyond the solar system, hints in the architectures of extrasolar systems also suggest a high rate of planet-planet scattering. Such evidence is typically drawn from the spacings and orbital properties of planetary systems, which often point toward dynamical sculpting beyond the planets' initial formation.

Perhaps the most direct line of evidence for a high rate of planetary ejection in extrasolar systems is the eccentricity distribution observed for giant exoplanets. Planet-planet scattering has long been invoked to explain the elevated eccentricities of exoplanet orbits, often in the context of hot Jupiter formation and high-eccentricity giant exoplanet orbital configurations (F. A. Rasio & E. B. Ford 1996; S. J. Weidenschilling & F. Marzari 1996; D. N. C. Lin & S. Ida 1997; F. C. Adams & G. Laughlin 2003; S. Chatterjee et al. 2008; M. Nagasawa et al. 2008; S. N. Raymond et al. 2009). Even extremely high eccentricities $e > 0.99$ may be reached by planet-planet scattering (D. Carrera et al. 2019).

Population-level studies have found that the high eccentricities of giant exoplanet systems are well-matched by models in which nearly all ($> 75 - 80\%$) systems underwent an orbital instability (M. Jurić & S. Tremaine 2008; S. N. Raymond et al. 2010; S. N. Raymond et al. 2011). Planets with a higher Safronov number also show a wider spread in orbital eccentricities (E. B. Ford & F. A. Rasio 2008, see also Figure 3 in this review), suggesting that at least a subset of these planets may have been dynamically excited to higher eccentricities through past scattering events. Planet-planet scattering notably offers a pathway toward elevated eccentricities while simultaneously reproducing observed features of the spin-orbit distribution for giant exoplanet systems (M. Rice et al. 2022; J. Rusznak et al. 2025; J. Esposito et al. 2026; J. Dong et al. 2026).

Another line of evidence used to argue for a high rate of orbital instabilities in exoplanet systems is the relative spacings of observed planets. The dynamical separation of planets may be measured with the critical spacing Δ, given as

$$\Delta \equiv \frac{a_2 - a_1}{R_H} \tag{11}$$

for semimajor axes a_1 and a_2, and Hill radius

$$R_H = \frac{a_1 + a_2}{2}\left(\frac{m_1 + m_2}{3M_*}\right)^{1/3} \tag{12}$$

with planet masses m_1 and m_2. B. Gladman (1993) showed that systems of two planets on circular, coplanar orbits are stable to orbit-crossing instabilities for $\Delta > 2\sqrt{3} \approx 3.46$. For higher-multiplicity systems, this spacing must be larger to ensure stability, with specific configurations (planet multiplicities and mass ratios) examined in further detail in a slew of later studies (J. E. Chambers et al. 1996; J.-L. Zhou et al. 2007; A. W. Smith & J. J. Lissauer 2009; B. Funk et al. 2010; B. Pu & Y. Wu 2015; D. Tamayo et al. 2015; S. J. Morrison & K. M. Kratter 2016; A. Obertas et al. 2017; D. R. Rice et al. 2018; A. Yalinewich & C. Petrovich 2020; P. Bartram et al. 2021; J. J. Lissauer & S. Gavino 2021; D. R. Rice & J. H. Steffen 2023; K. Volk & R. Malhotra 2024; D.-H. Wu et al. 2025; B. Outland et al. 2026; S. Gavino & J. J. Lissauer 2026).

Early work by R. Barnes & T. Quinn (2004), examining the 13 multiplanet systems known at the time, demonstrated that, while the known systems were stable, many fell precariously close to the edge of orbital instability. This led to the "packed planetary systems" hypothesis (R. Barnes & S. N. Raymond 2004), which suggests that *all* multiplanet systems are tightly packed, and those that appear to have larger spacings instead host planets below the detection limit within the observed gaps. This tight dynamical packing was later found to extend to many planetary systems that lack nearby gas giant planets (C. Lovis et al. 2011), including at least $\approx 30\%$ of multiplanet systems detected through the *Kepler* space mission (W. J. Borucki et al. 2010), pointed out by J. Fang & J.-L. Margot (2013).

Building upon these findings, B. Pu & Y. Wu (2015) showed that *Kepler* planets' spacings lie just beyond the stability threshold for survival over Gyr timescales, at $\Delta \approx 12$, leading the authors to propose that most short-period planetary systems originated in dynamically packed configurations that subsequently underwent instabilities. The instabilities in these systems would result in collisions due to the short-period orbits of *Kepler* systems, such that they would not directly produce ejections. However, this finding does point toward a high incidence of dynamical sculpting within plane-

tary systems—where analogous processes at wider orbits would result in ejections rather than collisions.

The paucity of mean-motion resonances (that is, orbital commensurabilities—formally, planet pairs with at least one librating resonant angle) in exoplanet systems, too, has been called upon as evidence for a high rate of orbital instabilities. J. J. Lissauer et al. (2011) found that *Kepler* planetary systems reported from the first four months of the mission (W. J. Borucki et al. 2011) show little to no statistical preference toward mean-motion resonance, with most systems lying wide of dominant resonances by up to a few percent. This result was further affirmed by D. C. Fabrycky et al. (2014) using a larger set of planet candidate from 16 months of *Kepler* data (N. M. Batalha et al. 2013).

The low occurrence of mean-motion resonances in exoplanet systems is unexpected as a direct consequence of formation. Commensurabilities are predicted to be common in planetary systems: the Jovian and Saturnian moon systems show an overabundance of mean-motion resonances (A. E. Roy & M. W. Ovenden 1954), and resonances play a key role in shaping the solar system's structure (S. J. Peale 1976; R. Malhotra 1998). Planetary migration models oriented toward exoplanet systems predict that planets should typically be found at or near commensurability after migration within the protoplanetary disk (M. H. Lee & S. J. Peale 2002; P. Cresswell & R. P. Nelson 2006; C. Terquem & J. C. Papaloizou 2007; S. N. Raymond et al. 2008; M. Ogihara & S. Ida 2009).

The low rate of present-day mean-motion resonances in the census of mature planetary systems implies a high rate of orbital instabilities during or soon after protoplanetary gas disk dispersal (e.g. M. Ogihara & S. Ida 2009; A. Izidoro et al. 2017; B. Liu et al. 2022; A. Izidoro et al. 2021)—or, as required to reproduce the suggestive high rate of mean-motion resonances in young ($\approx 10-60$ Myr) planetary systems (F. Dai et al. 2024), at delayed stages post-disk-dispersal. Suggested mechanisms for later-stage resonant chain disruption include delayed instability caused by remnant planetesimal disks in the systems (P. Griveaud et al. 2024; R. LoRusso et al. 2026; N. Choksi et al. 2026). While the low rate of commensurabilities in *Kepler* systems is specific to transiting planets, which lie in a parameter space in which instabilities would generally result in collisions rather than ejections, they may be indicative of system-wide disruption corresponding to planetary ejection in the outer system (e.g. P. Goldreich et al. 2004b).

Case studies of individual exoplanet systems have provided evidence that planet-planet scattering and consequent ejection may have occurred in the systems' histories, as well. E. B. Ford et al. (2005), for example, demonstrate that the excited orbital eccentricities in the 3-planet Upsilon Andromedae system may be naturally reproduced by a brief, $\approx$ 1000-year period of past instability and the ejection of a fourth planet. A. S. Bonomo et al. (2017) carried out a case study of the CoRoT-9 planetary system, which contains a single eccentric warm Jupiter planet on a $\approx$95-day orbit, to show that the previous ejection of a second, $\approx 50 M_\oplus$ planet well reproduces the system architecture. L. Yuan & M. H. Lee (2024) and T. Lu et al. (2026) present case studies for the 2-planet GJ 1148 and 14 Herculis systems, respectively, showing that if the high eccentricities of the systems result from planet-planet scattering, then a third planet was most likely ejected from the systems.

2.4. *Predictions and implications: planet-planet scattering*

2.4.1. *The present-day population of bound planets*

Ejected FFPs typically leave behind equal- or higher-mass planets that remain bound to the system. As a result, limits may be placed on the production of FFPs through ejection vs. *in situ* formation by examining the occurrence of high-mass bound exoplanets that show possible signatures of past instabilities.

The orbital configurations of giant exoplanet orbits suggest that instabilities are common, with an instability occurrence rate $\gtrsim 75-80\%$ that well reproduces the eccentricity distribution of Jupiter-mass planets (M. Jurić & S. Tremaine 2008; S. N. Raymond et al. 2010; S. N. Raymond et al. 2011). In the limit that *all* FFPs are ejected from their natal systems through planet-planet scattering with giant-planet neighbors, the number of FFPs per star $N_{\rm free}/N_{\rm stars}$ may be calculated as

$$\frac{N_{\rm free}}{N_{\rm stars}} = f_{\rm giant} f_{\rm unstable} n_{\rm ejec}, \tag{13}$$

where $f_{\rm giant}$ is the fraction of stars hosting giant planets (in particular, those with $\Theta \gg 1$), $f_{\rm unstable}$ is the fraction of those systems that undergo instabilities, and $n_{\rm ejec}$ is the typical number of planets ejected from each system that undergoes an instability (D. Veras & S. N. Raymond 2012; N. Miret-Roig et al. 2022).

The occurrence of wide-orbiting Jovian-mass planets is now relatively well-constrained in FGK star systems through a combination of microlensing (D. Suzuki et al. 2016), direct imaging (B. P. Bowler 2016; F. Baron et al. 2019; E. L. Nielsen et al. 2019), and radial velocity surveys (A. Cumming et al. 2008; M. Mayor et al. 2011; R. B. Fernandes et al. 2019; R. A. Wittenmyer et al. 2020; B. J. Fulton et al. 2021, see also C. Clanton & B. S. Gaudi (2016) for a synthesis of these methods). N.

Miret-Roig et al. (2022) demonstrated that in principle (that is, from an ejection rate standpoint), up to 100% of the highest-mass free-floating planets may be accounted for through single-star dynamical instabilities and subsequent ejection. Notably, this work focused primarily on high-mass young "planets" in star-forming regions, with formation pathways that remain under debate.

We repeat this exercise here, adopting the microlensing-constrained FFP mass function from T. Sumi et al. (2023)

$$\frac{dN}{d\log_{10} M} = 2.18 \left(\frac{M}{8\,M_\oplus}\right)^{-0.96} \text{dex}^{-1}\,\text{star}^{-1}, \quad (14)$$

which corresponds to 0.09 free-floating giant planets per star between 0.3 and 13 M_J. If all free-floating giant planets were produced via ejection by planet-planet scattering, then roughly one giant planet ($M > 0.3 M_J$) would need to be ejected per instability for a giant-planet occurrence rate $\approx 10 - 15\%$ (C. Clanton & B. S. Gaudi 2014) and instability rate 75-80%. The adopted giant-planet occurrence rate for this estimate is specific to M dwarf systems from C. Clanton & B. S. Gaudi (2014), in accordance with typical representatives of the galactic stellar population.

Jupiter-mass planets may not, however, be the sole (or even dominant) ejectors of their neighbors. Wide-orbiting Neptune-mass planets, too, may play a leading role. Observational limits from microlensing surveys (D. Suzuki et al. 2016; R. Poleski et al. 2021), alongside indirect evidence from axisymmetric protoplanetary disk substructures at tens of AU host-star separations (S. M. Andrews et al. 2018; S. Zhang et al. 2018), indicate that these wide-orbiting Neptunes are common. Recent studies have demonstrated that wide-orbiting Neptunes may be the dominant ejectors in many systems, resulting in the removal of equal- or lower-mass neighboring planets (S. Hadden & Y. Wu 2025; K. Guo et al. 2025; R. LoRusso et al. 2026).

2.4.2. *The mass distribution of FFPs*

The initial conditions of planetary systems—in particular, their typical spacings, orbit distributions, and masses—play a key role in setting the expected outcomes of planet-planet scattering. We describe population-level simulated trends for the outcomes of planet-planet scattering in this section, noting that specific predictions are strongly dependent upon the assumed initial conditions of the systems.

In systems with unequal-mass planets, lower-mass planets tend to be most efficiently ejected through scattering—generally pushing the mass function of ejected planets to be more bottom-heavy. However, competing effects complicate the interpretation of the mass function.

In equal-mass multiplanet systems, lower-mass ensembles and those with larger mutual separations typically take longer to eject planets (e.g. J. E. Chambers et al. 1996; F. Marzari & S. J. Weidenschilling 2002; P. Faber & A. C. Quillen 2007; S. Chatterjee et al. 2008; A. C. Petit et al. 2020), with a timescale dependence on the planet mass and the innermost planet's orbital period (S. Hadden & Y. Wu 2025; R. Zhai et al. 2025). For equal-mass, two-planet Hill stable planetary systems with $e \lesssim 0.3$, D. Veras & A. J. Mustill (2013) found a representative instability timescale

$$\log_{10} N_{\text{orb}} \approx 5.2 \left(\frac{\mu}{M_J/M_\odot}\right)^{-0.18} \quad (15)$$

given a mass ratio μ between each planet and the host star, corresponding to a number of inner planet orbits N_{orb}. For a suite of simulations with five equal-mass planets and constant fractional spacing between planets, S. Hadden & Y. Wu (2025) similarly found an empirical relation

$$T_{\text{ej}}(M_p) \approx 2.9 \times 10^7 \left(\frac{M_p}{M_{\text{Nep}}}\right)^{-1.64} P_{1,0} \quad (16)$$

for the time taken for the number of bound planets to decrease by one, with initial orbital period $P_{1,0}$ and where M_{Nep} corresponds to one Neptune mass. Thus, lower-mass crowded systems take longer to undergo instabilities than higher-mass crowded systems.

Because of this difference in instability timescale with planet mass, populations produced from early- vs. late-time instabilities may have differing properties. A natural time for the first wave of instabilities and ejections is early in a system's lifetime, as the mass distribution substantially shifts around the era of planet formation and disk dispersal. These instabilities would generally occur within the first few Myr of a system's lifetime (R. R. de Sousa et al. 2020), with possible delays in the instability timescale to within the first few hundred Myr based on the observed longevity of resonant chains in inner planetary systems (F. Dai et al. 2024; P. Griveaud et al. 2024; R. LoRusso et al. 2026; N. Choksi et al. 2026).

The first wave of instabilities should be bottom-heavy in its mass distribution, as the least massive planets would be ejected first. K. Guo et al. (2025) (see also S. Ma et al. (2016)) leveraged population-synthesis models from S. Ida et al. (2018) to forward-model the production of FFPs from planet-planet scattering in single-star systems within the core accretion paradigm. The authors found that most planets are ejected during in-

stabilities induced during these earlier stages, with a predicted mass distribution of FFPs that is highest (and roughly flat) around 0.1-10$M_\oplus$. Notably, higher-mass self-gravitating "fragments" of material—in some cases planet-mass—may be more readily ejected through early instabilities in the gravitational instability formation framework (J. C. Papaloizou et al. 2001; D. Forgan et al. 2015; D. H. Forgan et al. 2018; O. Schib et al. 2025a,b), with distinct implications from the core-accretion paradigm generally discussed within this section.

Over the remainder of the system's lifetime on the main sequence, additional instabilities may be triggered as well. These slower-acting instability mechanisms, induced by secular drift and AMD transfer, would most efficiently remove *higher*-mass planets, as discussed in S. Hadden & Y. Wu (2025). Specifically, high-mass planets in multi-giant-planet systems would be the first to be ejected through these mechanisms, whereas lower-mass sets of planets would be much longer-lived if they survived the initial phase of early instabilities.

Planets are not the only bodies that may become unbound through the process of scattering described throughout this section. Planet-planet scattering may also produce a large population of free-floating moons, though some FFPs with sufficiently short-period moons may retain their satellites even after ejection (J. H. Debes & S. Sigurdsson 2007; Y.-X. Gong et al. 2013; Y.-C. Hong et al. 2018; I. Rabago & J. H. Steffen 2019; X. Huang & D. Lai 2026). Tidally-induced migration in star-planet-moon systems (J. A. Alvarado-Montes et al. 2017), too, has the potential to trigger scattering events that destabilize and eject moons, with the efficiency of this process dictated by the system geometry and the host planet's tidal quality factor and Love number (A. Tokadjian & A. L. Piro 2020; M. Sucerquia et al. 2020; V. Dobos et al. 2021; E. Bolmont et al. 2025).

Furthermore, planet-planet scattering among wide-orbiting giant planets has been shown to efficiently eject planetary embryos (e.g. J. E. Chambers 2001; D. Veras & P. J. Armitage 2005; S. N. Raymond et al. 2005; T. Barclay et al. 2017), as well as planetesimals (e.g. S. N. Raymond et al. 2010; S. N. Raymond et al. 2011, 2012; F. Marzari 2014; S. N. Raymond et al. 2018; M. Rice & G. Laughlin 2019) that may contribute toward the high number density of free-floating interstellar objects inferred from recent detections (A. Do et al. 2018). These bodies would be ejected at a range of overlapping timescales: for example, planetary embryos would generally be ejected early in a system's lifetime, but they may heavily overlap in their mass distribution with moons that are commonly ejected alongside giant planets.

2.4.3. *The velocity distribution of FFPs*

Another observable that offers insight into the relative prevalence of FFP production mechanisms is the distribution of FFP excess velocities v_∞. The excess velocity is defined as

$$v_\infty = \sqrt{v^2 - v_{\rm esc,*}^2}, \tag{17}$$

where v is the velocity of the ejected planet at the distance where the body becomes unbound, and the escape velocity $v_{\rm esc,*}$ from the host star at that same position may be drawn from Equation 5.

X. Huang & D. Lai (2026) derived a useful expression for the critical velocity $v_{c,\rm 2pl}$ around which v_∞ is peaked for two-body scattering, provided as

$$v_{c,\rm 2pl} = \left(\frac{Gm_1}{0.12a_2}\right)^{1/2}\left(\frac{m_1}{m_1+m_2}\right)\left(\frac{a_1}{a_2}\right)^{1/4} \tag{18}$$

for two-planet systems with semimajor axes a_1, a_2 and planetary masses m_1, m_2. This expression was obtained by combining close-encounter-induced ejection rate estimates from B. Pu & D. Lai (2021) and J. Li et al. (2022) with principles of energy exchange. A comparable expression was also obtained by X. Huang & D. Lai (2026) for the critical velocity $v_{c,\rm 3pl}$ in the case of 3-body scattering, given as

$$v_{c,\rm 3pl} = \left(\frac{Gm_{\rm max}}{0.12a_3}\right)^{1/2}\left(\frac{m_{\rm max}}{m_{\rm max}+m_{\rm ejec}}\right)\left(\frac{a_1}{a_3}\right)^{1/4}. \tag{19}$$

Here $m_{\rm max}$ is the highest-mass planet in the system, while $m_{\rm eject}$ is the mass of the ejected planet and a_1, a_3 are the semimajor axes of the innermost and outermost planet, respectively. In both expressions, the critical velocity corresponds to the peak of a probability distribution of velocities, which has a larger width for systems with more constituent bodies.

Ejected planets from planet-planet scattering are predicted to have relatively low excess velocities < 10 km/s, with a median at $\approx 2-3$ km/s and lower excess velocities attained for planets ejected from larger initial semimajor axes (G. A. L. Coleman & W. DeRocco 2025; H. G. Bhaskar & H. B. Perets 2025; R. Zhai et al. 2025). Ejected planet-mass, self-gravitating fragments formed from gravitational instability, too, have comparably low expected excess velocities $\approx 4-5$ km/s (D. H. Forgan et al. 2018). H. G. Bhaskar & H. B. Perets (2025) showed that planets are typically ejected within 30° of the plane of the planetary system, such that their trajectories, in

addition to their velocities, may encode some information about their birth environments.

3. INSTABILITIES IN SYSTEMS WITH BOUND STELLAR COMPANIONS

Binary and multiple-star systems are ubiquitous across the galaxy: roughly half of sun-like stars host a bound stellar companion, with a higher occurrence of companions to higher-mass stars (A. Duquennoy & M. Mayor 1991; D. Raghavan et al. 2010; G. Duchêne & A. Kraus 2013; S. S. R. Offner et al. 2023). Planets in multi-star systems are susceptible to many of the same dynamical instability mechanisms that induce planetary ejection in single-star systems, such as planet-planet scattering and intra-system resonance overlap. In addition to these mechanisms, planets in binary systems may undergo further instabilities caused by perturbations from the companion star.

Exoplanets in multiple-star systems may be divided into two classes: circumstellar ("$s-$type," historically standing for "satellite-type") and circumbinary ("$p-$type," historically standing for "planet-type") planets (R. Dvorak 1984). Circumstellar planets (top center panel of Figure 1) orbit a single star in a binary or higher-multiplicity stellar system, such that these systems operate similarly to their single-star counterparts but with additional perturbations imposed by one or more additional, high-mass companions. Circumbinary planets (top right panel of Figure 1) instead orbit two stars[6] and therefore undergo qualitatively different evolutionary trajectories.

The three-body problem, including the circular restricted three-body problem that may be applied to planetary systems in certain cases—circular orbits and large mass ratios between the planet and stars—has an extensive history in astronomy. There have been correspondingly many studies of three-body systems' stability, spanning both analytic (e.g. V. Szebehely 1977, 1980) and numerical (e.g. M. Hénon & M. Guyot 1970; D. C. Black 1982; Y. J. Pendleton & D. C. Black 1983) results.

Many of these foundational studies impose stringent criteria on the orbit and mass-ratio regimes for their analyses, limiting their applicability to true systems. Therefore, we focus here on relatively general forms that account for orbital eccentricities and unequal stellar mass ratios, as are commonly observed in binary star systems (M. Moe & R. Di Stefano 2017; K. El-Badry et al. 2019; H.-C. Hwang et al. 2022).

We emphasize that instability is a necessary but not sufficient condition for planetary ejection. Many binary systems undergo instabilities that do not necessarily induce planetary ejection. Instabilities may instead lead to collisions with other planets or with stars within the system, or they may, in rare cases, introduce exchange reactions in which the planet becomes bound to a different star. Thus, we begin with an overview of instabilities in the context of potential planetary ejection, then discuss the implications of these instabilities for ejection rates.

3.1. *Instabilities of circumstellar planets in binary systems*

Of the possible configurations for circumstellar planets in non-single-star systems, circumstellar binaries are the most well-studied to date. This is likely in part due to their relative simplicity, and in part because they are the most commonly observed configuration to date for non-single-star planetary systems.

We divide instabilities in circumstellar binaries into two regimes: those most relevant for close binaries ($a \lesssim$ a few hundred au) where the instability limit is set by intra-system dynamics (Section 3.1.1), and those most relevant for very wide binaries ($a \gtrsim$ a few hundred au) where the instability limit is instead set by the influence of passing stars and the galactic tide (Section 3.1.2). The instability limits described in the "close stellar binaries" overview may also play an important role in high-eccentricity wide binaries with close periastron approaches.

3.1.1. *Circumstellar planets in close stellar binaries*

For circumstellar planetary orbits in close binary systems, there exists an outermost planetary semimajor axis for dynamical stability. Early derivations of this boundary were obtained through analytic approximations by V. Szebehely (1980) in the context of the planar, circular restricted three-body problem (enabling a wide range of binary mass ratios), as well as numerical calculations by G. Rabl & R. Dvorak (1988) for circular planetary orbits, equal-mass stars, and coplanar, eccentric planet-binary configurations. D. Benest (1988a,b, 1993) extended these frameworks to examine stability in the elliptic planar restricted three-body problem, including case studies of known binary systems.

M. J. Holman & P. A. Wiegert (1999) later conducted a large suite of numerical simulations in the elliptic restricted three-body problem—that is, with eccen-

[6] Note that we restrict this category to binary star systems, as over a dozen circumbinary planets have been found (e.g. L. R. Doyle et al. 2011; D. V. Martin et al. 2019; M. Thornton et al. 2026), whereas no planets have been confirmed encircling higher-multiplicity systems—though see J. L. Smallwood et al. (2021) for discussion of a tentative circumtriple planetary system in the GW Orionis system.

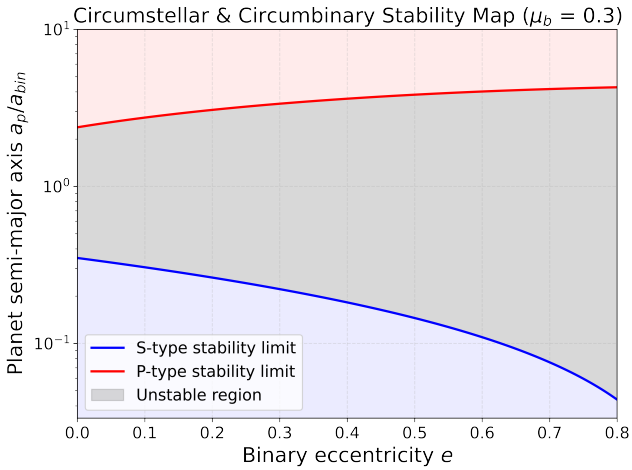

Figure 5. Example thresholds for $s-$type and $p-$type binary instabilities for stellar binary mass ratio $\mu_b = 0.3$, displayed as a function of the binary eccentricity and the ratio between the planet and binary semimajor axis. Boundaries are drawn directly from M. J. Holman & P. A. Wiegert (1999), provided in this work as Equations 20 and 21.

tric binary orbits and massless, test-particle planets—spanning 10^4 binary orbital periods and covering a range of binary separations and mass ratios. The commonly-adopted empirical formula for the outermost stable semi-major axis a_c derived by M. J. Holman & P. A. Wiegert (1999) is given as

$$\begin{aligned} a_c/a_b =&(0.464 \pm 0.006) + (-0.380 \pm 0.010)\mu_b \\ &+ (-0.631 \pm 0.034)e + (0.586 \pm 0.061)\mu_b e \\ &+ (0.150 \pm 0.041)e^2 + (-0.198 \pm 0.074)\mu_b e^2 \end{aligned} \tag{20}$$

where e is the binary eccentricity, a_b is the binary semi-major axis, and μ_b is the binary mass ratio. This stability limit is shown in blue in Figure 5 for a canonical binary mass ratio $\mu_b = 0.3$.

Notably, all planets were assumed to lie on circular orbits in M. J. Holman & P. A. Wiegert (1999). E. Pilat-Lohinger et al. (2002) built upon this work to consider eccentric planet orbits using the Fast Lyapunov Indicator method (C. Froeschlé et al. 1997), which rapidly identifies chaotic, unstable orbits. With this method, the authors numerically examined the stability of circumstellar planetary systems over 1000 binary orbital periods, demonstrating that planet eccentricity plays a minor role in setting stability relative to binary eccentricity. More recently, computational advances enabled an extensive new suite of ≈700 million $N-$body simulations that extended the expressions of M. J. Holman & P. A. Wiegert (1999) to non-coplanar orbits across the range of planetary orbital eccentricities (B. Quarles et al. 2020), considering integration times of 10^5 yr per system. B. Quarles et al. (2020) provide a series of new coefficients to Equation 20 for varying binary eccentricity (Table 3 of B. Quarles et al. (2020)) and planetary inclination (Table 4 of B. Quarles et al. (2020)), with interpolation maps for intermediate values.

Further studies have examined the stability of solar-system-like configurations in binary star systems, including a demonstration that a stellar companion supports planetary ejection during instabilities in the Jumping Jupiter model (F. Marzari et al. 2005), as well as a characterization of the planetary removal timescale within the instability region for Earth-like planets (E.-M. David et al. 2003).[7] M. Ávila-Bravo et al. (2026), too, carried out a suite of 2500 simulations following the 0.5-Gyr evolution of three giant planets on a circumstellar orbit with a stellar binary companion at $a = 50 - 1500$ AU, mapping the rate of planetary survivors as a function of binary properties. These contributions fold in the impact of neighboring planets and consider how planetary removal times scale with the periastron distance of the companion star.

L. R. Mudryk & Y. Wu (2006) applied semi-analytic models in the coplanar regime to provide useful intuition for the physical mechanisms underlying these numerically-characterized instability boundaries. Specifically, they showed that secular forcing is strong for planetary systems with nearby stellar companions, leading to significant overlap between subresonances of individual mean-motion resonances that triggers chaotic diffusion and planetary instability. L. R. Mudryk & Y. Wu (2006) demonstrated that, in practice, this leads to rapid ejection dominated by the influence of low-order resonances, with a jagged instability boundary as a function of eccentricity for a given mass ratio. This result remains in rough agreement with boundaries derived through orbital integrations, but demonstrates the more complex structure of the true stability boundary.

Most of this section has focused on instabilities in systems with fully-formed stars and fully-formed planets. However, in the presence of a growing stellar perturber, recent simulations have suggested that both Jovian-mass (A. Ćalović et al. 2026) and lower-mass (S. Nayakshin et al. 2026) planets formed through gravitational instability may be efficiently ejected through instabilities

[7] Note that the definition of "ejection" in E.-M. David et al. (2003) encompasses both planets that become unbound from the host star and planets that collide with the host star; hence, to avoid confusion we use the term "planetary removal" in this context.

with the neighboring, growing stars. Such planets would be expected to have low excess velocities around 1-3 km/s.

3.1.2. *Circumstellar planets in wide stellar binaries*

Over secular timescales, wide binaries may be perturbed to high orbital eccentricities through gravitational interactions with passing stars and the galactic tide (Y.-F. Jiang & S. Tremaine 2010), triggering orbital instabilities and planetary ejection. N. A. Kaib et al. (2013) simulated this scenario for systems hosting four solar-system-like giant planets and a wide, bound stellar companion at 1,000-30,000 AU separations, showing that $30-60\%$ of examined systems underwent at least one planetary ejection within 10 Gyr. J. A. Correa-Otto & R. A. Gil-Hutton (2017) extended this work to a broader set of wide binaries, excluding planets from their simulations but similarly finding that the widest (particularly $a > 10,000$ au) binaries and those with the highest orbital eccentricities ($e > 0.9$) have a high binary disruption rate that would potentially lead to corresponding planetary disruption.

Given the high rate of high-eccentricity wide binaries (H.-C. Hwang et al. 2022), this mechanism may serve as an important reservoir for FFPs. Indeed, E. Grishin et al. (2025) demonstrated that the ejection of giant planets from wide binary interactions with the galactic tide could account for $24^{+117}_{-15}\%$ of the population of free-floating Jovian-mass planets. This mechanism may contribute a significant subset of FFPs found at the high-mass end of the FFP mass function ($M_J \gtrsim$ a few M_J), where planet-planet scattering—which tends to liberate the lowest-mass planets present in systems—may efficiently remove planets only in the case of multi-super-Jupiter systems.

3.2. *Instabilities of circumbinary planets*

Well before the first circumbinary planetary system was discovered, numerical studies by R. Dvorak (1984) R. Dvorak (1986), and R. Dvorak et al. (1989) established that there exists a critical circumbinary separation—the innermost semimajor axis for stability—beyond which planetary orbits may remain stable. Using a large suite of numerical simulations, the location of this innermost semimajor axis a_c was empirically quantified by M. J. Holman & P. A. Wiegert (1999) as

$$\begin{aligned} a_c/a_b =&(1.60 \pm 0.04) + (5.10 \pm 0.05)e \\ &+ (-2.22 \pm 0.11)e^2 + (4.12 \pm 0.09)\mu_b \\ &+ (-4.27 \pm 0.17)e\mu_b + (-5.09 \pm 0.11)\mu_b^2 \\ &+ (4.61 \pm 0.36)e^2\mu_b^2 \end{aligned} \tag{21}$$

for systems of coplanar, circular orbits for binary semimajor axis a_b, binary mass ratio μ_b, and binary eccentricity e. This stability boundary is visualized in red in Figure 5 for a binary with mass ratio $\mu_b = 0.3$.

Later work that considered mutual inclinations between orbits demonstrated that islands of stability exist at high mutual inclinations for binaries on eccentric orbits. E. Pilat-Lohinger et al. (2003) applied numerical experiments to produce stability maps as a function of binary separation for planets that orbit equal-mass binaries at mutual orbital inclinations of up to $i = 50°$. This was followed by an analytic characterization of stability across binary orbital eccentricities and planetary inclinations, conducted by F. Farago & J. Laskar (2010) in the secular and quadrupolar approximations. Additional studies have demonstrated an island of stable libration toward polar orbits in circumbinary systems (S. Doolin & K. M. Blundell 2011; B. Quarles & J. J. Lissauer 2016; G. Li et al. 2016). While polar circumbinary planets have yet to be definitively detected, R. G. Martin et al. (2023) found that AC Herculis, which is a post-asymptotic giant branch star hosting a circumbinary disk, is consistent with this configuration.

More recent advances have extended this previous work by examining substantially larger-scale suites of numerical simulations (B. Quarles et al. 2018; N. Georgakarakos et al. 2024) and additional methods, such as deep neural networks (C. Lam & D. Kipping 2018). These approaches were leveraged to more thoroughly delineate the parameter space for stability in circumbinary planetary systems, including islands of stability that are not well-captured by the polynomial form of Equation 21.

3.3. *Planetary orbital instabilities in multi-star systems*

While most non-single-star stability studies to date have focused on binaries, planets may similarly undergo orbital instabilities in triple-star or higher-order systems. There are many possible configurations of planetary orbits in such systems, including both $s-$type and $p-$type orientations.

A few systematic studies have considered such systems. P. E. Verrier & N. W. Evans (2007) characterized the stability zones for planets within low-inclination hierarchical triple-star systems, demonstrating that the empirical results from M. J. Holman & P. A. Wiegert (1999) hold for triple-star systems with relatively low orbital eccentricities and sufficiently wide-orbiting, low-mass stars. F. Busetti et al. (2018) later applied $N-$body simulations to more extensively map plane-

tary stability in triple-star systems, considering both prograde and retrograde planetary configurations.

3.4. *Predictions and implications: instabilities in systems with bound stellar companions*

Orbital instabilities in binary and multi-star systems do not always lead to planetary ejection. Instead, they may result in planetary or stellar collisions, or in some cases capture into different orbits: for example, a planet in a circumbinary orbit may be captured into a circumstellar orbit.

Despite the extensive history of numerical simulation studies examining these systems, the distribution of these outcomes has not, to the authors' knowledge, been explicitly reported for binary systems with circumstellar planets. Instead, the systems are typically grouped only as "stable" vs. "unstable", without explicitly parsing the outcomes of the unstable systems. In circumbinary systems, by contrast, these outcomes have been explicitly traced and reported for some simulation suites.

R. A. Smullen et al. (2016) considered a range of planet populations and binary configurations to demonstrate that, for various initial condition parameterizations in the literature, instabilities in circumbinary star systems tend to lead to ejection within 10 Myr, with ejections occurring at a far higher rate (typically $\approx 50-70\%$) than in single-star systems (typically $\approx 25-50\%$). A. P. Sutherland & D. C. Fabrycky (2016) similarly conducted a numerical study of planets on tight (1-4 au) circular orbits in circumbinary systems with unequal stellar masses ($M_2/M_1 = 0.1$) and binary semi-major axis 1 AU, finding that roughly 80% of unstable systems culminated in planetary ejection—with higher-eccentricity stellar binaries taking longer on average to eject planets. A small but nonzero percent of unstable systems in this simulation suite ($0.16 \pm 0.06\%$) had the unstable planet captured into orbit around the secondary star.

Intuition for the outcomes of instability in circumbinary systems may be gained through examining the circular restricted three-body problem (see e.g. V. Szebehely & R. McKenzie 1981). For a three-body system setup with $m_1 > m_2$ and $m_1, m_2 \gg m_3$, as well as circular orbits, the Jacobi constant C_J is conserved, given as

$$C_J = 2n(x\dot{y} - y\dot{x}) + 2\left(\frac{\mu_1}{r_1} + \frac{\mu_2}{r_2}\right) - (\dot{x}^2 + \dot{y}^2 + \dot{z}^2) \quad (22)$$

for positions (x, y, z), velocities $(\dot{x}, \dot{y}, \dot{z})$, binary mean motion n, and parameterized masses $\mu_1 = Gm_1$ and $\mu_2 = Gm_2$. In this regime, zero-velocity curves may be calculated for a given C_J. R. A. Smullen et al. (2016) demonstrated that scattering is the only possible outcome for Jacobi constant $C_J > 3.46$; that is, collisions may not occur for $C_J > 3.46$. A wide swath of the instability region of circumbinary planets satisfies this condition, such that most systems that undergo instabilities in circumbinary systems are expected to undergo ejection, rather than collisions.

Using a combined disk evolution and $N-$body model designed to simulate the outcomes of core-accretion planet formation, G. A. L. Coleman (2024) found that free-floating planets ejected from circumbinary interactions have relatively high excess velocities 8-12 km/s, with velocity dispersions that are substantially higher ($\approx 3\times$ larger) than those of free-floating planets ejected from planet-planet interactions. M. Teasdale & D. Stamatellos (2026) simulated the process of disk fragmentation around circumbinary systems and found that orbital instabilities among the resulting population of planets—formed beyond 50 AU, and with a typical separation of 100 AU—would produce free-floating planets with lower ejection velocities, potentially making them more difficult to distinguish from planets ejected from scattering in single-star systems. Some giant ($\approx 10M_J$) planetary-mass objects have been found on such wide circumbinary orbits (J. L. Christiansen et al. 2025), though their prevalence at a demographic level is currently not well-constrained.

Follow-up population synthesis work by G. A. L. Coleman & W. DeRocco (2025) showed that instabilities in circumbinary systems may account for most of the inferred census of ejected high-mass ($> 1M_\oplus$) FFPs. G. A. L. Coleman & W. DeRocco (2025) offered quantitative predictions for the number density of ejected planets derived from orbital instabilities in single and binary star systems as a function of planet mass. Their results suggest that planetary ejection across the galactic population of stars should produce a trough in the mass distribution at roughly $0.8M_\oplus$—between the relatively high rate of very low-mass planets and the pebble isolation mass peak near $8M_\oplus$, above which fewer planets form and the number density of ejected planets turns back over.

Last, the relevance of an unstable region for planetary ejection implicitly relies on the formation or migration of planets into that region during the system lifetime. Do planets form or arrive in unstable regions in the first place? If planet formation is ubiquitous across wide swaths of parameter space in planetary systems, including these unstable regions, then large populations of FFPs may be produced through such instabilities. Otherwise, the census of ejected planets from such binaries may be much lower.

4. FLYBY-INDUCED EJECTIONS

Beyond intra-system dynamics, planets may also be dislodged from their primordial systems through dynamical interactions with passing neighbors that are not bound to the host star. A planet may be ejected from its host system in the case that the energy injected from the flyby perturber (or from the cumulative gravitational assists from several perturbers) overcomes the gravitational potential energy binding the planet to its host star.

An extensive set of literature exists both analytically and numerically constraining the outcomes of flyby interactions for a planetary system (e.g. D. C. Heggie 1975; J. G. Hills 1984; J. G. Hills & R. W. Dissly 1989; D. C. Heggie & F. A. Rasio 1996; F. C. Adams & G. Laughlin 2001; D. Malmberg et al. 2011; G. Li & F. C. Adams 2015; G. Brown & H. Rein 2022; N. A. Kaib & S. N. Raymond 2025). We do not attempt to provide a comprehensive overview of all possible outcomes of these flybys here. Instead, we focus on the occurrence of such encounters and relevant implications for planetary ejections. A useful overview of the relevant analytic formulae for the change in eccentricity and binding energy to two-body systems caused by flyby encounters is provided in Appendix A of R. Spurzem et al. (2009), which also draws upon prior results from D. C. Heggie (1975); D. C. Heggie & F. A. Rasio (1996); A. Roy & M. Haddow (2003); D. C. Heggie (2006).

In this section, we provide an overview of the expected rates of planetary ejection through close encounters with other stars and planets in the galaxy. We consider specific predictions for environments at a range of stellar densities.

4.1. *Flyby occurrence rates*

In general, the occurrence rate of stellar flyby interactions Γ may be estimated as

$$\Gamma = \langle n_* \rangle \sigma \langle v \rangle, \tag{23}$$

where $\langle n_* \rangle$ is the local mean stellar density, σ is the cross-section of interaction, and $\langle v \rangle$ is the mean relative velocity between stars. As shown by this expression, planetary systems in dense stellar environments (high $\langle n_* \rangle$) and hosting wide-orbiting planets (large σ) are most susceptible to disruption by stellar flybys and subsequent planetary ejection. We show a mapping of Γ as a function of stellar density and velocity dispersion in Figure 6 for two example planetary orbit cross-sections.

4.2. *Cross-sections for flyby interactions*

At first glance, it may appear that the cross-section of interaction for a planetary system on a circular orbit would correspond to πa^2 for a given semimajor axis a: the system's geometric cross-section. This is not, however, generally the case due to the influence of gravitational focusing.

Gravitational focusing, which describes how the gravitational influence between two bodies affects the effective cross-section for interaction, gives

$$\sigma = \pi a^2 \left(1 + \frac{v_{\rm esc,*}^2}{v_i^2}\right) \tag{24}$$

as the cross-section for a star interacting with a planet with semimajor axis a. Here v_i is the relative speed of encounter between the two systems, which for stellar flybys may be estimated as the velocity dispersion $v_{\rm disp}$ of the background stellar population, while $v_{\rm esc,*}$ is the escape velocity from the planet's orbit around its host star. We note that this formalism applies specifically for close approaches to individual planets' orbits, whereas flybys at more distant close approaches may still significantly perturb the system. This formalism is conceptually very similar to that of the Safronov number Θ introduced in Section 2.1.1, which was originally derived through the framework of gravitational focusing to characterize the efficiency of planetesimal accretion (V. S. Safronov & E. V. Zvjagina 1969).

Equation 5 shows that the escape velocity from the stellar system scales as $v_{\rm esc,*} \propto 1/\sqrt{r}$, which can be approximated as $v_{\rm esc,*} \propto 1/\sqrt{a}$ for near-circular orbits. Combining this escape velocity with Equation 24 reveals that the cross-section for flyby interactions scales with the planetary semimajor axis as $\sigma \propto a$ for $(v_{\rm esc,*}^2/v_i^2) \gg 1$. This criterion is typically satisfied in open clusters, which have $v_{\rm disp} \approx 1$ km/s, and for relatively short-period planets in globular clusters, with a higher typical velocity dispersion $v_{\rm disp} \approx 10$ km/s (for comparison, $v_{\rm esc,*} = 42, 19$, and 8 km/s at Earth's, Jupiter's, and Neptune's orbit). G. Li & F. C. Adams (2015) verified this result through numerical simulations and demonstrated that the cross-section for disruption of a given planet's orbit is nearly independent of that of neighboring planets in the system.

Field stars in the local solar neighborhood have typical relative velocities $v_{\rm disp} \approx 30 - 40$ km/s (B. Nordström et al. 2004) such that the approximation $(v_{\rm esc,*}^2/v_i^2) \gg 1$ breaks down particularly for wide-orbiting planets. In environments with very high velocity dispersions, such as the Milky Way bulge ($v_{\rm disp} \approx 120$ km/s) and core ($v_{\rm disp} \approx 170$ km/s), gravitational focusing plays a less dominant role and the geometric cross-section πa^2 is a more appropriate choice.

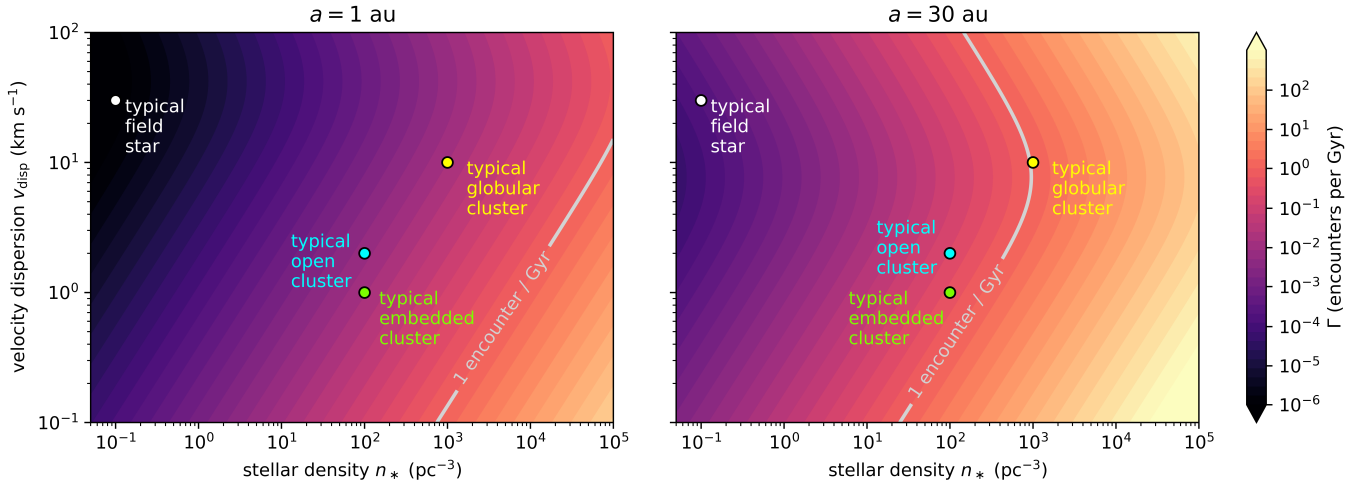

Figure 6. Flyby rates Γ as a function of stellar density and velocity dispersion. Representative values for example stellar environments are shown alongside a reference line tracing the threshold for one flyby encounter per Gyr. We visualize two cases, for a planetary orbit with $a = 1$ AU and another with $a = 30$ AU. Wide-orbiting planets are much more susceptible to disruption by flybys than shorter-period planets due to their larger cross-sections for interaction.

4.3. *Potential outcomes from stellar flyby interactions*

Depending on the timing of a flyby in the planetary system's evolution, as well as the relative masses and geometries of the flyby and planetary system, stellar flybys may result in several possible destabilizing outcomes. The implications of stellar flybys for planetary ejection have been examined in a range of contexts, including the solar system (G. Laughlin & F. C. Adams 2000; J. K. Zink et al. 2020; G. Brown & H. Rein 2022; S. N. Raymond et al. 2024; N. A. Kaib & S. N. Raymond 2025) and extrasolar systems (e.g. G. Laughlin & F. C. Adams 1998; D. Malmberg et al. 2011; G. Li & F. C. Adams 2015; F. Yu & D. Lai 2024). Frequent stellar flybys in dense environments have observable implications for lower-mass bodies, as well, producing a significant population of ejected planetesimals that become interstellar objects (T. O. Hands et al. 2019; S. Pfalzner et al. 2021).

In stellar clusters, binary star systems may become unbound through either individual nearby encounters or through a more gradual process of "evaporation", in which bound objects are driven above the cluster's escape velocity by distant, weak encounters. Transposing these mechanisms to the planetary regime, C. de la Fuente Marcos & R. de la Fuente Marcos (1999) showed that the evaporative process of ejection, while prevalent in binary star systems, is negligible for planets in single-star systems. Instead, using a series of N-body simulations, they found that planetary ejection in star clusters may occur through multi-star interactions that temporarily produce hierarchical triple or quadruple systems. This has the potential to launch newly unbound planets to velocities typically < 25 km/s, with a small tail toward much higher values (up to 120 km/s in the examined simulations).

Close stellar flybys ($\lesssim 100$ au) may induce the immediate ejection of neighboring planets or destabilize a system, leading to rapid ejection soon after the flyby event (J. G. Hills 1984). In some cases, close flybys with low-mass stars or brown dwarfs may lead to an exchange interaction in which the planet becomes bound to the intruder (D. Malmberg et al. 2011).

More distant stellar flybys tend to excite the orbital eccentricities and inclinations of planets that are left bound, with the most pronounced effect on the widest-orbiting planets in a system (D. Malmberg et al. 2011; M. X. Cai et al. 2018; D. Li et al. 2019; E. A. Ellithorpe & N. A. Kaib 2022; H. Rickman et al. 2023). Eccentricity and inclination disturbances for wide-orbiting planets propagate inward through the system through secular planet-planet interactions (N. L. Zakamska & S. Tremaine 2004), altering the orbits of closer-in planets. This reduces the timescale of orbital instabilities and planet-planet scattering, indirectly triggering planetary ejection over Myr to Gyr timescales (e.g. A. C. Boley et al. 2012). Orbital excitation that occurs while the protoplanetary disk is still present may, however, be efficiently erased due to planet-disk interactions (F. Marzari & G. Picogna 2013; G. Picogna & F. Marzari 2014). As a result, the long-term impact of dynamical excitation from stellar flybys is most pronounced post-disk-dispersal.

In rare cases with favorable orientations, a passing star with a close, edge-on encounter may induce the simultaneous ejection of two giant planets, producing Jupiter-mass binary objects (Y. Wang et al. 2024). While

such encounters are likely not common in the local solar neighborhood due to the low rate of close stellar encounters, the occurrence of such events may reach up to a few percent for initially wide-orbiting planetary systems residing in dense stellar clusters. Empirical upper limits on the occurrence of this mechanism may be placed by imaging surveys sensitive to binary planetary-mass objects (e.g. H. Bouy et al. 2026). Importantly, however, many such objects may have been formed *in situ*—through direct collapse—rather than through flyby-induced ejection (see Section 6.1 for further discussion).

4.4. *Substellar object flybys*

Close flyby encounters with substellar objects (that is, free-floating brown dwarfs and planets) may also lead to the disruption of planetary orbits, as well as subsequent planetary ejection. Direct disruptions occur at a rate that can be calculated using an equivalent formalism to that presented in Equation 23, but with the local mean stellar density and relative velocity replaced with the relevant values for free-floating substellar objects, rather than stars. In the presence of an underlying population of FFPs, close encounters between FFPs and bound planetary systems may dislodge additional planets or induce orbital instabilities, further growing the FFP population.

G. Brown et al. (2025) examined this scenario in the context of the solar system's mutual inclination and eccentricity excitation, finding from a suite of numerical simulations that close substellar object flybys often result in planetary ejection and could contribute $10^7 - 10^8$ free-floating planets ejected from the roughly 10^{10} sun-like star systems in the galaxy, assuming solar-system-like architectures. S. N. Raymond & N. A. Kaib (2026) considered a similar range of parameters to demonstrate that the flyby of a substellar object could have triggered a dynamical instability among the giant planets in the early solar system, finding a $\approx 1 - 5\%$ chance of this scenario depending on the adopted occurrence rate of free-floating planets.

The production of FFPs serves as a feedback loop that may enable the further production of FFPs. However, current projected rates of planetary ejection caused by substellar object flybys are relatively low: with only 1% of sun-like stars having planets directly ejected through substellar object flybys, direct ejection through this mechanism likely does not play a major role in the total rate of FFP production. An enhanced instability rate from substellar object flybys offers an indirect avenue to increase the rate of planetary ejection through substellar object flybys, which may ultimately induce planet-planet instabilities. This rate, too, is limited by the occurrence of free-floating planets required for such encounters.

4.5. *Predictions and implications: flyby encounters*

The projected contribution of flyby encounters in producing FFPs varies significantly with stellar environment. The stellar density and velocity dispersion, each of which varies dramatically across the birth cycle and environment of a star, play an important role in setting the occurrence of stellar flybys, as can be seen through examination of Equation 23. Therefore, we consider predictions for planetary ejection specifically in stellar cluster environments due to their relatively high stellar densities, focusing on embedded clusters (Section 4.5.1), evolved open clusters (Section 4.5.2), and globular cluster environments (Section 4.5.3).

4.5.1. *Predictions and implications: flybys in embedded clusters*

Stars are generally born in embedded clusters within molecular clouds, which are relatively high-density environments (typically $10^2 - 10^3$ stars pc^{-3}; C. J. Lada & E. A. Lada 2003). As a result, young stars experience a relatively high rate of stellar encounters that may trigger planetary ejection.

In embedded cluster environments, protoplanetary disks may be truncated, warped, or destroyed by flyby encounters (C. J. Clarke & J. E. Pringle 1993; A. Scally & C. Clarke 2001; F. C. Adams et al. 2006; M. M. Fragner & R. P. Nelson 2009; D. Forgan & K. Rice 2009; J. Craig & M. R. Krumholz 2013; G. P. Rosotti et al. 2014; X. Zheng et al. 2015; N. Cuello et al. 2020, 2023) and photoevaporation caused by Far Ultraviolet (FUV) and Extreme Ultraviolet (EUV) flux from nearby, high-mass stars (H. Störzer & D. Hollenbach 1999; P. J. Armitage 2000; A. Scally & C. Clarke 2001; F. C. Adams et al. 2004; A. J. Winter et al. 2018; R. J. Parker et al. 2021; A. J. Winter & T. J. Haworth 2022), potentially suppressing the planet formation process. F. C. Adams et al. (2006) and E.-M. Proszkow & F. C. Adams (2009) each found that these external effects should not prevent the formation of solar-system-like architectures in typical embedded clusters, though Jovian-mass planet formation may be suppressed in environments with the highest stellar densities ($\rho \gtrsim 10^4 M_\odot$ pc^{-3}; E. C. Daffern-Powell & R. J. Parker 2022).

For environments in which giant planets are born, those residing in multiplanet systems and on the widest orbits are most susceptible to ejection. G. Laughlin & F. C. Adams (1998) found that Jupiter analogs commonly have their orbits disrupted by flyby interactions with binary star companions in their natal clusters, with

roughly 5% of such planets ejected over the course of 100 Myr. For solar-system-like architectures, with four gas giants, planetary ejection in embedded clusters occurs at a higher rate over the same timescale (5-15%; D. Malmberg et al. 2007) due to the combined influence of direct ejection and orbital-instability-inducing eccentricity excitation within multiplanet systems (see also W. Hao et al. 2013). Wider-orbiting giant planets at 10-100 AU may be ejected at much higher rates of up to tens of percent in embedded cluster environments (R. J. Parker & S. P. Quanz 2012; W. Hao et al. 2013; M. S. Fujii & Y. Hori 2019).

Lower-mass planets may also be ejected through flybys in embedded clusters. S. Chatterjee et al. (2012) considered the stability of *Kepler*-detectable systems in open clusters, demonstrating that the short-period population of exoplanets accessible to the transit method should not generally be directly disrupted via cluster dynamics—though eccentricity excitation combined with planet-planet scattering may play an important indirect role in ejection rates. By comparing simulations of multi-Jupiter and multi-Earth systems at separations ranging from roughly 1-200 AU, M. X. Cai et al. (2017) found that lower-mass wide-orbiting planetary systems have consistently higher survival rates, likely associated with their longer instability timescales (see e.g. Section 2.1.2). In the case that every star forms with several planets spanning a wide range of masses and separations set by the E. Kokubo & S. Ida (1998) oligarchic growth model, A. van Elteren et al. (2019) found that flyby encounters in embedded clusters may produce 0.24-0.70 free-floating bodies per main-sequence star, spanning a wide mass range (0.01-130M_J; mean mass 1.4M_J) that includes and extends beyond the planetary regime.

4.5.2. *Predictions and implications: flybys in evolved open clusters*

After leaving their natal molecular clouds, many stars remain in loosely bound, lower-density ($\leq 10^2$ stars pc^{-3}) open clusters that slowly disperse through dynamical interactions with passing stars and the galactic tide. I. A. Bonnell et al. (2001) performed simulations of these older open cluster environments with a fiducial velocity dispersion of 2 km/s, which they used to show that planets with orbital separations < 10 AU generally survive disruption by stellar encounters in open clusters over their lifetimes ($\approx$1 Gyr). As such, only the widest-orbiting planets are likely ejected directly from stellar encounters in evolved open clusters. Giant exoplanets in evolved open clusters have been discovered with the radial velocity (A. Brucalassi et al. 2014; L. Malavolta et al. 2016) and transit methods (S. Meibom et al. 2013; A. W. Mann et al. 2016), all well interior to this orbital separation (at least in part due to limitations of these detection methods and available observational baselines).

Using Runge-Kutta orbital integrations in the restricted 3-body limit, K. W. Smith & I. A. Bonnell (2001) found a relatively high typical velocity of of planets liberated from equal-mass binary star systems in open clusters, peaking at around 6 km/s. Later N-body simulations by J. R. Hurley & M. M. Shara (2002), examining the ejection of Jupiter-sized planets, found a lower typical velocity of roughly 2 km/s, potentially due to their use of unequal-mass binaries and system masses following the more observationally-driven initial mass function (IMF) of P. Kroupa et al. (1993).

4.5.3. *Predictions and implications: flybys in globular clusters*

Globular clusters are high-density stellar environments with mean densities of 10^3 stars pc^{-3} and densities of up to $10^4 - 10^6$ stars pc^{-3} in their cores. While their specific formation mechanisms remain under debate, the Milky Way's globular clusters are classically thought to have originated through major mergers of disk galaxies, multiphase in situ collapse with highly efficient star formation early in the galaxy's history, and/or the accretion of dwarf galaxies (J. P. Brodie & J. Strader 2006). The extreme birth conditions of globular clusters enabled them to survive to the present-day despite their formation 10-13 Gyr in the past, whereas open clusters typically disperse well within 1 Gyr (C. J. Lada & E. A. Lada 2003).

Given the elevated stellar encounter rates of such high-density environments, S. Sigurdsson (1992) found that planets in globular clusters would typically be rendered unstable over the ages of their host systems, though follow-up work showed that planets on tight orbits ($a \lesssim 0.3$ au) or those in less dense parts of globular clusters may more easily survive (M. B. Davies & S. Sigurdsson 2001). I. A. Bonnell et al. (2001) modeled planetary ejection in globular cluster environments, adopting a fiducial velocity dispersion of 10 km/s and showing that planets with $a \gtrsim 1$ AU for stellar densities $> 10^3$ stars pc^{-3}, or $a \gtrsim 0.1$ AU for denser environments with $> 10^4$ stars pc^{-3}, are typically ejected within the age of the globular cluster. A. S. Hamers & S. Tremaine (2017) more recently showed that orbital eccentricity excitation from frequent flybys in globular clusters commonly induces planetary ejection in some systems while triggering high-eccentricity migration toward tightly bound, close-in orbits in others, providing a candidate hot-Jupiter formation pathway.

An important underlying requirement for FFP production through stellar encounters is that planets must first form within the systems of interest. Very few exo-

planets have been detected in globular clusters despite targeted searches (R. L. Gilliland et al. 2000; V. Nascimbeni et al. 2012), though the true implications for the occurrence of such planets remain under debate (e.g. V. Nascimbeni et al. 2012; K. Masuda & J. N. Winn 2017). Planets and planet candidates that have been found include the PSR B1620-26 b circumbinary planet (S. E. Thorsett et al. 1993; Z. Arzoumanian et al. 1996; S. Sigurdsson et al. 2003) as well as the M62H planetary-mass companion (though its high density, $\rho = 11$ g cm^{-3}, at a mass of a few Jupiter masses places its planetary nature in question; L. Vleeschower et al. (2024)), both orbiting pulsars.

An absence of detected planets could be interpreted as a natural outcome of rampant instabilities, or it could instead be indicative of formation limitations. In the case of globular clusters, the latter interpretation is supported by evidence from the demographic properties of single-star systems residing outside of globular cluster environments. Globular clusters are comprised of very low-metallicity stars, and demographic surveys for planets around similarly metal-poor stars in other environments have thus far discovered few to no planets (D. A. Fischer & J. Valenti 2005; K. M. Boley et al. 2024). This suggests that the conditions for planet formation may not be as easily met in globular cluster environments.

As introduced in Section 4.5.1, in cluster environments protoplanetary disks may be substantially truncated by photoevaporation from neighboring high-mass stars and tidal encounters from close flybys, which could suppress planet formation from its early stages. I. A. Bonnell et al. (2001) found that stellar densities must be relatively high, at $\gtrsim 10^4 - 10^5$ stars pc^{-3}, for disruptive disk encounters to occur within typical timescales for planet formation. These conditions are possible for young globular clusters, such that planet formation may be suppressed in these environments.

In the case that planets do form regularly in globular clusters, how would the resulting FFPs be distinguished? K. W. Smith & I. A. Bonnell (2001) mapped the velocity distributions of FFPs produced through ejection in globular clusters, demonstrating that they would typically have higher velocities ($11 - 12$ km/s) by comparison with FFPs ejected from open clusters. K. Kremer et al. (2019) carried out $N-$body simulations to show that up to 2×10^7 FFPs may be produced in the Galactic halo due to dynamical encounters and tidal loss in globular clusters, assuming that 10-50% of stars in globular clusters begin with planets. This population of FFPs, while small relative to the full population, may be distinguished through its differing galactic distribution: most other mechanisms would produce FFPs primarily originating in the galactic plane, whereas globular-cluster-produced FFPs should instead follow the spherically isotropic distribution of globular clusters that populate the galactic halo.

4.5.4. *How often do planets remain bound to the host cluster after being liberated from their host star?*

After they become unbound from their host star, cluster-ejected planets may either remain within their natal cluster or join the underlying population of FFPs within the galaxy, unbound from any stellar system. J. R. Hurley & M. M. Shara (2002) demonstrated that ejected planets may be liberated from dense cluster environments relatively slowly after being ejected from parent star systems toward the core of the cluster, drifting outward on timescales of 0.1-1 Gyr before joining the field population of FFPs. R. Spurzem et al. (2009) similarly found that FFPs in clusters do not exit immediately; in their $N-$body cluster simulations, only $\approx 10\%$ of FFPs typically escaped the cluster after a simulation time spanning a few million encounters between bound planets and passing stars. L. Wang et al. (2015) showed that planets liberated from their host cluster experience dozens of close encounters within 1000 AU prior to escape from the cluster's potential well, in some cases further perturbing bound systems or resulting in re-capture by another star.

R. J. Parker & S. P. Quanz (2012) found that roughly 30% of ejected Jovian-mass planets in their simulations become unbound from the birth cluster within 10 Myr. Planets that escape the cluster have relatively high velocities $5 - 10$ km/s, with lower velocities for planets ejected from wider orbits (30 AU orbits vs. 5 AU orbits in R. J. Parker & S. P. Quanz (2012)). X. Zheng et al. (2015) later applied $N-$body simulations to map out the range of outcomes from planetary disruption in cluster environments, showing the distribution of not only FFPs bound and unbound to the cluster, but also of star-planet systems that remain bound vs. ejected from the cluster. While some FFPs are ejected immediately and others remain bound longer in dispersing embedded clusters, all ejected FFPs in dispersing clusters ultimately become part of the background galactic population over $\approx$10 Myr timescales.

Within stellar clusters, how are FFPs radially distributed? F. Flammini Dotti et al. (2025) and F. Flammini Dotti et al. (2026) applied $N-$body simulations to show that ejected low-mass bodies, such as planets and free-floating comets in clusters, should not undergo observable mass segregation in clusters in the same way that higher-mass bodies such as brown dwarfs and stars do. This implies that the population of FFPs that re-

main bound to a cluster would be potentially detectable throughout the cluster.

5. POST-MAIN-SEQUENCE PLANETARY EJECTION

As a host star loses mass, the orbital properties of its surrounding planetary system correspondingly shift, in some cases making systems more susceptible to or directly inducing planetary ejection. In this section we consider how planetary orbits evolve in post-main-sequence systems, focusing on the implications for planetary ejection in two limits.

The first of these is slow, adiabatic mass loss, as during the asymptotic giant branch (AGB) phase of stellar evolution. The second is effectively instantaneous mass loss, appropriate to describe planetary evolution during the explosion of a Type II (core-collapse) supernova when the host star exhausts its fuel and undergoes runaway gravitational collapse that causes the star to explode. We note that the impulsive regime examined in this work may also be applicable for other cases in which the orbital period far exceeds the mass-loss timescale, such as the evolution of some Oort cloud objects during the tip of the red giant branch. More detailed discussion of post-main-sequence orbital evolution may be found in the review by D. Veras (2016).

5.1. *The general variable-mass two-body problem*

Where mass loss is assumed to be isotropic, the equations of motion in the variable-mass two-body problem are quantified as (T. B. Omarov 1962; J. D. Hadjidemetriou 1963; A. Deprit 1983; L.-S. Li 2008; D. Veras et al. 2011; G. Voyatzis et al. 2013)

$$\mu \equiv M_* + M_p \tag{25}$$

$$\frac{da}{dt} = -\frac{a(1+e^2+2e\cos f)}{1-e^2}\frac{1}{\mu}\frac{d\mu}{dt} \tag{26}$$

$$\frac{de}{dt} = -(e+\cos f)\frac{1}{\mu}\frac{d\mu}{dt} \tag{27}$$

$$\frac{di}{dt} = \frac{d\Omega}{dt} = 0 \tag{28}$$

$$\frac{d\omega}{dt} = \frac{d\varpi}{dt} = -\frac{\sin f}{e}\frac{1}{\mu}\frac{d\mu}{dt} \tag{29}$$

$$\frac{df}{dt} = -\frac{d\varpi}{dt} + \frac{n(1+e\cos f)^2}{(1-e^2)^{3/2}}. \tag{30}$$

These expressions describe the evolution of the orbit of a planet with mass M_p orbiting a star with mass M_*, where M_* is changing to produce a nonzero $d\mu/dt$. Here i is the planetary orbital inclination, ω is the argument of periastron, ϖ is the longitude of periastron, Ω is the longitude of ascending node, f is the true anomaly, and n is the mean motion $2\pi/P$ for orbital period P. The more general case of anisotropic and time-dependent mass loss was examined in D. Veras et al. (2013) (see Equations 34-38 in their work), which showed that the anisotropic terms' contributions scale as $\sqrt{a}$.

5.2. *The mass-loss index* Ψ

For a constant mass-loss rate α, the regimes of behavior may be described through a dimensionless "mass-loss index" Ψ introduced by D. Veras et al. (2011) as

$$\Psi \equiv \frac{\alpha}{n\mu}. \tag{31}$$

Here $n = 2\pi/P$ again corresponds to the planet's mean motion for orbital period P, while μ is the summed system mass (Equation 25). The mass-loss index quantifies the relative timescales between the planet's orbital period and the rate of stellar mass loss. Where $\Psi \ll 1$ a system falls into the adiabatic regime, in which the planet's orbital period is much shorter than the mass-loss timescale. For effectively instantaneous mass loss in the impulse approximation, $\Psi \to \infty$.

5.3. *Direct ejection from slow mass loss*

We first consider the evolution of an individual planet's orbit in the slow, adiabatic mass-loss regime—where the orbital period is significantly shorter than the mass-loss timescale. In this scenario, the planet's eccentricity remains roughly constant as the semimajor axis grows and the orbit gradually widens. The periastron q increases monotonically with mass loss as (D. Veras et al. 2011)

$$\frac{dq}{dt} = -\frac{a(1-e)(1-\cos f)}{1+e}\frac{1}{\mu}\frac{d\mu}{dt}, \tag{32}$$

which can be used to determine whether a planet's orbit is expanding more quickly than the radius of the stellar envelope. This can also be seen in Figure 2 of D. Veras et al. (2011), which shows a sample orbital evolution trajectory in the adiabatic regime.

Eventually, the widening orbit's period becomes comparable to the mass-loss timescale ($\Psi \approx 1$), transitioning the orbital evolution out of the adiabatic regime. When this transition takes place, df/dt begins to librate rather than circulating as in the adiabatic regime, introducing rapid, runaway evolution of the orbital eccentricity and semimajor axis. The range of possible behavior is described in detail throughout D. Veras et al. (2011), and we refer the reader to this work for a more in-depth

overview. Here we describe only certain orbital limits to provide insight into the qualitative behavior of systems transitioning out of the adiabatic regime.

Where f begins close to 0° or 180° and $\Psi \gg 1$, libration in the true anomaly is small and thus f can be treated as effectively constant. For $f = 0°$, this runaway is characterized as

$$e_{\rm runaway}|_{f=0°} = e_0 \frac{\mu_0}{\mu} + \left(\frac{\mu_0}{\mu} - 1\right) \tag{33}$$

$$a_{\rm runaway}|_{f=0°} = \frac{a_0(1-e_0)}{2 - \frac{\mu_0}{\mu}(1+e_0)} \tag{34}$$

for initial semimajor axis a_0, initial eccentricity e_0, and initial summed mass μ_0. In this regime, the eccentricity increases until the planet is ejected.

At the other extreme where $f = 180°$, the orbital eccentricity instead decreases toward $e = 0$. Once the orbit has circularized, $|d\varpi/dt|$ grows and forces df/dt to a nonzero value, changing f such that the planet's orbit lands on another evolutionary track. df/dt is nonzero for all true anomalies other than $f = 0°$, such that the value of f will continue to change until the system reaches $f = 0°$, the eccentricity reaches the runaway growth track, and the planet is ultimately ejected.

5.4. *Direct ejection in the impulse approximation*

We also consider the fast mass-loss limit in which all mass is lost instantaneously, corresponding to the impulse approximation. In this regime, $\Psi \to \infty$. The change in stellar mass from the initial value μ_i to the final value μ_f is characterized by the multiplicative factor β, given as

$$\mu_f = \beta \mu_i \tag{35}$$

for $0 < \beta \leq 1$. In the impulse approximation, D. Veras et al. (2011) showed that a planet is ejected in the case that

$$\beta < \frac{1 + e_0^2 + 2e_0 \cos f_0}{2(1 + e_0 \cos f_0)} \tag{36}$$

where initial eccentricity is e_0 and initial true anomaly is f_0.

We can see from Equation 36 that, for $e_0 = 0$ and the limiting case $\cos f_0 \to 0$, more than half of the stellar mass must be lost instantaneously to eject a planet. For highly eccentric planets, depending on the true anomaly the planets may be more or less readily ejected from the system. Systems that most easily survive lie on highly eccentric orbits with $f_0 \approx 180°$. Maps of the parameter space for bound and ejected planets are shown in Figure 7 for three example β values.

5.5. *Post-main-sequence planetary close encounters*

The orbital shifts induced by stellar evolution, in either the adiabatic regime or the impulse approximation regime, have the potential to trigger instabilities by pushing planetary orbits toward close approaches. As a result, the same planet-planet scattering instabilities described in Section 2 may be hastened through the stellar evolution process, even in the case that planets are not directly ejected by the host star's evolution.

Significant precedent from work leveraging $N-$body simulations has shown that planet-planet orbital instabilities are commonly triggered through the process of stellar evolution. Early work by M. J. Duncan & J. J. Lissauer (1998) used numerical simulations to show that the time to instability in the post-main-sequence solar system scales as a power law with the mass ratio between the sun and its neighboring planets, for ratios ≤ 0.4 times the current value. J. H. Debes & S. Sigurdsson (2002) generalized this result to a broader range of planetary system architectures, demonstrating that two-planet systems that began marginally Hill stable (G. W. Hill 1886; B. Gladman 1993)—that is, stable against close approaches between planets—can become quickly susceptible to planet-planet instabilities through post-main-sequence stellar mass loss.

The timescales of induced instabilities are often short relative to system lifetimes, such that they may have occurred in the past for many evolved star systems that host exoplanets. G. Voyatzis et al. (2013), for example, showed that instabilities in two-planet systems tend to occur in under 100 Myr for systems that undergo chaotic evolution due to stellar mass loss. A. J. Mustill et al. (2014) demonstrated that ejection-inducing instabilities are common for three-planet white dwarf systems, typically occurring at cooling ages of a few hundred Myr with ejections a factor of 3.9 times more likely during the white dwarf phase than during the host star's main-sequence phase. More recently, R. F. Maldonado et al. (2022) carried out a suite of $N-$body simulations examining systems with 2-6 planets, demonstrating that the instability rate increases with planet multiplicity irrespective of the planet masses and range of separations, but that ejection in particular (rather than orbit-crossing events that do not result in ejection) is most efficient for systems of multiple high-mass planets. Observed short-period giant exoplanets found around red giant branch stars show orbital eccentricities effectively tracing the upper limit predicted for planet-planet scattering at a given orbital separation (S. K. Grunblatt et al. 2022)—a suggestive signature of planet-planet orbital instabilities in the past histories of evolved planetary systems.

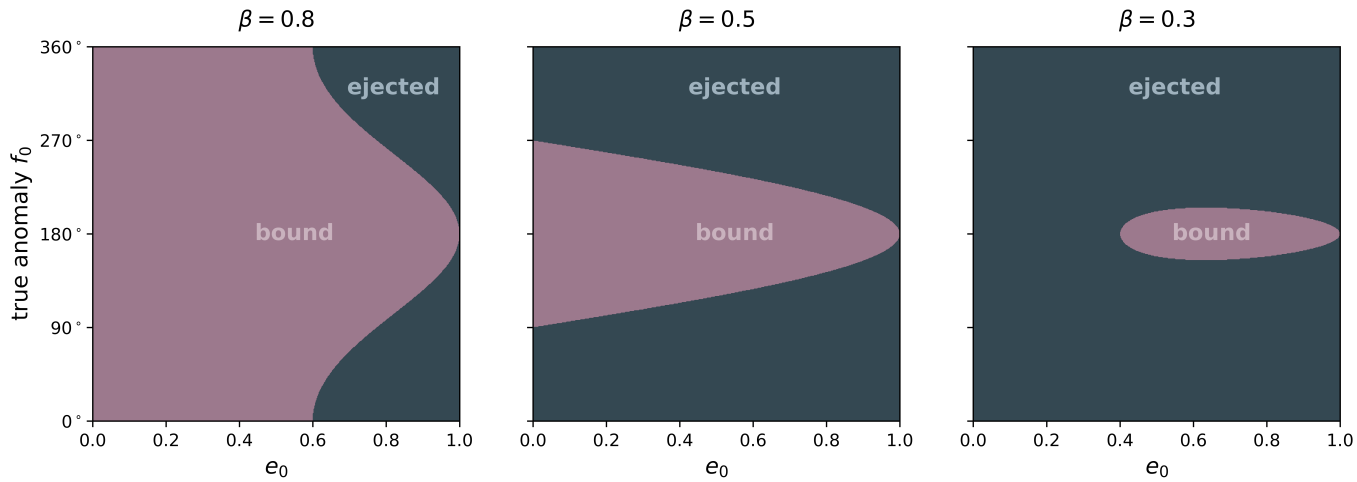

Figure 7. Planetary ejection regimes in the impulse approximation during a supernova explosion, shown for $\beta = 0.8$, 0.5, and 0.3 where $\beta = \mu_f/\mu_i$ is the fractional stellar mass that remains after near-instantaneous mass loss. Here e_0 and f_0 are the initial orbital eccentricity and true anomaly of the planetary orbit. For higher fractional mass loss (increasing left to right across the three panels), planets are ejected across a wider range of true anomaly values. Note that for a planet to be ejected, it must survive the supernova without being destroyed by interactions with the stellar ejecta.

5.6. *Increased susceptibility to flyby-induced ejection*

Another secondary planetary-ejection-related implication of stellar evolution is the increased flyby rate for surviving planets in an evolved system. Planetary orbits expand during post-main-sequence stellar evolution, such that the effective target area for a stellar or planetary flyby encounter also increases. This makes any given system that preserves its planets—that is, a system that does not have its full planetary system engulfed by the host star—more susceptible to planetary ejection through flybys.

In the limit of slow, spherically-symmetric mass loss, planetary orbital separations evolve as $a \propto M_*^{-1}$ due to the approximate conservation of specific angular momentum. This means that a star losing half its mass will have its neighboring planets' orbits expand by a factor of 2 in the gravitational focusing regime ($\sigma \propto a$), or a factor of 4 in the geometric cross-section regime ($\sigma \propto a^2$; see Section 4.2). The close stellar encounter occurrence rate (Equation 23) increases by a commensurate factor.

J. K. Zink et al. (2020) showed that the sun's orbital expansion will enable close stellar encounters to ultimately (within 100-1000 Gyr) destabilize all of the outer solar system giant planets. This process, however, is slow: the first planet is typically ejected within ≈ 30 Gyr in simulations considered by J. K. Zink et al. (2020). S. N. Raymond et al. (2024) found that individual flybys even within 100 AU would likely not destabilize any of the solar system planets: instead, multiple stellar flybys would generally be necessary to produce a sufficiently large change in acceleration to trigger planetary ejection.

Flybys in post-main-sequence systems were examined in further detail and within a Galactic context by D. Veras et al. (2014), who predicted a high rate of FFP production from stellar flybys in the galactic bulge. R. J. Parker & D. Veras (2026) recently simulated the evolution of planets orbiting white dwarf progenitor stars with $1 \leq M/M_\odot < 2.5$ in dense ($10^4 M_\odot$ pc^{-3}) embedded cluster environments, simultaneously modeling the influence of stellar evolution and $N-$body interactions. Incorporating the influence of orbit-widening from white dwarf evolution, R. J. Parker & D. Veras (2026) showed that up to 48% of their simulated planets orbiting white dwarfs, which include Jupiter-mass planets uniformly placed at 0.1-50 AU initial orbital separations, were disrupted to become FFPs. Their work predicts that many white dwarfs may subsequently capture these ejected FFPs, culminating in a population of wide-orbiting white-dwarf planets with semimajor axes $a > 100$ AU and high orbital eccentricities $e > 0.5$.

5.7. *White dwarf kicks*

Anisotropies—that is, deviations from perfect spherical symmetry—in mass loss during the AGB phase of stellar evolution produce a recoil kick of $\lesssim 2$ km/s on the stellar remnant, often referred to as a "white dwarf kick" (M. Fellhauer et al. 2003; K. El-Badry & H.-W. Rix 2018). The dynamical influence of mass-loss anisotropies has been examined within the impulse approximation (J. G. Hills 1983) as well as within the slower, adiabatic mass-loss regime (H.-C. Hwang & N. L. Zakamska 2025; C. E. O'Connor 2026).

The implications of white dwarf kicks for planetary ejection have been most explicitly modeled in the impulse approximation, appropriate for wide binaries at separations < 1000 au (C. E. O'Connor 2026). In this case, A. P. Stephan & K. G. Stassun (2026) leveraged $N-$body models together with the velocity distribution of white dwarf kicks derived in K. El-Badry & H.-W. Rix (2018) to demonstrate that white dwarf kicks rarely trigger direct planetary ejection ($\lesssim 1-2\%$ of known exoplanet systems). Instead, they tend to excite orbital eccentricities and inclinations that induce instabilities over time in multi-planet systems (see also Section 5.5). A. P. Stephan & K. G. Stassun (2026) finds that such instabilities result in planetary ejection within 5 Myr for $\sim 40-50\%$ of known exoplanet systems in which the planetary orbits would not be engulfed during the AGB phase of stellar evolution. Although A. P. Stephan & K. G. Stassun (2026) finds that FFPs produced by white dwarf kicks can reproduce only of order a few percent of the total FFP population, they also predict that such planets should slowly drift from their hosts at a rate of roughly 0.75 pc/Myr (0.73 km/s), offering a potential avenue toward identification.

5.8. *The role of binarity in planetary ejection for evolving stellar systems*

Up to this point, this section has focused primarily on planetary ejection in the case that an evolving single star is the planet host, unbound to any companion stars. The range of ejection scenarios is, however, more expansive when considering binary and higher-multiplicity systems, including influences from Type II supernovae of both stars, Type Ia supernovae, and common envelope evolution.

These possibilities were mapped by D. Veras & C. A. Tout (2012), who delineated the critical semimajor axes beyond which planets became unbound as a function of binary parameters, metallicity, and changing mass loss rate. This work showed that circumbinary ($p-$type) planets are particularly susceptible to ejection during the post-main-sequence evolution of one or both stars in their system, with projected ejection rates that are highly dependent upon the binary properties and initial planet semimajor axes. A. Nigioni et al. (2026) built upon this work by examining comparable two, three, four, and five-planet circumbinary systems. These authors showed that planetary ejection is common in such systems and that a modest sample of remnant, lower-multiplicity bound planets may be detectable with the future Laser Interferometer Space Antenna (LISA) gravitational wave observatory (P. Amaro-Seoane et al. 2017).

While D. Veras & C. A. Tout (2012) did not explicitly model evolving binary systems with $s-$type planets, they noted that planets in close binaries are likely to be destroyed by stellar evolution, whereas planets in wider binaries evolve more similarly to single-star systems with evolving stellar hosts. K. M. Kratter & H. B. Perets (2012) showed that for planets on $s-$type orbits in binary star systems, stellar evolution may lead to an exchange of planets between stars for relatively large semimajor axis ratios $a_p/a_* \gtrsim 0.1$, though their simulations were set up such that the minimum Jacobi constant reached by their simulations precluded ejection as a potential outcome. D. Veras et al. (2017) later modeled the dynamical evolution of $s-$type two-planet systems in which the planet host undergoes stellar evolution with a bound stellar companion—showing that systems remain stable over 14 Gyr in the case that an $e = 0$ binary companion is at least seven times as distant as the outer planetary orbit, with higher instability rates for more eccentric binaries.

5.9. *Predictions and implications: post-main-sequence planetary ejection*

While each of the aforementioned mechanisms has the potential to produce FFPs, direct planetary ejection from post-main-sequence stellar evolution likely plays a relatively minor role in producing FFPs. By evolving stars along their evolutionary tracks, D. Veras et al. (2011) showed that only planets on extremely wide orbits—typically at semimajor axes of hundreds to thousands of AU—are ejected during the AGB phase of stellar evolution. The same authors showed that nearly all planets that are not engulfed are ejected from orbit around a Type II supernova: the runaway regime is reached for all true anomalies except for a narrow range around $f_0 = 180°$. However, these high-mass stars are uncommon, as the stellar IMF is heavily tilted toward lower-mass M stars.

Planets forming at the wide separations necessary for AGB ejection are likely rare, as protoplanetary disks typically have dust disk radii of roughly 30-45 AU (J. J. Tobin et al. 2020). Nevertheless, it is possible that a small fraction of planetary systems ($1-5\%$) retain very-wide-orbiting planets at orbital separations of a few hundred to a few thousand AU, trapped after near-ejection by dynamical instabilities during the embedded cluster phase. Some objects ranging from planet- to brown-dwarf-mass have been found at these wide orbital separations (e.g. K. L. Luhman et al. 2011; V. Bailey et al. 2014; A. J. Bohn et al. 2020; M. Janson et al. 2021; A. J. Bohn et al. 2021).

Although only a small fraction of all stars undergo Type II supernovae, the population of FFPs produced by this mechanism may be distinguishable from other FFP sub-populations due to their high ejection velocities. Z. Regály et al. (2022) modeled high-velocity (1,000-10,000 km/s) stellar envelope ejections and found a wide range of resulting planetary ejection velocities, ranging from $\approx 1 - 275$ km/s and a mean ejection velocity of $\langle v_{\rm ejec} \rangle = 18$ km/s.

Secondary influences from post-main-sequence stellar evolution, including enhanced rates of orbital instabilities and disruptive stellar flybys, also contribute to FFP production. Given the low rate of FFPs expected directly from slow mass loss, together with the small fraction of stars that undergo Type II supernovae, these secondary effects likely represent the most dominant mechanisms for FFP production through post-main-sequence stellar evolution.

6. DISCUSSION

6.1. *Relative rates of FFP production*

As discussed in the previous sections, several planetary ejection mechanisms have been examined in detail, with differing FFP production rates across stellar environments. These mechanisms each contribute to the occurrence rate of free-floating planetary-mass objects. Therefore, FFPs as a whole will not follow any individual predicted distribution that focuses on only a subset of stellar populations. Instead, they will emerge with overlapping distributions of properties.

We provide a high-level summary of planetary ejection mechanisms in Table 1 alongside the projected properties of FFPs produced by each mechanism. The efficiency of ejection is described under the assumption that all stars host planets following known limits on exoplanet demographics. We also report the typical projected excess ejection velocity $\langle v_\infty \rangle$ for each mechanism, noting that the velocity distributions are dependent on the system configuration at the time of ejection, with differing planet populations required for ejection across mechanisms. Several FFP production mechanisms have the potential to contribute a large fraction of the underlying population, including planet-planet scattering, embedded cluster encounters, and binary instabilities.

To estimate rates in Table 1, we adopt the assumption from G. A. L. Coleman & W. DeRocco (2025) that planets on $p-$type orbits may form around binaries with separations of up to 3 AU. Considering binary instability rates from M. J. Holman & P. A. Wiegert (1999); B. Quarles et al. (2018), we use planet-to-star semimajor axis ratio $a_p/a_b \gtrsim 0.1$ as a threshold for $s-$type binary instability and assume that planets are typically located at a maximum semimajor axis of 30 AU, such that circumstellar planets in binaries with $a_b \lesssim 300$ AU may be prone to instabilities. We also assume that circumstellar planets cannot form unless the host stars are separated by at least a factor of three times the typical snow line separation 3 AU, corresponding to binary separations of roughly $a_b \gtrsim 10$ AU. Last, we consider only binaries with $a_b > 1000$ AU as candidates for a substantial influence from the Galactic tide.

Binary companion fractions are drawn as a function of stellar mass from S. S. R. Offner et al. (2023), and we approximate that the same separation distributions extend over slightly wider mass ranges from $M_* = 0.075 - 0.225 M_\odot$, $M_* = 0.225 - 0.675 M_\odot$, and $M_* > 0.675 M_\odot$. The adopted separation distributions are shown in Figure 8 for reference. Combining these fits with the piecewise power-law IMF from P. Kroupa (2001), from which we find that 63%, 29%, and 8% of stars fit into the listed low-, medium-, and high-mass bins, we find that 9% of stars have a binary companion that may induce $p-$type binary instabilities if circumbinary planets form within the system, and 10% of stars have a binary companion that may induce $s-$type binary instabilities for circumstellar planets. The true rate of initial planet formation in these unstable regions is not well-characterized, such that it is possible that all such systems eject one or more planetary companions.

For open (globular) clusters, we consider densities of roughly 10^2 (10^3) star pc^{-3} and report ejection rates for planets that would be disrupted within 1 (10) Gyr at orbital separations 3 AU (I. A. Bonnell et al. 2001). Embedded cluster encounters may result in either a very low or very high rate of planetary ejection depending on the planetary multiplicity and primordial orbital separation distribution (W. Hao et al. 2013); therefore, we report a range corresponding to outcomes for planets originating in multiplanet systems and spanning orbital separations of one to tens of AU.

We also assume that the galactic tide and stellar flybys in wide binaries typically induce planet-planet scattering comparable to that experienced by single stars, corresponding to a similar ejection velocity and source distribution of planets. The ejection rate reported in Table 1 for wide binary star systems corresponds to that of N. A. Kaib et al. (2013) with a four-giant-planet outer solar system analog and binary separations 1,000-30,000 AU. We note that the "low-mass" label within Table 1 refers to planets below the highest-mass planet within the system, but that planet-planet scattering—including that induced by galactic tide interactions—may still eject giant planets if multiple are present.

Mechanism	% stars	ej. rate	typical planet ejected	$\langle v_\infty \rangle$	References
Planet-planet scattering	100%	up to 100%	low-mass, wide-orbiting	2-6 km/s	[1,2,3,4]
$s-$type binary instability	10%	up to 100%	any mass, wide-orbiting	?	[3,4]
$p-$type binary instability	9%	up to 100%	any mass, close-orbiting	2-12 km/s	[3,4,5,6]
Embedded cluster encounters	100%	30-70%	any mass, wide-orbiting	5-10 km/s	[7,14]
Evolved open cluster encounters	10%	10%	any mass, wide-orbiting	1-2 km/s	[8]
Globular cluster encounters	0.5%	80%	any mass, wide-orbiting	11-12 km/s	[9,10]
Galactic tide + wide binaries	2%	30-60%	low-mass, wide-orbiting	2-6 km/s	[11]
AGB-phase stellar evolution	5%	$\lesssim$2%	any mass, wide-orbiting	0.5-1 km/s	[12,15,16]
Type II supernovae	0.1-1%	100%	any mass, any orbit	18 km/s	[12,13]

Table 1. Summary of the relative prevalence of and predictions for planetary ejection mechanisms. "% stars" refers to the percent of all stars that are susceptible to a given mechanism, and "ej. rate" refers to the percent of those systems that are predicted to eject at least one planet. The efficiency of planet ejection varies significantly with the locations and masses of formed planets; therefore, we describe the "typical planet ejected" in the fourth column. Typical excess velocities $\langle v_\infty \rangle$ are listed in the fifth column. We note that FFPs may populate different parts of parameter space: for example, those ejected from clusters do not all immediately join the latent background population, and planets ejected from encounters in globular clusters may populate the galactic halo. References are as follows: [1] H. G. Bhaskar & H. B. Perets (2025), [2] K. Guo et al. (2025), [3] G. A. L. Coleman & W. DeRocco (2025), [4] S. S. R. Offner et al. (2023), [5] G. A. L. Coleman (2024), [6] M. Teasdale & D. Stamatellos (2026), [7] R. J. Parker & S. P. Quanz (2012), [8] J. R. Hurley & M. M. Shara (2002), [9] K. W. Smith & I. A. Bonnell (2001), [10] I. A. Bonnell et al. (2001), [11] N. A. Kaib et al. (2013), [12] D. Veras et al. (2011), [13] Z. Regály et al. (2022), [14] W. Hao et al. (2013), [15] M. W. O'Brien et al. (2024), [16] A. P. Stephan & K. G. Stassun (2026)

Importantly, not all free-floating planets are the products of planetary ejection. Some FFPs may form *in situ* as the lowest-mass tail of the stellar initial mass function (K. L. Luhman 2012), including from erosion of prestellar cores in the vicinity of high-energy radiation from OB stars (A. P. Whitworth & H. Zinnecker 2004; J. L. Diamond & R. J. Parker 2024). Indeed, hundreds of planetary-mass objects have been discovered in star-forming regions since the turn of the century (e.g. Y. Oasa et al. 1999; P. W. Lucas & P. F. Roche 2000; M. R. Zapatero Osorio et al. 2000; K. L. Luhman 2004; A. Scholz et al. 2009; K. Mužić et al. 2012; K. L. Luhman et al. 2016; J. Gagné et al. 2017; M. Robberto et al. 2020; M. Gennaro & M. Robberto 2020; N. Miret-Roig et al. 2022; S. G. Pearson & M. J. McCaughrean 2023; K. L. Luhman et al. 2024; A. B. Langeveld et al. 2024; M. De Furio et al. 2025). Nevertheless, the high projected occurrence rate of low-mass FFPs (T. Sumi et al. 2023), together with new limits on the lowest-mass self-luminous objects in young star-forming regions—which taper off below roughly $3-5M_J$ (A. B. Langeveld et al. 2024; M. De Furio et al. 2025)—indicates that many FFPs, if they are truly unbound and free-floating, must have formed in and subsequently been ejected from circumstellar systems.

Another important caveat is that apparent FFPs observed through microlensing are not necessarily unbound. Many of these bodies may instead be wide-orbiting bound planets, with stellar hosts at sufficiently large projected separations such that they were not captured by the microlensing event that identified the FFP. Thus, the true occurrence rate of FFPs retains significant ambiguity. Observations before or after a microlensing event, when the lens is tens to hundreds of mas in angular separation from its source, may be used to search for a potential host star and distinguish between these scenarios. This typically requires at least several years in temporal separation, considering lens proper motion rates at microlensing event distances. A small number of searches have been conducted to date using post-event follow-up imaging (P. Mróz et al. 2024) and precovery searches with archival data (M. Kapusta et al. 2026), with no significant detections of host stars to date.

Even with a high rate of dynamical instabilities, not all scattered bodies are fully ejected. B. Gladman et al. (2002) found that planet-planet scattering could push Mars-sized embryos to extremely wide orbits of a few hundred AU, and this scenario was revisited by K. Silsbee & S. Tremaine (2018) to further delineate the parameter space for planetary embryos that may remain bound to the solar system in the present day. C. Scharf & K. Menou (2009) and D. Veras et al. (2009) showed that even giant planets can be feasibly left on wide-

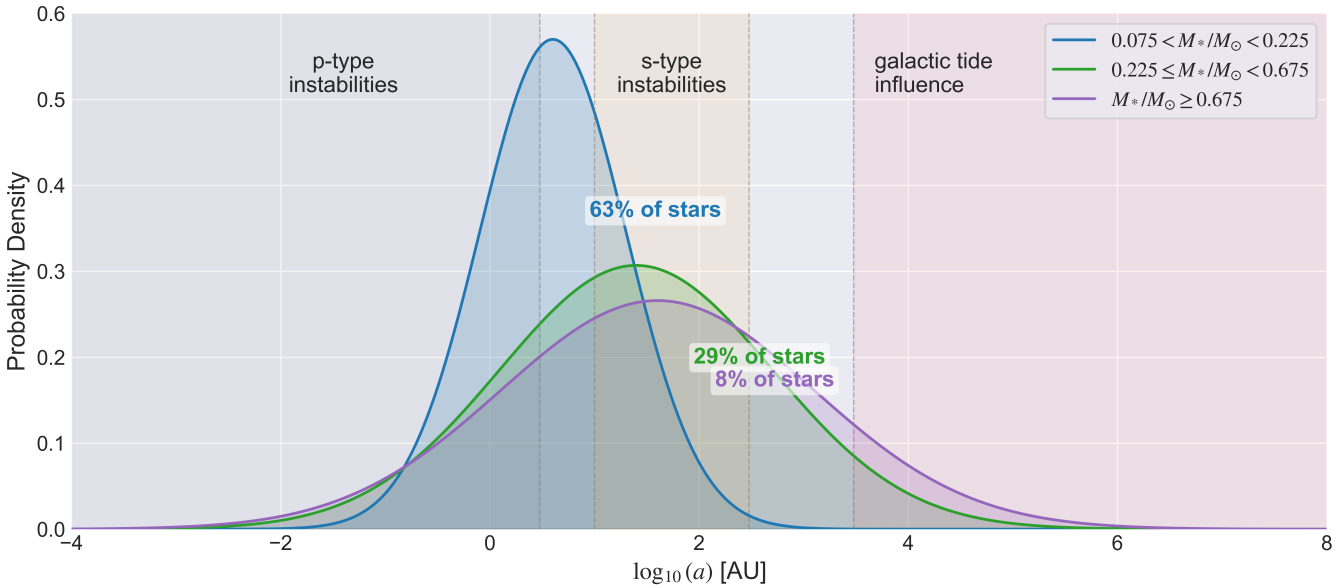

Figure 8. Log-normal binary separation distributions adopted from S. S. R. Offner et al. (2023) and derived from data drawn from D. Raghavan et al. (2010). The adopted limiting regimes for three categories of binary-driven instabilities are shown as the shaded background regions. The percentage of all stars falling in a given mass range, derived from the P. Kroupa (2001) IMF, is shown together with the binary separation distribution for stars in that mass range that host a bound stellar companion.

orbiting, bound orbits at separations of hundreds of AU as the remnants of planet-planet scattering. In rare cases, scattered planets may be captured at orbital separations of thousands of AU as an Oort cloud population of exoplanets (D. Veras et al. 2009; N. Bailey & D. Fabrycky 2019; S. N. Raymond et al. 2023; A. Izidoro et al. 2025). S. Hadden & Y. Wu (2025) leveraged scattering simulations in conjunction with updated microlensing constraints to predict that about half of Neptune-mass bodies that appear as FFPs may be on wide, bound orbits, rather than being truly free-floating. While the mechanisms described in Table 1 *can* account for all candidate FFPs, not all such objects should necessarily be accounted for as unbound products of planetary ejection.

6.2. *Observed properties of candidate FFPs*

Discoveries of free-floating planets have been made for decades using direct imaging, and more recently using the gravitational microlensing method. Directly imaged FFPs in star-forming regions, all of which have been super-Jupiter-mass ($\geq 3 - 5M_J$) to date (A. B. Langeveld et al. 2024; M. De Furio et al. 2025), are generally consistent with formation through direct collapse with no need to invoke planetary ejection to produce the population. As a result, we focus in this section on the FFPs identified through gravitational microlensing.

Ground-based gravitational microlensing surveys for free-floating and bound exoplanets include the Optical Gravitational Lensing Experiment (OGLE; A. Udalski et al. 2015), the Korea Microlensing Telescope Network (KMTNet; D.-J. Kim et al. 2018; C. B. Henderson et al. 2014), and the Microlensing Observations in Astrophysics (MOA; J. B. Hearnshaw et al. 2006) project. The threshold for FFP candidate events is typically placed at the bottom edge of the "Einstein desert", which corresponds to a dearth of microlensing events found with angular Einstein radii $10\,\mu\text{as} \lesssim \theta_E \lesssim 30\,\mu\text{as}$ (H.-W. Kim et al. 2021; Y.-H. Ryu et al. 2021). FFP candidates are generally reported for $\theta_E \lesssim 10\,\mu\text{as}$, where the Einstein timescale t_E and the angular Einstein radius θ_E are defined as

$$t_E = \frac{\theta_E}{\mu_{\rm rel}} \tag{37}$$

and

$$\theta_E \equiv \sqrt{\kappa M_L \pi_{\rm rel}} \tag{38}$$

for

$$\kappa \equiv \frac{4G}{c^2\ \text{au}}. \tag{39}$$

Here M_L is the lens mass, $\pi_{\rm rel}$ is the relative lens-source parallax, and $\mu_{\rm rel}$ is the lens-source relative proper motion.

Roughly a dozen microlensing FFP candidates have been reported to date that are attributed to low-mass (super-Earth-mass or below) planets that are unlikely to

have formed through direct collapse (T. Sumi et al. 2011; P. Mróz et al. 2017; P. Mróz et al. 2018; P. Mróz et al. 2019; P. Mró z et al. 2020; P. Mróz et al. 2020; H.-W. Kim et al. 2021; Y.-H. Ryu et al. 2021; N. Koshimoto et al. 2023; Y. K. Jung et al. 2024; R. Poleski et al. 2025; T. Inyanya et al. 2026; S. Dong et al. 2026a; Y.-H. Ryu et al. 2026). The completeness-corrected high occurrence of these isolated objects has been leveraged to argue for a high rate of FFPs particularly at the low-mass end, with estimates from T. Sumi et al. (2023) corresponding to a total of $80^{+73}_{-47} M_\oplus$ ejected per star for objects in the mass range $0.33 < M/M_\oplus < 6660$.

The history of any individual FFP ranges from difficult to impossible to definitively determine. This is for the same reasons that it is difficult to definitively show the origin system of the interstellar object 'Oumuamua, as discussed by A. Morbidelli et al. (2020): the processes that produce FFPs are chaotic, and it is impossible to integrate an object's trajectory backward in time to determine its origin (which would violate the second law of thermodynamics). In combination with the short dynamical lifetimes of free-floating bodies in the Galaxy, this means that orbital paths cannot be directly traced backward to origin systems unless the objects were ejected in the recent past. Some efforts have been made to identify possible progenitor systems for observed interstellar objects under the assumption of recent ejection, with plausible hosts reported for each discovered interstellar object (Q. Zhang 2018; F. Feng & H. R. A. Jones 2018; P. A. Dybczyński & M. Królikowska 2018; C. A. L. Bailer-Jones et al. 2018; S. Portegies Zwart et al. 2018; J. I. Zuluaga et al. 2018; C. A. L. Bailer-Jones et al. 2020; S. Portegies Zwart 2021; Y. Guo et al. 2025).

Some information may still be gleaned from the velocities of FFPs, even if their specific histories are difficult (or impossible) to unambiguously disentangle. In most cases, microlensing events associated with FFPs do not correspond to directly measured masses; instead, microlensing measurements provide t_E, which is a degenerate combination of the true mass, the object velocity, and the distance to the lensing body. The measurement of finite-source effects (H. J. Witt & S. Mao 1994) can break one of these degeneracies; however, an intrinsic degeneracy typically remains. This final degeneracy was broken in one recent case reported by S. Dong et al. (2026a), in which combined observations from ground-based telescopes (OGLE and KMTNet) and the *Gaia* spacecraft provided a parallax measurement of the event alongside measurements of t_E and θ_E. The most favored solution for the system corresponds to lens transverse velocities $v_{l,l,\mathrm{VSR}} = -48^{+23}_{-41}$ km/s and $v_{l,b,\mathrm{VSR}} = 79 \pm 12$ km/s relative to the vicinity standard of rest (VSR) describing neighboring stars. While the velocity deviation of the FFP from the VSR is consistent with the Galactic velocity distributions within 2σ, the potentially high observed velocity of this object is suggestive of ejection through a mechanism that can impart high relative velocities, such as instabilities in a tight circumbinary system or a Type II supernova explosion.

6.3. *Sub-planetary-mass ejected bodies*

In addition to planetary-mass ejected bodies, lower-mass free-floating objects are, in many cases, subject to the same ejection mechanisms described within this review. Understanding the properties of sub-planetary-mass ejected bodies may therefore offer useful insights into the ejection rates and mechanisms relevant for the FFP population. We do not attempt to provide a comprehensive overview of results oriented around the ejection of these sub-planetary-mass objects here. Instead, we provide a few key points to contextualize the lower-mass ejected population in light of current constraints on planetary-mass objects' ejection.

In the past decade, the first three interstellar objects—1I/'Oumuamua (G. V. Williams et al. 2017; K. J. Meech et al. 2017), 2I/Borisov (G. Borisov et al. 2019; D. Jewitt & J. Luu 2019; P. Guzik et al. 2020), and 3I/ATLAS (L. Denneau et al. 2025; B. T. Bolin et al. 2025; D. Z. Seligman et al. 2025)—were discovered. These objects have radii of $\sim 0.1 - 3$ km (K. J. Meech et al. 2017; D. Jewitt et al. 2017; M. M. Knight et al. 2017; M. Drahus et al. 2018; D. Jewitt et al. 2020; D. Jewitt & D. Z. Seligman 2023; D. Jewitt et al. 2025), and they were discovered passing through the solar system on hyperbolic orbits, unbound to the sun.

Several studies have explored the ejection of small bodies from their host planetary systems, largely with the goal of explaining the demographics of interstellar objects (for a review, see e.g. 'Oumuamua ISSI Team et al. 2019). These studies have made several key points. First, the known exoplanet population, which has been largely discovered by the transit and radial velocity methods, contains relatively few planets capable of efficiently ejecting small bodies (G. Laughlin & K. Batygin 2017; M. Rice & G. Laughlin 2019). Nevertheless, statistical evidence from planet searches that are less biased toward short-period planets, including suggestive evidence drawn from protoplanetary disk gaps in S. Zhang et al. (2018) and microlensing searches in D. Suzuki et al. (2016), indicates that wide-orbiting, Neptune-mass planets—efficient interstellar object ejectors (M. Rice & G. Laughlin 2019)—are common. Second, comet-like planetesimals are far more likely to be

ejected than asteroid-like ones (S. N. Raymond et al. 2018). This result stems from the expectation that rocky planetesimals are found much closer to their host stars, where they are typically accreted rather than ejected. Beyond the snow line there is also far more space to form planetesimals, for simple geometric reasons, enabling the production of a large population of icy interstellar object seeds. Third, planetesimals may undergo significant processing on their pathway to ejection, including tidal disruption and thermal processing (M. Ćuk 2018; S. N. Raymond et al. 2018; Y. Zhang & D. N. C. Lin 2020).

Like FFPs, interstellar objects may be produced by mechanisms other than scattering in single-star systems—including ejection from close binary star systems (A. P. Jackson et al. 2018) and gravitational stripping of distant objects during stellar flybys (K. Vincke & S. Pfalzner 2016; S. Portegies Zwart et al. 2018; T. O. Hands et al. 2019). The projected velocity distributions of interstellar objects may in principle be differentiated between formation scenarios: S. Pfalzner et al. (2021) modeled differences in interstellar object velocities for the cases of production by stellar evolution (typically < 0.5 km/s), flybys (typically < 1 km/s), and planet-planet scattering (typically above 2-3 km/s). Ejection from circumbinary systems would likely produce interstellar objects at even higher velocities (G. A. L. Coleman 2024).

Unlike interstellar objects, the detection of free-floating exomoons remains elusive. Nevertheless, useful limits may be placed in the near future on moon-mass objects that remain bound to their host stars. Microlensing observations with the NASA *Nancy Grace Roman* space telescope (D. Spergel et al. 2015; R. Akeson et al. 2019) are projected to enable the first population-level studies of moon-mass, bound objects (M. T. Penny et al. 2019) down to a Ganymede mass ($0.025 M_\oplus$), demonstrating the rate at which sub-Earth-mass bodies persist on wide orbits without having undergone either collisions or ejections. Considering true solar-system analog exomoons, projections indicate that of order one bound exomoon with moon-planet mass ratio $10^{-4}-10^{-2}$ around a wide-separation (0.3−30 au) giant ($30M_\oplus - 10M_{\rm Jup}$) planet will be detectable with the current *Roman* observing strategy (M. Lastovka et al. 2025). S. A. Johnson et al. (2020) and W. DeRocco et al. (2026) each showed that *Roman* will be sensitive to free-floating objects down to roughly the mass of Mars ($0.1M_\oplus$), with sensitivity that drops rapidly at lower masses. Some FFPs detected by *Roman* may have originated as moons if a subset of exoplanets hosts moons more massive than those in the solar system. For such low-mass free-floating bodies, it will likely be difficult to distinguish between objects that were initially moons and those that were planetesimals in their natal systems.

6.4. *Future prospects*

We stand at a key inflection point, with rich prospects for future observations from which we may glean insights into the processes underlying planetary ejection. Upcoming space missions with dedicated surveys amenable to microlensing FFP searches have the potential to provide unprecedented observational constraints on the properties of FFP populations.

The NASA *Nancy Grace Roman* space telescope, with projected launch in late 2026, offers tremendous prospects for upcoming microlensing detections of FFPs. Hundreds of FFPs are projected to be discovered by the mission's Core Community Surveys (S. A. Johnson et al. 2020), which would increase the number of known FFPs by a factor of ten. With a sufficiently large census of planets discovered to enable population studies, the FFPs discovered by *Roman* are projected to enable distinctions between current, competing models for the FFP mass function (W. DeRocco et al. 2026).

The Earth 2.0 mission, led by the Shanghai Astronomical Observatory through the Chinese Academy of Sciences for projected launch in late 2028, is also expected to find hundreds of FFPs during its four-year primary mission. Notably, this includes roughly 150 FFPs for which true masses will be measured from simultaneous parallax measurements through synergistic observations with KMTNet (J. Ge et al. 2022). These parallax measurements offer an unprecedented opportunity to characterize the transverse velocities of the lenses at scale, as in S. Dong et al. (2026b), for comparison with excess velocities imparted through distinct planetary ejection models.

On the theoretical side, inroads that would be particularly useful in advancing planetary ejection include clear formation-informed predictions for the planetary mass function at wide separations. How commonly do low-mass planets form at and beyond the ice line of a protoplanetary disk, where planetary ejection is efficient? How often do planets form on wide orbits in $s-$type binary star systems and in dense stellar cluster environments? Inroads have been made in connecting microlensing, direct imaging, and ALMA disk constraints with the stellar and planetary mass functions (J. C. Yee & S. J. Kenyon 2025), and further such limits offer a pathway toward determining what fraction of FFP candidates are truly unbound.

The observed occurrence of FFPs provides an opportunity to characterize the total mass budget available for planet formation—which the classic minimum-mass so-

lar nebula (S. J. Weidenschilling 1977) and its extrasolar analog (E. Chiang & G. Laughlin 2013) would generally underestimate relative to the population of free-floating planets. Heavier Class 0/I disks may be necessary to invoke to account for the high observed mass budget, if it is confirmed with upcoming observations (E. J. Lee et al. 2026). Constraints on the initial mass budgets of planetary systems have the potential to further inform the relative rates with which contributions from individual planetary ejection mechanisms may be capped.

7. SUMMARY

Planetary ejection is ubiquitous across environment, stellar multiplicity, and the life cycle of a stellar system: where planets form, planets are ejected. For a planetary system to form, its building blocks must have undergone instabilities, leading to orbit crossing and subsequent collisions through which planets grow. This process does not end with the formation of planets. In some cases, these continued instabilities may culminate in planetary ejection.

In this review, we have discussed the dynamical mechanisms relevant for planetary ejection, including both underlying principles and the current state of the field. We provide some high-level summary points as follows.

- Roughly a dozen candidate low-mass, sub-Jovian FFPs have been discovered by microlensing surveys. When incorporating survey completeness metrics, this discovery rate corresponds to a vast background population of low-mass FFPs. While higher-mass, directly-imaged FFPs—often found in star-forming regions—may form *in situ* through direct collapse, lower-mass FFPs demand an alternative explanation. This implies a high rate of planetary ejection.

- Planets may be ejected from their host systems through dynamical mechanisms including planet-planet scattering, binary instabilities (including resonance-overlap-driven orbital evolution, as well as eccentricity excitation by passing stars and the galactic tide), stellar and planetary flybys, and post-main-sequence orbital evolution. All of these mechanisms make some contribution to the population of FFPs.

- Though multiple mechanisms play a role in producing the FFP population, planet-planet scattering, embedded cluster encounters, and binary instabilities are likely predominant in FFP production. The true prevalence of planetary ejection via each mechanism examined in this work is set by the initial mass and semimajor axis distribution of planets forming across stellar environments.

- Radial-velocity and transiting exoplanet observations have revealed a prevalence of highly eccentric orbits among observed giant planets, together with architectural trends such as the dense packing of planetary systems on the brink of instability, that are suggestive of past planetary system instabilities. At a population level, these architectural vestiges may be the signposts of previous planetary ejection events.

- Upcoming microlensing surveys have the potential to place limits on the planetary initial mass function from the occurrence of FFPs while also improving constraints on the occurrence of wide-orbiting, sub-Jupiter-mass planets. In these ways, among others, upcoming surveys will inform the characteristics of both FFPs and their potential parent populations.

Understanding the dynamics of planetary ejection requires an overarching synergy of techniques. It is informed by the occurrence of mature long-period planets that remain bound after planetary ejection, measured through radial velocity and astrometry surveys. It is informed by the transit-identified dearth of resonant chains, and by the fingerprints of those few pristine remnant resonant systems that have evaded instability. It is informed by the prevalence of young, wide-orbiting giant planets from interferometric protoplanetary disk imaging, by direct-imaging limits in the cradles of planet formation, and by the discovery of FFPs and the demographics of wide-orbiting planets offered through microlensing.

Each nexus in this web of constraints provides a small piece of the broader puzzle of planetary ejection. Planetary ejection extends to the heart of fundamental questions about how planetary systems form and evolve: how are planets distributed at birth? In which environments do they form? And in what ways does the current set of bound systems differ from the demographics at various points in the planetary systems' life cycles?

These are large-scale problems, yet they are remarkably tractable. Significant, substantive progress has been made and remains to be made in coming decades—from the discovery of the first exoplanets only a few decades ago to the advent of ground- and space-based exoplanet-oriented surveys today. It has become possible to map not only the demographics of planetary systems, but also the demographics of the *now-invisible*, past states of planetary systems. A complete picture of

planetary systems' life cycles—at least the fuzzy outline, if not the fully sharpened image—may not be so far out of reach.

ACKNOWLEDGMENTS

We are grateful to the organizers of the 2025 Rogue Worlds Two conference, through which the core content of this article was originally presented as a review talk. We also thank the anonymous reviewer for helpful feedback that has strengthened this manuscript. M.R. acknowledges support from the Heising-Simons Foundation through Grants #2021-2802 and #2023-4478. S.N.R. is grateful to the ANR's PEPR-Origins and CNRS/INSU's PNP programs for support. W.D. was supported by NSF grant PHY-2210361 and the Maryland Center for Fundamental Physics.

AUTHOR CONTRIBUTIONS

M.R. was responsible for formulating and writing the manuscript. W.D. and S.N.R. each provided feedback on and contributed ideas toward refining the manuscript.

Software: `astropy` (Astropy Collaboration et al. 2013; A. M. Price-Whelan et al. 2018; Astropy Collaboration et al. 2022), `astroquery` (A. Ginsburg et al. 2019), `matplotlib` (J. D. Hunter 2007), `numpy` (T. E. Oliphant 2006; S. v. d. Walt et al. 2011; C. R. Harris et al. 2020), `pandas` (W. McKinney 2010), `scipy` (P. Virtanen et al. 2020)

REFERENCES

Adams, F. C., Hollenbach, D., Laughlin, G., & Gorti, U. 2004, ApJ, 611, 360, doi: 10.1086/421989

Adams, F. C., & Laughlin, G. 2001, Icarus, 150, 151, doi: 10.1006/icar.2000.6567

Adams, F. C., & Laughlin, G. 2003, Icarus, 163, 290, doi: 10.1016/S0019-1035(03)00081-2

Adams, F. C., Proszkow, E. M., Fatuzzo, M., & Myers, P. C. 2006, ApJ, 641, 504, doi: 10.1086/500393

Akeson, R., Armus, L., Bachelet, E., et al. 2019, arXiv e-prints, arXiv:1902.05569, doi: 10.48550/arXiv.1902.05569

Alvarado-Montes, J. A., Zuluaga, J. I., & Sucerquia, M. 2017, MNRAS, 471, 3019, doi: 10.1093/mnras/stx1745

Amaro-Seoane, P., Audley, H., Babak, S., et al. 2017, arXiv e-prints, arXiv:1702.00786, doi: 10.48550/arXiv.1702.00786

Andrews, S. M., Huang, J., Pérez, L. M., et al. 2018, ApJL, 869, L41

Armitage, P. J. 2000, A&A, 362, 968, doi: 10.48550/arXiv.astro-ph/0007044

Arzoumanian, Z., Joshi, K., Rasio, F. A., & Thorsett, S. E. 1996, in Astronomical Society of the Pacific Conference Series, Vol. 105, IAU Colloquium 160: Pulsars: Problems and Progress, ed. S. Johnston, M. A. Walker, & M. Bailes, 525–530, doi: 10.48550/arXiv.astro-ph/9605141

Astropy Collaboration, Robitaille, T. P., Tollerud, E. J., et al. 2013, A&A, 558, A33, doi: 10.1051/0004-6361/201322068

Astropy Collaboration, Price-Whelan, A. M., Lim, P. L., et al. 2022, ApJ, 935, 167, doi: 10.3847/1538-4357/ac7c74

Ávila-Bravo, M., Charalambous, C., & Aguilera-Gómez, C. 2026, A&A, 706, A121, doi: 10.1051/0004-6361/202557225

Bailer-Jones, C. A. L., Farnocchia, D., Meech, K. J., et al. 2018, AJ, 156, 205, doi: 10.3847/1538-3881/aae3eb

Bailer-Jones, C. A. L., Farnocchia, D., Ye, Q., Meech, K. J., & Micheli, M. 2020, A&A, 634, A14, doi: 10.1051/0004-6361/201937231

Bailey, N., & Fabrycky, D. 2019, AJ, 158, 94, doi: 10.3847/1538-3881/ab2d2a

Bailey, V., Meshkat, T., Reiter, M., et al. 2014, ApJL, 780, L4, doi: 10.1088/2041-8205/780/1/L4

Barclay, T., Quintana, E. V., Raymond, S. N., & Penny, M. T. 2017, ApJ, 841, 86, doi: 10.3847/1538-4357/aa705b

Barnes, R., & Quinn, T. 2004, ApJ, 611, 494, doi: 10.1086/421321

Barnes, R., & Raymond, S. N. 2004, ApJ, 617, 569, doi: 10.1086/423419

Baron, F., Lafrenière, D., Artigau, É., et al. 2019, AJ, 158, 187, doi: 10.3847/1538-3881/ab4130

Bartram, P., Wittig, A., Lissauer, J. J., Gavino, S., & Urrutxua, H. 2021, MNRAS, 506, 6181, doi: 10.1093/mnras/stab1465

Batalha, N. M., Rowe, J. F., Bryson, S. T., et al. 2013, ApJS, 204, 24, doi: 10.1088/0067-0049/204/2/24

Batygin, K., & Brown, M. E. 2010, ApJ, 716, 1323, doi: 10.1088/0004-637X/716/2/1323

Batygin, K., Brown, M. E., & Betts, H. 2012, ApJL, 744, L3, doi: 10.1088/2041-8205/744/1/L3

Benest, D. 1988a, Celestial Mechanics, 43, 47, doi: 10.1007/BF01234553

Benest, D. 1988b, A&A, 206, 143

Benest, D. 1993, Celestial Mechanics and Dynamical Astronomy, 56, 45, doi: 10.1007/BF00699718

Bhaskar, H. G., & Perets, H. B. 2025, The Astrophysical Journal, 991, 132, doi: 10.3847/1538-4357/adf4e2

Black, D. C. 1982, AJ, 87, 1333, doi: 10.1086/113220

Bohn, A. J., Kenworthy, M. A., Ginski, C., et al. 2020, ApJL, 898, L16, doi: 10.3847/2041-8213/aba27e

Bohn, A. J., Ginski, C., Kenworthy, M. A., et al. 2021, A&A, 648, A73, doi: 10.1051/0004-6361/202140508

Boley, A. C., Payne, M. J., & Ford, E. B. 2012, ApJ, 754, 57, doi: 10.1088/0004-637X/754/1/57

Boley, K. M., Christiansen, J. L., Zink, J., et al. 2024, AJ, 168, 128, doi: 10.3847/1538-3881/ad6570

Bolin, B. T., Belyakov, M., Fremling, C., et al. 2025, MNRAS, 542, L139, doi: 10.1093/mnrasl/slaf078

Bolmont, E., Galantay, E., Blanco-Cuaresma, S., Oza, A. V., & Mordasini, C. 2025, A&A, 704, A9, doi: 10.1051/0004-6361/202554625

Bonnell, I. A., Smith, K. W., Davies, M. B., & Horne, K. 2001, Monthly Notices of the Royal Astronomical Society, 322, 859, doi: 10.1046/j.1365-8711.2001.04171.x

Bonomo, A. S., Hébrard, G., Raymond, S. N., et al. 2017, A&A, 603, A43, doi: 10.1051/0004-6361/201730624

Borisov, G., Durig, D. T., Sato, H., et al. 2019, Comet C/2019 Q4 (Borisov),, Central Bureau Electronic Telegrams, No. 4666

Borucki, W. J., Koch, D., Basri, G., et al. 2010, Science, 327, 977

Borucki, W. J., Koch, D. G., Basri, G., et al. 2011, ApJ, 736, 19, doi: 10.1088/0004-637X/736/1/19

Bouy, H., Duchêne, G., Strampelli, G., et al. 2026, A&A, 708, A218, doi: 10.1051/0004-6361/202555031

Bowler, B. P. 2016, PASP, 128, 102001, doi: 10.1088/1538-3873/128/968/102001

Brasil, P. I. O., Roig, F., Nesvorný, D., et al. 2016, Icarus, 266, 142, doi: 10.1016/j.icarus.2015.11.015

Brodie, J. P., & Strader, J. 2006, ARA&A, 44, 193, doi: 10.1146/annurev.astro.44.051905.092441

Brown, G., Malhotra, R., & Rein, H. 2025, The Open Journal of Astrophysics, 8, E161, doi: 10.33232/001c.146688

Brown, G., & Rein, H. 2022, MNRAS, 515, 5942, doi: 10.1093/mnras/stac1763

Brucalassi, A., Pasquini, L., Saglia, R., et al. 2014, A&A, 561, L9, doi: 10.1051/0004-6361/201322584

Busetti, F., Beust, H., & Harley, C. 2018, A&A, 619, A91, doi: 10.1051/0004-6361/201833097

Cai, M. X., Kouwenhoven, M. B. N., Portegies Zwart, S. F., & Spurzem, R. 2017, MNRAS, 470, 4337, doi: 10.1093/mnras/stx1464

Cai, M. X., Portegies Zwart, S., & van Elteren, A. 2018, MNRAS, 474, 5114, doi: 10.1093/mnras/stx3064

Ćalović, A., Nayakshin, S., Casewell, S., & Miret-Roig, N. 2026, MNRAS, 545, staf2097, doi: 10.1093/mnras/staf2097

Carrera, D., Raymond, S. N., & Davies, M. B. 2019, A&A, 629, L7, doi: 10.1051/0004-6361/201935744

Chambers, J. E. 2001, Icarus, 152, 205, doi: 10.1006/icar.2001.6639

Chambers, J. E., Wetherill, G. W., & Boss, A. P. 1996, Icarus, 119, 261, doi: 10.1006/icar.1996.0019

Chatterjee, S., Ford, E. B., Geller, A. M., & Rasio, F. A. 2012, MNRAS, 427, 1587, doi: 10.1111/j.1365-2966.2012.22057.x

Chatterjee, S., Ford, E. B., Matsumura, S., & Rasio, F. A. 2008, ApJ, 686, 580

Chen, J., & Kipping, D. 2017, ApJ, 834, 17, doi: 10.3847/1538-4357/834/1/17

Chiang, E., & Laughlin, G. 2013, MNRAS, 431, 3444, doi: 10.1093/mnras/stt424

Chirikov, B. V. 1979, PhR, 52, 263, doi: 10.1016/0370-1573(79)90023-1

Choksi, N., Lithwick, Y., Chiang, E., & Li, R. 2026, arXiv e-prints, arXiv:2604.05035, doi: 10.48550/arXiv.2604.05035

Christiansen, J. L., McElroy, D. L., Harbut, M., et al. 2025, PSJ, 6, 186, doi: 10.3847/PSJ/ade3c2

Clanton, C., & Gaudi, B. S. 2014, ApJ, 791, 90, doi: 10.1088/0004-637X/791/2/90

Clanton, C., & Gaudi, B. S. 2016, ApJ, 819, 125, doi: 10.3847/0004-637X/819/2/125

Clarke, C. J., & Pringle, J. E. 1993, MNRAS, 261, 190, doi: 10.1093/mnras/261.1.190

Clement, M. S., Deienno, R., Kaib, N. A., et al. 2021a, Icarus, 367, 114556, doi: 10.1016/j.icarus.2021.114556

Clement, M. S., Kaib, N. A., Raymond, S. N., & Walsh, K. J. 2018, Icarus, 311, 340, doi: 10.1016/j.icarus.2018.04.008

Clement, M. S., Raymond, S. N., Kaib, N. A., et al. 2021b, Icarus, 355, 114122, doi: 10.1016/j.icarus.2020.114122

Cloutier, R., Tamayo, D., & Valencia, D. 2015, ApJ, 813, 8, doi: 10.1088/0004-637X/813/1/8

Coleman, G. A. L. 2024, Monthly Notices of the Royal Astronomical Society, 530, 630, doi: 10.1093/mnras/stae903

Coleman, G. A. L., & DeRocco, W. 2025, Monthly Notices of the Royal Astronomical Society, 537, 2303, doi: 10.1093/mnras/staf138

Correa-Otto, J. A., & Gil-Hutton, R. A. 2017, A&A, 608, A116, doi: 10.1051/0004-6361/201731229

Craig, J., & Krumholz, M. R. 2013, ApJ, 769, 150, doi: 10.1088/0004-637X/769/2/150

Cresswell, P., & Nelson, R. P. 2006, A&A, 450, 833, doi: 10.1051/0004-6361:20054551

Cuello, N., Ménard, F., & Price, D. J. 2023, European Physical Journal Plus, 138, 11, doi: 10.1140/epjp/s13360-022-03602-w

Cuello, N., Louvet, F., Mentiplay, D., et al. 2020, MNRAS, 491, 504, doi: 10.1093/mnras/stz2938

Ćuk, M. 2018, ApJ, 852, L15, doi: 10.3847/2041-8213/aaa3db

Cumming, A., Butler, R. P., Marcy, G. W., et al. 2008, PASP, 120, 531, doi: 10.1086/588487

Daffern-Powell, E. C., & Parker, R. J. 2022, MNRAS, 517, 2103, doi: 10.1093/mnras/stac2797

Dai, F., Goldberg, M., Batygin, K., et al. 2024, AJ, 168, 239, doi: 10.3847/1538-3881/ad83a6

David, E.-M., Quintana, E. V., Fatuzzo, M., & Adams, F. C. 2003, PASP, 115, 825, doi: 10.1086/376395

Davies, M. B., Adams, F. C., Armitage, P., et al. 2014, in Protostars and Planets VI, ed. H. Beuther, R. S. Klessen, C. P. Dullemond, & T. Henning, 787–808, doi: 10.2458/azu_uapress_9780816531240-ch034

Davies, M. B., & Sigurdsson, S. 2001, MNRAS, 324, 612, doi: 10.1046/j.1365-8711.2001.04336.x

De Furio, M., Meyer, M. R., Greene, T., et al. 2025, ApJL, 981, L34, doi: 10.3847/2041-8213/adb96a

de la Fuente Marcos, C., & de la Fuente Marcos, R. 1999, NewA, 4, 21, doi: 10.1016/S1384-1076(98)00043-8

de Sousa, R. R., Morbidelli, A., Raymond, S. N., et al. 2020, Icarus, 339, 113605, doi: 10.1016/j.icarus.2019.113605

Debes, J. H., & Sigurdsson, S. 2002, The Astrophysical Journal, 572, 556, doi: 10.1086/340291

Debes, J. H., & Sigurdsson, S. 2007, ApJL, 668, L167, doi: 10.1086/523103

Deienno, R., Morbidelli, A., Gomes, R. S., & Nesvorný, D. 2017, AJ, 153, 153, doi: 10.3847/1538-3881/aa5eaa

Deienno, R., Nesvorný, D., Vokrouhlický, D., & Yokoyama, T. 2014, AJ, 148, 25, doi: 10.1088/0004-6256/148/2/25

Denneau, L., Siverd, R., Tonry, J., et al. 2025, Minor Planet Electronic Circulars, 2025-N12, doi: 10.48377/MPEC/2025-N12

Deprit, A. 1983, Celestial Mechanics, 31, 1, doi: 10.1007/BF01272557

DeRocco, W., Johnson, S. A., Zohrabi, F., Penny, M. T., & McGill, P. 2026, AJ, 172, 7, doi: 10.3847/1538-3881/ae6e36

Diamond, J. L., & Parker, R. J. 2024, ApJ, 975, 204, doi: 10.3847/1538-4357/ad8644

Do, A., Tucker, M. A., & Tonry, J. 2018, ApJL, 855, L10

Dobos, V., Charnoz, S., Pál, A., Roque-Bernard, A., & Szabó, G. M. 2021, PASP, 133, 094401, doi: 10.1088/1538-3873/abfe04

Dong, J., Lee, E. J., Kokubo, E., Murray-Clay, R., & Gupta, A. 2026, arXiv e-prints, arXiv:2603.22426, doi: 10.48550/arXiv.2603.22426

Dong, S., Wu, Z., Ryu, Y.-H., et al. 2026a, Science, 391, 96, doi: 10.1126/science.adv9266

Dong, S., Wu, Z., Ryu, Y.-H., et al. 2026b, Science, 391, 96, doi: 10.1126/science.adv9266

Doolin, S., & Blundell, K. M. 2011, MNRAS, 418, 2656, doi: 10.1111/j.1365-2966.2011.19657.x

Doyle, L. R., Carter, J. A., Fabrycky, D. C., et al. 2011, Science, 333, 1602, doi: 10.1126/science.1210923

Drahus, M., Guzik, P., Waniak, W., et al. 2018, Nature Astronomy, 2, 407, doi: 10.1038/s41550-018-0440-1

Duchêne, G., & Kraus, A. 2013, ARA&A, 51, 269, doi: 10.1146/annurev-astro-081710-102602

Duncan, M. J., & Lissauer, J. J. 1998, Icarus, 134, 303, doi: 10.1006/icar.1998.5962

Duquennoy, A., & Mayor, M. 1991, A&A, 248, 485

Dvorak, R. 1984, Celestial Mechanics, 34, 369, doi: 10.1007/BF01235815

Dvorak, R. 1986, A&A, 167, 379

Dvorak, R., Froeschle, C., & Froeschle, C. 1989, A&A, 226, 335

Dybczyński, P. A., & Królikowska, M. 2018, A&A, 610, L11, doi: 10.1051/0004-6361/201732309

El-Badry, K., & Rix, H.-W. 2018, MNRAS, 480, 4884, doi: 10.1093/mnras/sty2186

El-Badry, K., Rix, H.-W., Tian, H., Duchêne, G., & Moe, M. 2019, MNRAS, 489, 5822, doi: 10.1093/mnras/stz2480

Ellithorpe, E. A., & Kaib, N. A. 2022, MNRAS, 515, 2914, doi: 10.1093/mnras/stac1973

Esposito, J., Li, G., & Wang, S. 2026, arXiv e-prints, arXiv:2603.22409, doi: 10.48550/arXiv.2603.22409

Faber, P., & Quillen, A. C. 2007, MNRAS, 382, 1823, doi: 10.1111/j.1365-2966.2007.12490.x

Fabrycky, D. C., Lissauer, J. J., Ragozzine, D., et al. 2014, ApJ, 790, 146

Fang, J., & Margot, J.-L. 2013, ApJ, 767, 115, doi: 10.1088/0004-637X/767/2/115

Farago, F., & Laskar, J. 2010, MNRAS, 401, 1189, doi: 10.1111/j.1365-2966.2009.15711.x

Fellhauer, M., Lin, D. N. C., Bolte, M., Aarseth, S. J., & Williams, K. A. 2003, ApJL, 595, L53, doi: 10.1086/379005

Feng, F., & Jones, H. R. A. 2018, ApJL, 852, L27, doi: 10.3847/2041-8213/aaa404

Fernandes, R. B., Mulders, G. D., Pascucci, I., Mordasini, C., & Emsenhuber, A. 2019, ApJ, 874, 81, doi: 10.3847/1538-4357/ab0300

Fernandez, J. A., & Ip, W.-H. 1984, Icarus, 58, 109, doi: 10.1016/0019-1035(84)90101-5

Fischer, D. A., & Valenti, J. 2005, ApJ, 622, 1102

Flammini Dotti, F., Kouwenhoven, M. B. N., Berczik, P., Shu, Q., & Spurzem, R. 2025, A&A, 693, A166, doi: 10.1051/0004-6361/202452441

Flammini Dotti, F., Kouwenhoven, M. B. N., Wu, K., et al. 2026, A&A, 706, A219, doi: 10.1051/0004-6361/202557334

Ford, E. B. 2014, Proceedings of the National Academy of Science, 111, 12616, doi: 10.1073/pnas.1304219111

Ford, E. B., & Chiang, E. I. 2007, The Astrophysical Journal, 661, 602, doi: 10.1086/513598

Ford, E. B., Lystad, V., & Rasio, F. A. 2005, Nature, 434, 873, doi: 10.1038/nature03427

Ford, E. B., & Rasio, F. A. 2008, ApJ, 686, 621, doi: 10.1086/590926

Forgan, D., Parker, R. J., & Rice, K. 2015, MNRAS, 447, 836, doi: 10.1093/mnras/stu2504

Forgan, D., & Rice, K. 2009, MNRAS, 400, 2022, doi: 10.1111/j.1365-2966.2009.15596.x

Forgan, D. H., Hall, C., Meru, F., & Rice, W. K. M. 2018, MNRAS, 474, 5036, doi: 10.1093/mnras/stx2870

Fragner, M. M., & Nelson, R. P. 2009, A&A, 505, 873, doi: 10.1051/0004-6361/200912292

Froeschlé, C., Gonczi, R., & Lega, E. 1997, Planet. Space Sci., 45, 881, doi: 10.1016/S0032-0633(97)00058-5

Fujii, M. S., & Hori, Y. 2019, Astronomy & Astrophysics, 624, A110, doi: 10.1051/0004-6361/201834677

Fulton, B. J., Rosenthal, L. J., Hirsch, L. A., et al. 2021, ApJS, 255, 14

Funk, B., Wuchterl, G., Schwarz, R., Pilat-Lohinger, E., & Eggl, S. 2010, A&A, 516, A82, doi: 10.1051/0004-6361/200912698

Gagné, J., Faherty, J. K., Mamajek, E. E., et al. 2017, ApJS, 228, 18, doi: 10.3847/1538-4365/228/2/18

Gavino, S., & Lissauer, J. J. 2026, A&A, 710, A119, doi: 10.1051/0004-6361/202557642

Ge, J., Zhang, H., Zang, W., et al. 2022, arXiv e-prints, arXiv:2206.06693, doi: 10.48550/arXiv.2206.06693

Gennaro, M., & Robberto, M. 2020, ApJ, 896, 80, doi: 10.3847/1538-4357/ab911a

Georgakarakos, N., Eggl, S., Ali-Dib, M., & Dobbs-Dixon, I. 2024, AJ, 168, 224, doi: 10.3847/1538-3881/ad7a78

Gilliland, R. L., Brown, T. M., Guhathakurta, P., et al. 2000, ApJL, 545, L47, doi: 10.1086/317334

Ginsburg, A., Sipőcz, B. M., Brasseur, C., et al. 2019, AJ, 157, 98

Gladman, B. 1993, Icarus, 106, 247, doi: 10.1006/icar.1993.1169

Gladman, B., Holman, M., Grav, T., et al. 2002, Icarus, 157, 269, doi: 10.1006/icar.2002.6860

Goldreich, P., Lithwick, Y., & Sari, R. 2004a, ARA&A, 42, 549, doi: 10.1146/annurev.astro.42.053102.134004

Goldreich, P., Lithwick, Y., & Sari, R. 2004b, ApJ, 614, 497, doi: 10.1086/423612

Gomes, R., Levison, H. F., Tsiganis, K., & Morbidelli, A. 2005, Nature, 435, 466, doi: 10.1038/nature03676

Gong, Y.-X., Zhou, J.-L., Xie, J.-W., & Wu, X.-M. 2013, ApJL, 769, L14, doi: 10.1088/2041-8205/769/1/L14

Gould, A., Jung, Y. K., Hwang, K.-H., et al. 2022, Journal of Korean Astronomical Society, 55, 173, doi: 10.5303/JKAS.2022.55.5.173

Grishin, E., Winter, J., & Alvarado-Montes, J. A. 2025, arXiv e-prints, arXiv:2512.13773, doi: 10.48550/arXiv.2512.13773

Griveaud, P., Crida, A., Petit, A. C., Lega, E., & Morbidelli, A. 2024, A&A, 688, A202, doi: 10.1051/0004-6361/202450340

Grunblatt, S. K., Saunders, N., Sun, M., et al. 2022, AJ, 163, 120, doi: 10.3847/1538-3881/ac4972

Guo, K., Ida, S., & Ogihara, M. 2025, Formation of Free-Floating Planets via Ejection: Population Synthesis with a Realistic IMF and Comparison to Microlensing Observations, arXiv, doi: 10.48550/arXiv.2511.03246

Guo, Y., Zhang, L., Feng, F., et al. 2025, AJ, 170, 362, doi: 10.3847/1538-3881/ae1833

Guzik, P., Drahus, M., Rusek, K., et al. 2020, Nature Astronomy, 4, 53

Hadden, S., & Wu, Y. 2025, Free Floating or Merely Detached? arXiv, doi: 10.48550/arXiv.2507.08968

Hadjidemetriou, J. D. 1963, Icarus, 2, 440, doi: 10.1016/0019-1035(63)90072-1

Hamers, A. S., & Tremaine, S. 2017, AJ, 154, 272, doi: 10.3847/1538-3881/aa9926

Hands, T. O., Dehnen, W., Gration, A., Stadel, J., & Moore, B. 2019, MNRAS, 490, 21, doi: 10.1093/mnras/stz1069

Hao, W., Kouwenhoven, M. B. N., & Spurzem, R. 2013, MNRAS, 433, 867, doi: 10.1093/mnras/stt771

Harris, C. R., Millman, K. J., van der Walt, S. J., et al. 2020, Nature, 585, 357

Hearnshaw, J. B., Abe, F., Bond, I. A., et al. 2006, in The 9th Asian-Pacific Regional IAU Meeting, ed. W. Sutantyo, P. W. Premadi, P. Mahasena, T. Hidayat, & S. Mineshige, 272, doi: 10.48550/arXiv.astro-ph/0509420

Heggie, D. C. 1975, MNRAS, 173, 729, doi: 10.1093/mnras/173.3.729

Heggie, D. C. 2006, in Few-Body Problem: Theory and Computer Simulations, 20, doi: 10.48550/arXiv.astro-ph/0512504

Heggie, D. C., & Rasio, F. A. 1996, MNRAS, 282, 1064, doi: 10.1093/mnras/282.3.1064

Henderson, C. B., Gaudi, B. S., Han, C., et al. 2014, ApJ, 794, 52, doi: 10.1088/0004-637X/794/1/52

Hénon, M., & Guyot, M. 1970, in Periodic Orbits Stability and Resonances, ed. G. E. O. Giacaglia, 349

Hill, G. W. 1886 Acta Mathematica, 8, 1

Hills, J. G. 1983, ApJ, 267, 322, doi: 10.1086/160871

Hills, J. G. 1984, AJ, 89, 1559, doi: 10.1086/113659

Hills, J. G., & Dissly, R. W. 1989, AJ, 98, 1069, doi: 10.1086/115197

Holman, M. J., & Wiegert, P. A. 1999, AJ, 117, 621, doi: 10.1086/300695

Hong, Y.-C., Raymond, S. N., Nicholson, P. D., & Lunine, J. I. 2018, The Astrophysical Journal, 852, 85, doi: 10.3847/1538-4357/aaa0db

Huang, X., & Lai, D. 2026, ApJ, 998, 245, doi: 10.3847/1538-4357/ae394f

Hunter, J. D. 2007, Computing in science & engineering, 9, 90

Hurley, J. R., & Shara, M. M. 2002, ApJ, 565, 1251, doi: 10.1086/337921

Hwang, H.-C., Ting, Y.-S., & Zakamska, N. L. 2022, MNRAS, 512, 3383, doi: 10.1093/mnras/stac675

Hwang, H.-C., & Zakamska, N. L. 2025, ApJ, 991, 226, doi: 10.3847/1538-4357/adfa1c

Ida, S., Tanaka, H., Johansen, A., Kanagawa, K. D., & Tanigawa, T. 2018, ApJ, 864, 77, doi: 10.3847/1538-4357/aad69c

Inyanya, T., Jung, Y. K., Yang, H., et al. 2026, KMT-2024-BLG-3237: Another Free-Floating Planet Candidate with Angular Einstein Radius Measurement, https://arxiv.org/abs/2602.22709

Izidoro, A., Bitsch, B., Raymond, S. N., et al. 2021, A&A, 650, A152, doi: 10.1051/0004-6361/201935336

Izidoro, A., Morbidelli, A., Raymond, S. N., Hersant, F., & Pierens, A. 2015, A&A, 582, A99, doi: 10.1051/0004-6361/201425525

Izidoro, A., Ogihara, M., Raymond, S. N., et al. 2017, Monthly Notices of the Royal Astronomical Society, 470, 1750

Izidoro, A., Raymond, S. N., Kaib, N. A., Morbidelli, A., & Isella, A. 2025, Nature Astronomy, 9, 982, doi: 10.1038/s41550-025-02556-0

Jackson, A. P., Tamayo, D., Hammond, N., Ali-Dib, M., & Rein, H. 2018, MNRAS: Letters, 478, L49

Jakubík, M., Morbidelli, A., Neslušan, L., & Brasser, R. 2012, A&A, 540, A71, doi: 10.1051/0004-6361/201117687

Janson, M., Gratton, R., Rodet, L., et al. 2021, Nature, 600, 231, doi: 10.1038/s41586-021-04124-8

Jewitt, D., Hui, M.-T., Kim, Y., et al. 2020, ApJL, 888, L23, doi: 10.3847/2041-8213/ab621b

Jewitt, D., Hui, M.-T., Mutchler, M., Kim, Y., & Agarwal, J. 2025, ApJL, 990, L2, doi: 10.3847/2041-8213/adf8d8

Jewitt, D., & Luu, J. 2019, ApJL, 886, L29, doi: 10.3847/2041-8213/ab530b

Jewitt, D., Luu, J., Rajagopal, J., et al. 2017, arXiv preprint arXiv:1711.05687

Jewitt, D., & Seligman, D. Z. 2023, ARA&A, 61, 197, doi: 10.1146/annurev-astro-071221-054221

Jiang, Y.-F., & Tremaine, S. 2010, MNRAS, 401, 977, doi: 10.1111/j.1365-2966.2009.15744.x

Johnson, S. A., Penny, M., Gaudi, B. S., et al. 2020, AJ, 160, 123, doi: 10.3847/1538-3881/aba75b

Jung, Y. K., Hwang, K.-H., Yang, H., et al. 2024, AJ, 168, 152, doi: 10.3847/1538-3881/ad6b12

Jurić, M., & Tremaine, S. 2008, ApJ, 686, 603, doi: 10.1086/590047

Kaib, N. A., Parsells, A., Grimm, S., Quarles, B., & Clement, M. S. 2024, Icarus, 415, 116057, doi: 10.1016/j.icarus.2024.116057

Kaib, N. A., & Raymond, S. N. 2025, Icarus, 439, 116632, doi: 10.1016/j.icarus.2025.116632

Kaib, N. A., Raymond, S. N., & Duncan, M. 2013, Nature, 493, 381, doi: 10.1038/nature11780

Kapusta, M., Mróz, P., Ryu, Y.-H., et al. 2026, A&A, 706, A110, doi: 10.1051/0004-6361/202555863

Kim, D.-J., Kim, H.-W., Hwang, K.-H., et al. 2018, AJ, 155, 76, doi: 10.3847/1538-3881/aaa47b

Kim, H.-W., Hwang, K.-H., Gould, A., et al. 2021, The Astronomical Journal, 162, 15, doi: 10.3847/1538-3881/abfc4a

Knight, M. M., Protopapa, S., Kelley, M. S., et al. 2017, ApJL, 851, L31

Kokubo, E., & Ida, S. 1998, Icarus, 131, 171, doi: 10.1006/icar.1997.5840

Koshimoto, N., Sumi, T., Bennett, D. P., et al. 2023, AJ, 166, 107, doi: 10.3847/1538-3881/ace689

Kratter, K. M., & Perets, H. B. 2012, The Astrophysical Journal, 753, 91, doi: 10.1088/0004-637X/753/1/91

Kremer, K., D'Orazio, D. J., Samsing, J., Chatterjee, S., & Rasio, F. A. 2019, The Astrophysical Journal, 885, 2, doi: 10.3847/1538-4357/ab44d1

Kroupa, P. 2001, MNRAS, 322, 231, doi: 10.1046/j.1365-8711.2001.04022.x

Kroupa, P., Tout, C. A., & Gilmore, G. 1993, MNRAS, 262, 545, doi: 10.1093/mnras/262.3.545

Lada, C. J., & Lada, E. A. 2003, ARA&A, 41, 57, doi: 10.1146/annurev.astro.41.011802.094844

Lam, C., & Kipping, D. 2018, MNRAS, 476, 5692, doi: 10.1093/mnras/sty022

Langeveld, A. B., Scholz, A., Mužić, K., et al. 2024, AJ, 168, 179, doi: 10.3847/1538-3881/ad6f0c

Laplace, P.-S. 1878, Œuvres complètes de Laplace, Vol. 1 (Paris: Gauthier-Villars)

Laskar, J. 1997, A&A, 317, L75

Laskar, J. 2000, PhRvL, 84, 3240, doi: 10.1103/PhysRevLett.84.3240

Laskar, J., & Petit, A. C. 2017, A&A, 605, A72, doi: 10.1051/0004-6361/201630022

Lastovka, M., Gaudi, B. S., Johnson, S. A., et al. 2025, AJ, 170, 258, doi: 10.3847/1538-3881/ae0196

Laughlin, G., & Adams, F. C. 1998, The Astrophysical Journal, 508, L171, doi: 10.1086/311736

Laughlin, G., & Adams, F. C. 2000, Icarus, 145, 614, doi: 10.1006/icar.2000.6355

Laughlin, G., & Batygin, K. 2017, Research Notes of the AAS, 1, 43

Lee, E. J., DeRocco, W., Hadden, S., & Gaudi, B. S. 2026, The Astrophysical Journal Letters, 1005, L18, doi: 10.3847/2041-8213/ae796f

Lee, M. H., & Peale, S. J. 2002, ApJ, 567, 596

Levison, H. F., Dones, L., Chapman, C. R., et al. 2001, Icarus, 151, 286, doi: 10.1006/icar.2001.6608

Levison, H. F., Morbidelli, A., Tsiganis, K., Nesvorný, D., & Gomes, R. 2011, AJ, 142, 152, doi: 10.1088/0004-6256/142/5/152

Li, D., Mustill, A. J., & Davies, M. B. 2019, MNRAS, 488, 1366, doi: 10.1093/mnras/stz1794

Li, G., & Adams, F. C. 2015, MNRAS, 448, 344, doi: 10.1093/mnras/stv012

Li, G., Holman, M. J., & Tao, M. 2016, ApJ, 831, 96, doi: 10.3847/0004-637X/831/1/96

Li, J., Lai, D., & Rodet, L. 2022, ApJ, 934, 154, doi: 10.3847/1538-4357/ac7c0d

Li, L.-S. 2008, Astronomy Reports, 52, 806, doi: 10.1134/S106377290810003X

Lin, D. N. C., & Ida, S. 1997, ApJ, 477, 781, doi: 10.1086/303738

Lissauer, J. J., & Gavino, S. 2021, Icarus, 364, 114470, doi: 10.1016/j.icarus.2021.114470

Lissauer, J. J., Ragozzine, D., Fabrycky, D. C., et al. 2011, ApJS, 197, 8

Lithwick, Y., & Wu, Y. 2011, ApJ, 739, 31

Lithwick, Y., & Wu, Y. 2014, Proceedings of the National Academy of Science, 111, 12610, doi: 10.1073/pnas.1308261110

Liu, B., Raymond, S. N., & Jacobson, S. A. 2022, Nature, 604, 643, doi: 10.1038/s41586-022-04535-1

LoRusso, R., Petrovich, C., & Gautham Bhaskar, H. 2026, arXiv e-prints, arXiv:2604.08383, doi: 10.48550/arXiv.2604.08383

Lovis, C., Ségransan, D., Mayor, M., et al. 2011, A&A, 528, A112, doi: 10.1051/0004-6361/201015577

Lu, T., Millholland, S. C., Rice, M., et al. 2026, arXiv preprint arXiv:2605.30177. https://arxiv.org/abs/2605.30177

Lucas, P. W., & Roche, P. F. 2000, MNRAS, 314, 858, doi: 10.1046/j.1365-8711.2000.03515.x

Luhman, K. L. 2004, ApJ, 617, 1216, doi: 10.1086/425647

Luhman, K. L. 2012, ARA&A, 50, 65, doi: 10.1146/annurev-astro-081811-125528

Luhman, K. L., Alves de Oliveira, C., Baraffe, I., et al. 2024, AJ, 167, 19, doi: 10.3847/1538-3881/ad00b7

Luhman, K. L., Burgasser, A. J., & Bochanski, J. J. 2011, ApJL, 730, L9, doi: 10.1088/2041-8205/730/1/L9

Luhman, K. L., Esplin, T. L., & Loutrel, N. P. 2016, ApJ, 827, 52, doi: 10.3847/0004-637X/827/1/52

Ma, S., Mao, S., Ida, S., Zhu, W., & Lin, D. N. C. 2016, MNRAS, 461, L107, doi: 10.1093/mnrasl/slw110

Malavolta, L., Nascimbeni, V., Piotto, G., et al. 2016, A&A, 588, A118, doi: 10.1051/0004-6361/201527933

Maldonado, R. F., Villaver, E., Mustill, A. J., & Chávez, M. 2022, MNRAS, 512, 104, doi: 10.1093/mnras/stac481

Malhotra, R. 1993, Nature, 365, 819, doi: 10.1038/365819a0

Malhotra, R. 1995, AJ, 110, 420, doi: 10.1086/117532

Malhotra, R. 1998, in Astronomical Society of the Pacific Conference Series, Vol. 149, Solar System Formation and Evolution, ed. D. Lazzaro, R. Vieira Martins, S. Ferraz-Mello, & J. Fernandez, 37

Malmberg, D., Davies, M. B., & Chambers, J. E. 2007, MNRAS, 377, L1, doi: 10.1111/j.1745-3933.2007.00291.x

Malmberg, D., Davies, M. B., & Heggie, D. C. 2011, MNRAS, 411, 859, doi: 10.1111/j.1365-2966.2010.17730.x

Mann, A. W., Gaidos, E., Mace, G. N., et al. 2016, ApJ, 818, 46, doi: 10.3847/0004-637X/818/1/46

Martin, D. V., Triaud, A. H. M. J., Udry, S., et al. 2019, A&A, 624, A68, doi: 10.1051/0004-6361/201833669

Martin, R. G., Lubow, S. H., Vallet, D., Anugu, N., & Gies, D. R. 2023, ApJL, 957, L28, doi: 10.3847/2041-8213/ad0730

Marzari, F. 2014, MNRAS, 444, 1419, doi: 10.1093/mnras/stu1544

Marzari, F. 2025, MNRAS, 536, 422, doi: 10.1093/mnras/stae2602

Marzari, F., & Picogna, G. 2013, A&A, 550, A64, doi: 10.1051/0004-6361/201220436

Marzari, F., & Weidenschilling, S. J. 2002, Icarus, 156, 570, doi: 10.1006/icar.2001.6786

Marzari, F., Weidenschilling, S. J., Barbieri, M., & Granata, V. 2005, ApJ, 618, 502, doi: 10.1086/425976

Masuda, K., & Winn, J. N. 2017, AJ, 153, 187, doi: 10.3847/1538-3881/aa647c

Mayor, M., Marmier, M., Lovis, C., et al. 2011, arXiv e-prints, arXiv:1109.2497, doi: 10.48550/arXiv.1109.2497

McKinney, W. 2010, in Proceedings of the 9th Python in Science Conference, Vol. 445, Austin, TX, 51–56

Meech, K. J., Weryk, R., Micheli, M., et al. 2017, Nature, 552, 378

Meibom, S., Torres, G., Fressin, F., et al. 2013, Nature, 499, 55, doi: 10.1038/nature12279

Miret-Roig, N., Bouy, H., Raymond, S. N., et al. 2022, Nature Astronomy, 6, 89, doi: 10.1038/s41550-021-01513-x

Moe, M., & Di Stefano, R. 2017, ApJS, 230, 15, doi: 10.3847/1538-4365/aa6fb6

Morbidelli, A. 2018, in Handbook of Exoplanets, ed. H. J. Deeg & J. A. Belmonte, 145, doi: 10.1007/978-3-319-55333-7_145

Morbidelli, A., Batygin, K., Brasser, R., & Raymond, S. N. 2020, MNRAS, 497, L46, doi: 10.1093/mnrasl/slaa111

Morbidelli, A., Levison, H. F., Tsiganis, K., & Gomes, R. 2005, Nature, 435, 462

Morrison, S. J., & Kratter, K. M. 2016, ApJ, 823, 118, doi: 10.3847/0004-637X/823/2/118

Mróz, P., Ban, M., Marty, P., & Poleski, R. 2024, AJ, 167, 40, doi: 10.3847/1538-3881/ad1106

Mróz, P., Udalski, A., Skowron, J., et al. 2017, Nature, 548, 183, doi: 10.1038/nature23276

Mróz, P., Udalski, A., Skowron, J., et al. 2017, Nature, 548, 183, doi: 10.1038/nature23276

Mróz, P., Udalski, A., Bennett, D. P., et al. 2019, A&A, 622, A201, doi: 10.1051/0004-6361/201834557

Mró z, P., Poleski, R., Han, C., et al. 2020, The Astronomical Journal, 159, 262, doi: 10.3847/1538-3881/ab8aeb

Mróz, P., Ryu, Y.-H., Skowron, J., et al. 2018, The Astronomical Journal, 155, 121, doi: 10.3847/1538-3881/aaaae9

Mróz, P., Poleski, R., Gould, A., et al. 2020, The Astrophysical Journal Letters, 903, L11, doi: 10.3847/2041-8213/abbfad

Mudryk, L. R., & Wu, Y. 2006, The Astrophysical Journal, 639, 423, doi: 10.1086/499347

Mustill, A. J., Veras, D., & Villaver, E. 2014, MNRAS, 437, 1404, doi: 10.1093/mnras/stt1973

Mužić, K., Scholz, A., Geers, V., Jayawardhana, R., & Tamura, M. 2012, ApJ, 744, 134, doi: 10.1088/0004-637X/744/2/134

Nagasawa, M., Ida, S., & Bessho, T. 2008, ApJ, 678, 498, doi: 10.1086/529369

Nascimbeni, V., Bedin, L. R., Piotto, G., De Marchi, F., & Rich, R. M. 2012, A&A, 541, A144, doi: 10.1051/0004-6361/201118655

Nayakshin, S., Zhang, L., Ćalović, A., et al. 2026, MNRAS, 546, stag043, doi: 10.1093/mnras/stag043

Nesvorný, D. 2015a, AJ, 150, 73, doi: 10.1088/0004-6256/150/3/73

Nesvorný, D. 2015b, AJ, 150, 68, doi: 10.1088/0004-6256/150/3/68

Nesvorný, D., Vokrouhlický, D., & Deienno, R. 2014a, ApJ, 784, 22, doi: 10.1088/0004-637X/784/1/22

Nesvorný, D., Vokrouhlický, D., Deienno, R., & Walsh, K. J. 2014b, AJ, 148, 52, doi: 10.1088/0004-6256/148/3/52

Nesvorný, D., Vokrouhlický, D., & Morbidelli, A. 2013, ApJ, 768, 45, doi: 10.1088/0004-637X/768/1/45

Nesvorný, D. 2011, The Astrophysical Journal, 742, L22, doi: 10.1088/2041-8205/742/2/L22

Nesvorný, D., & Morbidelli, A. 2012, The Astronomical Journal, 144, 117, doi: 10.1088/0004-6256/144/4/117

Nielsen, E. L., De Rosa, R. J., Macintosh, B., et al. 2019, AJ, 158, 13

Nigioni, A., Turrini, D., Danielski, C., Polychroni, D., & Chambers, J. E. 2026, A&A, 706, A96, doi: 10.1051/0004-6361/202452890

Nordström, B., Mayor, M., Andersen, J., et al. 2004, A&A, 418, 989, doi: 10.1051/0004-6361:20035959

Oasa, Y., Tamura, M., & Sugitani, K. 1999, ApJ, 526, 336, doi: 10.1086/307964

Obertas, A., Van Laerhoven, C., & Tamayo, D. 2017, Icarus, 293, 52, doi: 10.1016/j.icarus.2017.04.010

O'Brien, M. W., Tremblay, P.-E., Klein, B. L., et al. 2024, MNRAS, 527, 8687, doi: 10.1093/mnras/stad3773

O'Connor, C. E. 2026, ApJ, 998, 280, doi: 10.3847/1538-4357/ae3b26

Offner, S. S. R., Moe, M., Kratter, K. M., et al. 2023, in Astronomical Society of the Pacific Conference Series, Vol. 534, Protostars and Planets VII, ed. S. Inutsuka, Y. Aikawa, T. Muto, K. Tomida, & M. Tamura, 275, doi: 10.48550/arXiv.2203.10066

Ogihara, M., & Ida, S. 2009, ApJ, 699, 824, doi: 10.1088/0004-637X/699/1/824

Oliphant, T. E. 2006, A guide to NumPy, Vol. 1 (Trelgol Publishing USA)

Omarov, T. B. 1962, Akademiia Nauk Kazakhskoi SSR, Izvestiia, Seriia Fiziko-Matematicheskaia, 14, 66

'Oumuamua ISSI Team, Bannister, M. T., Bhandare, A., et al. 2019, Nature Astronomy, 3, 594, doi: 10.1038/s41550-019-0816-x

Outland, B., Noble, G., Smith, A. W., & Lissauer, J. J. 2026, Icarus, 452, 117025, doi: 10.1016/j.icarus.2026.117025

Papaloizou, J. C., Nelson, R. P., & Masset, F. 2001, A&A, 366, 263

Papaloizou, J. C. B., & Terquem, C. 2006, Reports on Progress in Physics, 69, 119, doi: 10.1088/0034-4885/69/1/R03

Parker, R. J., Alcock, H. L., Nicholson, R. B., Panić, O., & Goodwin, S. P. 2021, ApJ, 913, 95, doi: 10.3847/1538-4357/abf4cc

Parker, R. J., & Quanz, S. P. 2012, MNRAS, 419, 2448, doi: 10.1111/j.1365-2966.2011.19911.x

Parker, R. J., & Veras, D. 2026, arXiv e-prints, arXiv:2607.00080. https://arxiv.org/abs/2607.00080

Peale, S. J. 1976, ARA&A, 14, 215, doi: 10.1146/annurev.aa.14.090176.001243

Pearson, S. G., & McCaughrean, M. J. 2023, arXiv e-prints, arXiv:2310.01231, doi: 10.48550/arXiv.2310.01231

Pendleton, Y. J., & Black, D. C. 1983, AJ, 88, 1415, doi: 10.1086/113430

Penny, M. T., Gaudi, B. S., Kerins, E., et al. 2019, ApJS, 241, 3, doi: 10.3847/1538-4365/aafb69

Petit, A. C., Pichierri, G., Davies, M. B., & Johansen, A. 2020, A&A, 641, A176, doi: 10.1051/0004-6361/202038764

Pfalzner, S., Aizpuru Vargas, L. L., Bhandare, A., & Veras, D. 2021, A&A, 651, A38, doi: 10.1051/0004-6361/202140587

Picogna, G., & Marzari, F. 2014, A&A, 564, A28, doi: 10.1051/0004-6361/201322816

Pilat-Lohinger, E., Funk, B., & Dvorak, R. 2003, A&A, 400, 1085, doi: 10.1051/0004-6361:20021811

Pilat-Lohinger, E., Funk, B., Freistetter, F., & Dvorak, R. 2002, in ESA Special Publication, Vol. 518, Exo-Astrobiology, ed. H. Lacoste, 547–548

Poleski, R., Skowron, J., Mróz, P., et al. 2021, AcA, 71, 1, doi: 10.32023/0001-5237/71.1.1

Poleski, R., Ryu, Y.-H., Udalski, A., et al. 2025, AcA, 75, 279, doi: 10.32023/0001-5237/75.4.1

Portegies Zwart, S. 2021, A&A, 647, A136, doi: 10.1051/0004-6361/202038888

Portegies Zwart, S., Torres, S., Pelupessy, I., Bédorf, J., & Cai, M. X. 2018, MNRAS, 479, L17, doi: 10.1093/mnrasl/sly088

Price-Whelan, A. M., Sipőcz, B. M., Günther, H. M., et al. 2018, AJ, 156, 123, doi: 10.3847/1538-3881/aabc4f

Proszkow, E.-M., & Adams, F. C. 2009, ApJS, 185, 486, doi: 10.1088/0067-0049/185/2/486

Pu, B., & Lai, D. 2021, MNRAS, 508, 597, doi: 10.1093/mnras/stab2504

Pu, B., & Wu, Y. 2015, ApJ, 807, 44, doi: 10.1088/0004-637X/807/1/44

Quarles, B., Li, G., Kostov, V., & Haghighipour, N. 2020, AJ, 159, 80, doi: 10.3847/1538-3881/ab64fa

Quarles, B., & Lissauer, J. J. 2016, AJ, 151, 111, doi: 10.3847/0004-6256/151/5/111

Quarles, B., Satyal, S., Kostov, V., Kaib, N., & Haghighipour, N. 2018, ApJ, 856, 150, doi: 10.3847/1538-4357/aab264

Quillen, A. C. 2011, MNRAS, 418, 1043, doi: 10.1111/j.1365-2966.2011.19555.x

Rabago, I., & Steffen, J. H. 2019, MNRAS, 489, 2323, doi: 10.1093/mnras/sty2552

Rabl, G., & Dvorak, R. 1988, A&A, 191, 385

Raghavan, D., McAlister, H. A., Henry, T. J., et al. 2010, ApJS, 190, 1, doi: 10.1088/0067-0049/190/1/1

Rasio, F. A., & Ford, E. B. 1996, Science, 274, 954

Raymond, S. N., Armitage, P. J., & Gorelick, N. 2009, ApJL, 699, L88, doi: 10.1088/0004-637X/699/2/L88

Raymond, S. N., Armitage, P. J., & Gorelick, N. 2010, ApJ, 711, 772

Raymond, S. N., Armitage, P. J., & Veras, D. 2018, ApJL, 856, L7

Raymond, S. N., Armitage, P. J., Veras, D., Quintana, E. V., & Barclay, T. 2018, MNRAS, 476, 3031, doi: 10.1093/mnras/sty468

Raymond, S. N., Barnes, R., & Mandell, A. M. 2008, MNRAS, 384, 663, doi: 10.1111/j.1365-2966.2007.12712.x

Raymond, S. N., Izidoro, A., & Kaib, N. A. 2023, MNRAS, 524, L72, doi: 10.1093/mnrasl/slad079

Raymond, S. N., Izidoro, A., & Morbidelli, A. 2020, in Planetary Astrobiology, ed. V. S. Meadows, G. N. Arney, B. E. Schmidt, & D. J. Des Marais, 287, doi: 10.2458/azu_uapress_9780816540068

Raymond, S. N., & Kaib, N. A. 2026, Icarus, 447, 116910, doi: 10.1016/j.icarus.2025.116910

Raymond, S. N., Kaib, N. A., Selsis, F., & Bouy, H. 2024, MNRAS, 527, 6126, doi: 10.1093/mnras/stad3604

Raymond, S. N., Quinn, T., & Lunine, J. I. 2005, ApJ, 632, 670, doi: 10.1086/433179

Raymond, S. N., Armitage, P. J., Moro-Martín, A., et al. 2011, A&A, 530, A62, doi: 10.1051/0004-6361/201116456

Raymond, S. N., Armitage, P. J., Moro-Martín, A., et al. 2012, A&A, 541, A11, doi: 10.1051/0004-6361/201117049

Regály, Z., Fröhlich, V., & Vinkó, J. 2022, The Astrophysical Journal, 941, 121, doi: 10.3847/1538-4357/aca1ba

Rice, D. R., Rasio, F. A., & Steffen, J. H. 2018, MNRAS, 481, 2205, doi: 10.1093/mnras/sty2418

Rice, D. R., & Steffen, J. H. 2023, MNRAS, 520, 4057, doi: 10.1093/mnras/stad393

Rice, M., & Laughlin, G. 2019, ApJL, 884, L22

Rice, M., Wang, S., & Laughlin, G. 2022, ApJL, 926, L17

Rickman, H., Wajer, P., Przyłuski, R., et al. 2023, MNRAS, 520, 637, doi: 10.1093/mnras/stac3705

Robberto, M., Gennaro, M., Ubeira Gabellini, M. G., et al. 2020, ApJ, 896, 79, doi: 10.3847/1538-4357/ab911e

Rosotti, G. P., Dale, J. E., de Juan Ovelar, M., et al. 2014, MNRAS, 441, 2094, doi: 10.1093/mnras/stu679

Roy, A., & Haddow, M. 2003, Celestial Mechanics and Dynamical Astronomy, 87, 411, doi: 10.1023/B:CELE.0000006767.34371.2f

Roy, A. E., & Ovenden, M. W. 1954, MNRAS, 114, 232, doi: 10.1093/mnras/114.2.232

Rusznak, J., Wang, X.-Y., Rice, M., & Wang, S. 2025, ApJL, 983, L42, doi: 10.3847/2041-8213/adc129

Ryu, Y.-H., Mróz, P., Gould, A., et al. 2021, AJ, 161, 126, doi: 10.3847/1538-3881/abd55f

Ryu, Y.-H., Gould, A., Hwang, K.-H., et al. 2026, arXiv e-prints, arXiv:2606.27725. https://arxiv.org/abs/2606.27725

Safronov, V. S., & Zvjagina, E. V. 1969, Icarus, 10, 109, doi: 10.1016/0019-1035(69)90013-X

Scally, A., & Clarke, C. 2001, MNRAS, 325, 449, doi: 10.1046/j.1365-8711.2001.04274.x

Scharf, C., & Menou, K. 2009, ApJL, 693, L113, doi: 10.1088/0004-637X/693/2/L113

Schib, O., Mordasini, C., Emsenhuber, A., & Helled, R. 2025a, A&A, 704, A27, doi: 10.1051/0004-6361/202556262

Schib, O., Mordasini, C., Emsenhuber, A., & Helled, R. 2025b, A&A, 704, A28, doi: 10.1051/0004-6361/202556261

Scholz, A., Geers, V., Jayawardhana, R., et al. 2009, ApJ, 702, 805, doi: 10.1088/0004-637X/702/1/805

Seligman, D. Z., Micheli, M., Farnocchia, D., et al. 2025, ApJL, 989, L36, doi: 10.3847/2041-8213/adf49a

Sigurdsson, S. 1992, ApJL, 399, L95, doi: 10.1086/186615

Sigurdsson, S., Richer, H. B., Hansen, B. M., Stairs, I. H., & Thorsett, S. E. 2003, Science, 301, 193, doi: 10.1126/science.1086326

Silsbee, K., & Tremaine, S. 2018, AJ, 155, 75

Smallwood, J. L., Nealon, R., Chen, C., et al. 2021, MNRAS, 508, 392, doi: 10.1093/mnras/stab2624

Smith, A. W., & Lissauer, J. J. 2009, Icarus, 201, 381, doi: 10.1016/j.icarus.2008.12.027

Smith, K. W., & Bonnell, I. A. 2001, Monthly Notices of the Royal Astronomical Society, 322, L1, doi: 10.1046/j.1365-8711.2001.04321.x

Smullen, R. A., Kratter, K. M., & Shannon, A. 2016, Monthly Notices of the Royal Astronomical Society, 461, 1288, doi: 10.1093/mnras/stw1347

Spergel, D., Gehrels, N., Baltay, C., et al. 2015, arXiv e-prints, arXiv:1503.03757, doi: 10.48550/arXiv.1503.03757

Spurzem, R., Giersz, M., Heggie, D. C., & Lin, D. N. C. 2009, The Astrophysical Journal, 697, 458, doi: 10.1088/0004-637X/697/1/458

Stephan, A. P., & Stassun, K. G. 2026, arXiv e-prints, arXiv:2607.02653. https://arxiv.org/abs/2607.02653

Störzer, H., & Hollenbach, D. 1999, ApJ, 515, 669, doi: 10.1086/307055

Sucerquia, M., Ramírez, V., Alvarado-Montes, J. A., & Zuluaga, J. I. 2020, MNRAS, 492, 3499, doi: 10.1093/mnras/stz3548

Sumi, T., Kamiya, K., Bennett, D. P., et al. 2011, Nature, 473, 349, doi: 10.1038/nature10092

Sumi, T., Koshimoto, N., Bennett, D. P., et al. 2023, AJ, 166, 108, doi: 10.3847/1538-3881/ace688

Sutherland, A. P., & Fabrycky, D. C. 2016, The Astrophysical Journal, 818, 6, doi: 10.3847/0004-637X/818/1/6

Suzuki, D., Bennett, D. P., Sumi, T., et al. 2016, ApJ, 833, 145, doi: 10.3847/1538-4357/833/2/145

Szebehely, V. 1977, Celestial Mechanics, 15, 107, doi: 10.1007/BF01229051

Szebehely, V. 1980, Celestial Mechanics, 22, 7, doi: 10.1007/BF01228750

Szebehely, V., & McKenzie, R. 1981, Celestial Mechanics, 23, 3, doi: 10.1007/BF01228541

Tamayo, D., Murray, N., Tremaine, S., & Winn, J. 2021, AJ, 162, 220, doi: 10.3847/1538-3881/ac1c6a

Tamayo, D., Triaud, A. H. M. J., Menou, K., & Rein, H. 2015, ApJ, 805, 100, doi: 10.1088/0004-637X/805/2/100

Teasdale, M., & Stamatellos, D. 2026, arXiv e-prints, arXiv:2604.24420, doi: 10.48550/arXiv.2604.24420

Terquem, C., & Papaloizou, J. C. 2007, ApJ, 654, 1110

Thommes, E. W., Duncan, M. J., & Levison, H. F. 1999, Nature, 402, 635, doi: 10.1038/45185

Thommes, E. W., Duncan, M. J., & Levison, H. F. 2002, AJ, 123, 2862, doi: 10.1086/339975

Thornton, M., Montet, B. T., White, R., Shao, A., & Kumar, D. T. 2026, MNRAS, 548, stag515, doi: 10.1093/mnras/stag515

Thorsett, S. E., Arzoumanian, Z., & Taylor, J. H. 1993, ApJL, 412, L33, doi: 10.1086/186933

Tobin, J. J., Sheehan, P. D., Megeath, S. T., et al. 2020, ApJ, 890, 130, doi: 10.3847/1538-4357/ab6f64

Tokadjian, A., & Piro, A. L. 2020, AJ, 160, 194, doi: 10.3847/1538-3881/abb29e

Tsiganis, K., Gomes, R., Morbidelli, A., & Levison, H. 2005, Nature, 435, 459

Udalski, A., Szymański, M. K., & Szymański, G. 2015, AcA, 65, 1, doi: 10.48550/arXiv.1504.05966

Valencia, D., O'Connell, R. J., & Sasselov, D. 2006, Icarus, 181, 545, doi: 10.1016/j.icarus.2005.11.021

van Elteren, A., Portegies Zwart, S., Pelupessy, I., Cai, M. X., & McMillan, S. L. W. 2019, A&A, 624, A120, doi: 10.1051/0004-6361/201834641

Veras, D. 2016, Royal Society Open Science, 3, 150571, doi: 10.1098/rsos.150571

Veras, D., & Armitage, P. J. 2005, ApJL, 620, L111, doi: 10.1086/428831

Veras, D., Crepp, J. R., & Ford, E. B. 2009, ApJ, 696, 1600, doi: 10.1088/0004-637X/696/2/1600

Veras, D., Evans, N. W., Wyatt, M. C., & Tout, C. A. 2014, MNRAS, 437, 1127, doi: 10.1093/mnras/stt1905

Veras, D., Georgakarakos, N., Dobbs-Dixon, I., & Gänsicke, B. T. 2017, MNRAS, 465, 2053, doi: 10.1093/mnras/stw2699

Veras, D., Hadjidemetriou, J. D., & Tout, C. A. 2013, MNRAS, 435, 2416, doi: 10.1093/mnras/stt1451

Veras, D., & Mustill, A. J. 2013, MNRAS, 434, L11, doi: 10.1093/mnrasl/slt067

Veras, D., & Raymond, S. N. 2012, Monthly Notices of the Royal Astronomical Society: Letters, 421, L117, doi: 10.1111/j.1745-3933.2012.01218.x

Veras, D., & Tout, C. A. 2012, Monthly Notices of the Royal Astronomical Society, 422, 1648, doi: 10.1111/j.1365-2966.2012.20741.x

Veras, D., Wyatt, M. C., Mustill, A. J., Bonsor, A., & Eldridge, J. J. 2011, MNRAS, 417, 2104

Verrier, P. E., & Evans, N. W. 2007, MNRAS, 382, 1432, doi: 10.1111/j.1365-2966.2007.12493.x

Vincke, K., & Pfalzner, S. 2016, ApJ, 828, 48, doi: 10.3847/0004-637X/828/1/48

Virtanen, P., Gommers, R., Oliphant, T. E., et al. 2020, Nature Methods, 17, 261

Vleeschower, L., Corongiu, A., Stappers, B. W., et al. 2024, MNRAS, 530, 1436, doi: 10.1093/mnras/stae816

Volk, K., & Malhotra, R. 2024, AJ, 167, 271, doi: 10.3847/1538-3881/ad3de5

Voyatzis, G., Hadjidemetriou, J. D., Veras, D., & Varvoglis, H. 2013, MNRAS, 430, 3383, doi: 10.1093/mnras/stt137

Walt, S. v. d., Colbert, S. C., & Varoquaux, G. 2011, Computing in Science & Engineering, 13, 22

Wang, L., Kouwenhoven, M. B. N., Zheng, X., Church, R. P., & Davies, M. B. 2015, MNRAS, 449, 3543, doi: 10.1093/mnras/stv542

Wang, Y., Perna, R., & Zhu, Z. 2024, Nature Astronomy, 8, 756, doi: 10.1038/s41550-024-02239-2

Weidenschilling, S. J. 1975, AJ, 80, 145, doi: 10.1086/111727

Weidenschilling, S. J. 1977, Ap&SS, 51, 153, doi: 10.1007/BF00642464

Weidenschilling, S. J., & Marzari, F. 1996, Nature, 384, 619, doi: 10.1038/384619a0

Whitworth, A. P., & Zinnecker, H. 2004, A&A, 427, 299, doi: 10.1051/0004-6361:20041131

Williams, G. V., Sato, H., Sarneczky, K., et al. 2017, Central Bureau Electronic Telegrams, 4450, 1

Winter, A. J., Clarke, C. J., Rosotti, G., et al. 2018, MNRAS, 478, 2700, doi: 10.1093/mnras/sty984

Winter, A. J., & Haworth, T. J. 2022, European Physical Journal Plus, 137, 1132, doi: 10.1140/epjp/s13360-022-03314-1

Witt, H. J., & Mao, S. 1994, ApJ, 430, 505, doi: 10.1086/174426

Wittenmyer, R. A., Wang, S., Horner, J., et al. 2020, MNRAS, 492, 377, doi: 10.1093/mnras/stz3436

Wu, D.-H., Jin, S., & Steffen, J. H. 2025, AJ, 169, 28, doi: 10.3847/1538-3881/ad9388

Wu, Y., & Lithwick, Y. 2011, ApJ, 735, 109

Wyatt, M. C., Bonsor, A., Jackson, A. P., Marino, S., & Shannon, A. 2017, MNRAS, 464, 3385, doi: 10.1093/mnras/stw2633

Yalinewich, A., & Petrovich, C. 2020, ApJL, 892, L11, doi: 10.3847/2041-8213/ab75dc

Yee, J. C., & Kenyon, S. J. 2025, AJ, 170, 132, doi: 10.3847/1538-3881/adeb84

Yu, F., & Lai, D. 2024, ApJ, 970, 97, doi: 10.3847/1538-4357/ad4f81

Yuan, L., & Lee, M. H. 2024, ApJ, 967, 98, doi: 10.3847/1538-4357/ad3ba4

Zakamska, N. L., & Tremaine, S. 2004, AJ, 128, 869, doi: 10.1086/422023

Zapatero Osorio, M. R., Béjar, V. J. S., Martín, E. L., et al. 2000, Science, 290, 103, doi: 10.1126/science.290.5489.103

Zhai, R., Lee, M. H., Gan, T., & Mao, S. 2025, ApJ, 990, 74, doi: 10.3847/1538-4357/adf557

Zhang, Q. 2018, ApJL, 852, L13, doi: 10.3847/2041-8213/aaa2f7

Zhang, S., Zhu, Z., Huang, J., et al. 2018, ApJL, 869, L47

Zhang, Y., & Lin, D. N. C. 2020, Nature Astronomy, 4, 852, doi: 10.1038/s41550-020-1065-8

Zheng, X., Kouwenhoven, M. B. N., & Wang, L. 2015, MNRAS, 453, 2759, doi: 10.1093/mnras/stv1832

Zhou, J.-L., Lin, D. N. C., & Sun, Y.-S. 2007, ApJ, 666, 423, doi: 10.1086/519918

Zink, J. K., Batygin, K., & Adams, F. C. 2020, AJ, 160, 232, doi: 10.3847/1538-3881/abb8de

Zuluaga, J. I., Sánchez-Hernández, O., Sucerquia, M., & Ferrín, I. 2018, AJ, 155, 236, doi: 10.3847/1538-3881/aabd7c